SHORT-TERM AND LONG-TERM RELIABILITY STUDIES

IN DEREGULATED POWER SYSTEMS

A Dissertation

by

YISHAN LI

Submitted to the Office of Graduate Studies of
Texas A&M University
in partial fulfillment of the requirements for the degree of

DOCTOR OF PHILOSOPHY

December 2005

Major Subject: Electrical Engineering

SHORT-TERM AND LONG-TERM RELIABILITY STUDIES

IN DEREGULATED POWER SYSTEMS

A Dissertation

by

YISHAN LI

Submitted to the Office of Graduate Studies of
Texas A&M University
in partial fulfillment of the requirements for the degree of

DOCTOR OF PHILOSOPHY

Approved by:

Chair of Committee,	Garng M. Huang
Committee Members,	Chanan Singh
	Aniruddha Datta
	Vivek Sarin
Head of Department,	Chanan Singh

December 2005

Major Subject: Electrical Engineering

ABSTRACT

Short-term and Long-term Reliability Studies in Deregulated Power Systems.

(December 2005)

Yishan Li, B.S., Shanghai Jiao Tong University;

M.S., Shanghai Jiao Tong University

Chair of Advisory Committee: Dr. Garng M. Huang

The electric power industry is undergoing a restructuring process. The major goals of the change of the industry structure are to motivate competition, reduce costs and improve the service quality for consumers. In the meantime, it is also important for the new structure to maintain system reliability. Power system reliability is comprised of two basic components, adequacy and security. In terms of the time frame, power system reliability can mean short-term reliability or long-term reliability. Short-term reliability is more a security issue while long-term reliability focuses more on the issue of adequacy. This dissertation presents techniques to address some security issues associated with short-term reliability and some adequacy issues related to long-term reliability in deregulated power systems.

Short-term reliability is for operational purposes and is mainly concerned with security. Thus the way energy is dispatched and the actions the system operator takes to remedy an insecure system state such as transmission congestion are important to short-term reliability. Our studies on short-term reliability are therefore focused on these two aspects. We first investigate the formulation of the auction-based dispatch by the law of supply and demand. Then we develop efficient algorithms to solve the auction-based dispatch with different types of bidding functions. Finally we propose a new Optimal Power Flow (OPF) method based on sensitivity factors and the technique of aggregation to manage congestion, which results from the auction-based dispatch. The algorithms and the new OPF method proposed here are much faster and more efficient than the conventional algorithms and methods.

With regard to long-term reliability, the major issues are adequacy and its improvement. Our research thus is focused on these two aspects. First, we develop a probabilistic methodology to assess composite power system long-term reliability with both adequacy and security included by using the sequential Monte Carlo simulation method. We then investigate new ways to improve composite power system adequacy in the long-term. Specifically, we propose to use Flexible AC Transmission Systems (FACTS) such as Thyristor Controlled Series Capacitor (TCSC), Static Var Compensator (SVC) and Thyristor Controlled Phase Angle Regulator (TCPAR) to enhance reliability.

DEDICATION

To my wife, parents and brothers

ACKNOWLEDGEMENTS

I would like to express my most sincere gratitude to my advisor, Dr. Garng M. Huang, for his invaluable guidance throughout my entire graduate program at Texas A&M University. Without his knowledege, patience, support and encouragement, my research would never have been possible.

I also want to extend my gratitude to my committee members, Dr. Chanan Singh, Dr. Aniruddha Datta and Dr. Vivek Sarin, for their precious time and support. I am especially thankful to Dr. Chanan Singh for his inspiring suggestions during the project meetings.

Acknowledgement is extended to my friends Qing Zhao, Rebecca Morrison and Jason Shutt for their constant help and encouragement during my studies at Texas A&M University.

I would also like to thank my colleagues Yan Ou, Ping Yan, Jun Li, Xingbin Yu and Nirmal-Kumar Nair.

Finally, from the bottom of my heart, I would like to thank my parents, wife and brothers for shaping my life and encouraging me all the time.

TABLE OF CONTENTS

Page

CHAPTER Page

CHAPTER Page

CHAPTER Page

LIST OF FIGURES

FIGURE Page

LIST OF TABLES

TABLE Page

CHAPTER I

INTRODUCTION

1.1 Deregulated Power Systems

Over the past two decades, the power industry around the world has been experiencing a change towards deregulation. Utilities that were previously vertically integrated have become divided into three sectors: generation companies, transmission companies, and distribution companies [1-5]. It is expected that the competition among generation companies together with open access to the transmission system will lead to lower electricity prices and better service for customers.

In the new deregulated power systems, electricity is considered a commodity which can be traded in a free market by generators and loads. At present there are two major market coordination models: the bilateral model and the pool model [1, 4-8]. In a bilateral market, the generators and loads enter into direct negotiations to decide the power quantities and prices. In a pool market, the amounts and prices of generations and loads are determined by the auction-based dispatch.

To facilitate the operation of power markets, the transmission system remains a regulated monopoly which should be open to all transmission users and should treat them on a fair and non-discriminatory basis. To achieve this requirement, an Independent System Operator (ISO) is designated to operate the transmission system and provide transmission services to all transmission users [1, 2]. As part of the system operations, the ISO has the responsibility to maintain the system reliability. The ISO's reliability functions include two aspects:

- Short-term reliability. This is for operational purposes. The ISO should monitor the state of the transmission system and re-dispatch generation if necessary to eliminate transmission congestion and maintain the reliability of the system.

This dissertation follows the style and format of *IEEE Transactions on Power Systems*.

- Long-term reliability. This is for planning purposes. The ISO needs to carry out studies to evaluate the reliability of the system over a long period of time. If the reliability level is not sufficient, the ISO should propose ways to improve the reliability. For instance, the ISO could suggest constructing new power plants or new transmission lines at weak locations.

1.2 Short-term and Long-term Reliability

The reliability analysis for a composite power system consists of two basic components namely, adequacy and security [9-12]. Adequacy "is mainly concerned with the ability of the electric system to supply the aggregate electrical demand and energy requirements of customers at all times taking into account scheduled and expected unscheduled outages of system elements". On the other hand security "deals with the ability of the system to withstand sudden disturbances such as short circuits or unanticipated system component failures" [9].

According to the time frame, reliability can be classified into short-term reliability and long-term reliability. Short-term reliability is related to the system behavior in the near future such as several hours away. On the other hand, long-term reliability is associated with the system behavior over a long period of time like years. Both the short-term and long-term reliability studies need to consider adequacy and security. And both studies have the same procedure in evaluating power system reliability, namely

- State selection
- State evaluation
- Reliability index calculation

State selection is to decide the states of all system components such as transmission lines and generators. For instance, suppose each component has only two states: up and down. The state selection will determine which components are in the up state and which are in the down state. Based on the states of the components, we evaluate the system to see whether or not the load is supplied sufficiently. If there is a loss of load, we need to

update reliability indices. We keep repeating the above three steps until a certain stopping criterion is reached.

Though the short-term and long-term reliability studies have the above similarities, due to their significant difference in time domain concerned, these two types of reliability studies are different in several aspects. This point can be demonstrated by using a simple two-state component.

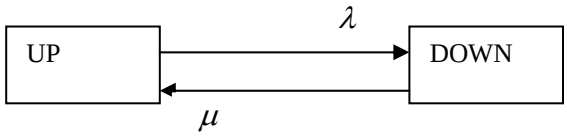

Fig. 1.1. State-space Model of a Two-state Component

Fig.1.1 shows the state-space model of a two-state component. The failure and repair rates are λ, μ respectively. The probabilities of the component in the up and down states at time t are given by [13]:

$$p_{UP}(t) = \frac{\mu}{\lambda + \mu} + (p_{UP}(0) - \frac{\mu}{\lambda + \mu})e^{-(\lambda+\mu)t} \tag{1.1}$$

$$p_{DOWN}(t) = \frac{\lambda}{\lambda + \mu} + (p_{DOWN}(0) - \frac{\lambda}{\lambda + \mu})e^{-(\lambda+\mu)t} \tag{1.2}$$

In the above two equations, "0" means time instant 0. $p_{UP}(t)$ and $p_{DOWN}(t)$ represent the up and down state probabilities at time instant *t* separately. For the long-term reliability study, the time concerned is long. Thus the second term in the above two equations is generally very close to zero and can be ignored. Therefore the state probability of the component is only determined by the failure rate λ and the repair rate μ. In comparison, in the short-term reliability study, we only consider a short period of time on the order of hours. As a result, usually the second term in (1.1) and (1.2) should not be neglected.

That means the state probability of the component is determined by not only the failure and repair rates but also the initial state and the time. As discussed earlier, state selection is the first step of reliability analysis. Therefore the difference of the short-term and long-term reliability studies in calculation of the component state probability could lead to other differences such as the result and the application. Below we show these differences through a simple system.

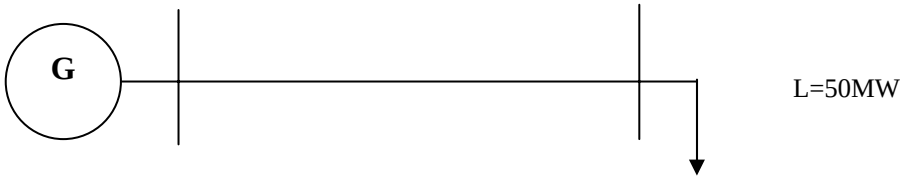

Fig. 1.2. A Simple Test System

For the system in Fig. 1.2, we assume that

- The generator has a capacity 60MW and is 100% reliable.
- The load is 50MW.
- The transmission line has 70MW capacity. It has two states: up and down. The failure rate is $\lambda = 3.65$/year and the repair rate is $\mu = 365$/year.
- The reliability index is Loss Of Load Probability (*LOLP*).

1.2.1 Case Study 1: Line Up at t=0

Suppose at time *t*=0 the transmission line is up and we are interested in the short-term reliability at time *t*=1 hour and the long-term reliability of 10 years. Obviously the system is not reliable when the line is down. In other words, reliability index *LOLP* is equal to the down probability of the line. In terms of (1.2), we can easily obtain the down probability of the line for the short-term and long-term reliability. Specifically for the short-term reliability,

$$p_{DOWN}(\frac{1}{8760}) = \frac{3.65}{3.65+365} + (0 - \frac{3.65}{3.65+365})e^{-(3.65+365)/8760} = 0.04\%$$

It is noted that 1 hour is 1/8760 year. Similarly, for the long-term reliability, we can get

$$p_{DOWN}(10) = \frac{3.65}{3.65+365} + (0 - \frac{3.65}{3.65+365})e^{-(3.65+365)\times 10} = 0.99\%$$

$P_{DOWN}(10)$ is exactly the same as $\left(3.65/\left(3.65+365\right)\right)$. Based on these results, we can see that

- The system has a very high short-term reliability. The *LOLP* is only 0.04%.
- The long-term reliability differs significantly from the short-term reliability. For a period of 10 years, the *LOLP* is 0.99%, much higher than that of the short-term reliability.
- Only the failure and repair rates affect the result of the long-term reliability.

1.2.2 Case Study 2: Line Down at t=0

To find out more information about the short-term and long-term reliability, we next assume at time *t*=0 the transmission line is down. We still calculate the short-term reliability at time *t*=1 hour and the long-term reliability for 10 years. Again (1.2) is used to decide the down probability of the transmission line, which is also the *LOLP* in this system. For the short-term reliability,

$$p_{DOWN}(\frac{1}{8760}) = \frac{3.65}{3.65+365} + (1 - \frac{3.65}{3.65+365})e^{-(3.65+365)/8760} = 95.92\%$$

For the long-term reliability, the result is

$$p_{DOWN}(10) = \frac{3.65}{3.65+365} + (1 - \frac{3.65}{3.65+365})e^{-(3.65+365)\times 10} = 0.99\%$$

We can see that

- The short-term reliability now has a very high probability for the loss of load: 95.92%.
- The long-term reliability has the same *LOLP* as the first case study.

By comparing the two sets of results of the case studies, we observe that the short-term reliability is closely related to the initial state while the long-term reliability is independent of the initial state. Specifically, when the transmission line is up at t=0, the short-term reliability is very high: *LOLP* is only 0.04%. But when the transmission line is down at t=0, *LOLP* of the short-term reliability is more than 95%. In a word, the short-term reliability is almost the same as the current reliability. In comparison, for the long-term reliability, no matter whether the line is up or down at t=0, the results are the same, *LOLP* = 0.99%. The different effects of the initial state on the short-term and long-term reliability are expected. Notice that the short-term reliability is about the system reliability only hours away. The period of time concerned is so short that the probability a component will change its state is very small. Therefore the current state can be a good indicator of the reliability in a short-term. That also implies deterministic methods are appropriate to analyze the short-term reliability. On the other hand, the long-term reliability is about the system behavior over a long period of time. Correspondingly a component can experience each state and repeat each state many times. That implies the initial state actually has no influence over the long-term reliability. Further, for the long-term reliability, probabilistic methods should be used so that all possible system states and their likelihood can be considered.

The above case studies also tell us that the short-term reliability and the long-term reliability have different focuses on adequacy and security. When the line is down initially, the short-term *LOLP* is very high: more than 95%. That implies security is a serious problem in the short-term reliability. In fact if we also consider the failure of generators in reliability analysis, we can find that the short-term reliability emphasizes security whereas the long-term reliability focuses on adequacy. The reasons are as follows.

For the short-term reliability, adequacy is mainly concerned about the dispatch of energy to meet demand fully. In practical operation, unit commitment (UC) is operated on a daily or weekly basis to supply load. In addition, energy dispatch is run very frequently. For instance, economic dispatch (ED) occurs every 15 to 30 minutes. That

means, in normal situations, there should have enough generation in the short-term reliability since those failing generators have been excluded in the UC and ED. Thus adequacy is less critical. On the other hand, in the ED or UC we implicitly assume the transmission lines are always available to deliver, which may not be true when faults occur. That implies the failure of transmission lines is a more significant problem than that of generators in the short-term reliability since the failure of lines is not well planned against. As a result, security instead of adequacy stands out as the major problem in the short-term reliability.

With regard to the long-term reliability, adequacy becomes a major issue. As we know, over a long period of time, there are no plans like UC and ED to guarantee enough generation. Thus we have to consider the failure of transmission lines as well as generators in the long-term reliability. Normally it takes much more time to repair a failed generator than a failed line. This is true especially for large size units, which can take up to 10 times time to be repaired than a line. That means in the long-term reliability, the failure of generators is a more serious problem than that of transmission lines. In other words, adequacy rather than security is the major concern of the long-term reliability.

To conclude, the short-term reliability is more a security issue while the long-term reliability focuses more an adequacy issue. It is noted that this conclusion applies to both the regulated power systems and the deregulated power systems. Though markets have brought many changes to the operation and planning of power systems, some fundamental features of the short-term and long-term reliability from earlier discussions remain the same in the deregulated systems:

- The short-term reliability still has a strong tie with the initial state and the adequacy in the initial state is always satisfied.
- The long-term reliability still needs to worry about the outage of components since its initial states are too many to be precisely known.

Therefore in the deregulated systems, security remains as the main issue for the short-term reliability and adequacy is still a major issue for the long-term reliability.

1.3 Focuses of the Dissertation

This research attempts to evolve an analytical framework to cope with some challenging issues associated with the short-term and long-term reliability in the deregulated power systems.

In terms of the analysis in section 1.2, we know that the short-term reliability study is for operational purposes and is mainly concerned with security. Our studies on the short-term reliability consist of “auction-based dispatch” and “congestion management”. The auction-based dispatch handles the dispatch of energy during operation. The congestion management eliminates the congestion on the transmission line in operation and maintains the security and thus the short-term reliability of the system. Deterministic methods are used for these studies considering the feature of the short-term reliability.

The long-term reliability is mainly for planning purposes. As discussed earlier, in the long-term reliability, adequacy and its improvement are the major issues. Accordingly, our studies on the long-term reliability are focused on these two areas. Our first topic evaluates the composite power system reliability with both adequacy and security included. The second topic is to improve the adequacy of the composite power system. In order to consider the effects of uncertainties, probabilistic methods are adopted for these two studies. Below we outline the four proposed focus areas.

1.3.1 Focus 1: Auction-based Dispatch in Deregulated Power Systems

As we know, in the regulated power systems, the economic dispatch is used to dispatch generators. The objective of the classic economic dispatch is to supply loads with the least cost. On the other hand, in the deregulated power systems, energy is procured from a power market, which can be either a bilateral market or a pool market. If it is a bilateral market, the seller and the buyer can negotiate by themselves to decide the price and quantity of the energy to be exchanged. If it is a pool market, the price and

quantity of the energy is determined by a central auction, i.e., the auction-based dispatch. The features of the auction-based dispatch are as follows:

- Loads are not necessarily constant.
- Both generators and loads can submit bids to the auction.
- Usually the bids of generators are convex quadratic functions whereas the bids of loads are concave quadratic functions or linear incremental functions.

Obviously this dispatch is much more complex than the classic economic dispatch. The formulation and algorithm of the economic dispatch are not applicable to the auction-based dispatch. That requires a study on the formulation of the auction-based dispatch. Accordingly new algorithms should be developed to solve the auction-based dispatch.

1.3.2 Focus 2: Congestion Management in Deregulated Power Systems

A significant feature of the deregulated power systems is that the procurement of energy is through markets, which neglect the constraint of the transmission system. To maximize their profits, people tend to buy electricity from the inexpensive sources. As a result, transmission congestion occurs more often than before deregulation. Correspondingly, the short-term reliability level declines in the deregulated power systems [14, 15]. Clearly, to maintain the reliability, it is important to eliminate congestion efficiently. One method to eliminate congestion is the Optimal Power Flow (OPF) model [16-18]. This model is arguably the most accurate and effective method for strongly networked transmission systems [19]. A typical formulation of the OPF model can be found in [20]. However, in this formulation all generators and loads are involved in congestion management. As a consequence, the optimization program has too many variables for large-size systems, which makes it hard to solve. Thus more efficient and reasonable methods must be found to manage congestion.

1.3.3 Focus 3: Composite Power System Long-term Reliability Analysis in Both Adequacy and Security

The above two focuses are related to the short-term reliability. As we know, in addition to the short-term reliability, the ISO also has the responsibility to take care of the long-term reliability. That is the ISO should evaluate the long-term reliability of the system for each planning. Furthermore, in coordination with the transmission owners and other market participants, the ISO should propose ways to improve the reliability of the system. Our work on the long-term reliability is thus focused on these two aspects, namely the evaluation and improvement of the system reliability in the long-term. To simplify the matter, we assume that power markets are mature and robust. Therefore we can focus on power systems themselves.

As we know, power system reliability analysis comprises adequacy and security. So far the majority thrust in reliability research has been on adequacy. For evaluating security component of reliability analysis, one can incorporate effects of static or dynamic security [21-23]. In analysis involving static security, researchers have studied the subject both deterministically and probabilistically [23, 24]. But in most of the work involving dynamic security, researchers tend to use deterministic methods for studies. The probabilistic nature of security involving dynamic effects is mostly neglected, which leads to somewhat conservative results [11]. Accordingly, the probabilistic analysis for dynamic security on the long-term reliability still needs to be investigated and developed.

1.3.4 Focus 4: Composite Power System Reliability Improvement

Reliable supply of power is one of the key constituents for a prospering society. However, the reliability degree has declined in the deregulated power systems. This greatly affects the continuing development of the society. Thus it is an important task to strengthen the system and improve the reliability of the system. Conventionally people would tend to build new transmission lines or new power plants. Though this can

definitely enhance the reliability, it is hard to implement this option due to various limitations such as economics, politics, environment, etc. It is imperative to find other methods to improve system reliability and make new investment cost-effective.

1.4 Objectives of the Dissertation

This dissertation is intended to develop techniques to address the above observed problems associated with the short-term and long-term reliability in the deregulated power systems. It has the following objectives.

1.4.1 Objective 1: Investigate the Formulation of the Auction-based Dispatch and Develop Efficient Algorithms for the Auction-based Dispatch

In the auction-based dispatch, in addition to generators, loads can also submit bids. As a result, some researchers propose to minimize loads' payment for the auction-based dispatch [25]. Whereas some plans still favor generators by maximizing the market saving for generators [26, 27]. On the other hand, reference [17] considers both generators and loads. Its objective is to maximize the social welfare, namely the bid difference between loads and generators. In this dissertation, we will use the law of supply and demand to analyze the formulation of the auction-based dispatch. By checking the conditions of the equilibrium, which is the intersection point of the market supply and demand curves, and the necessary conditions of the optimal solution of the formulation in [17], we conclude that the maximization of the social welfare is the most reasonable formulation for the auction-based dispatch.

If the conventional algorithm is employed to solve the auction-based dispatch problem, all the possible combinations of the states of variables, i.e., generators and loads need to be investigated. As each variable can have three states, namely on the upper limit, on the lower limit, or within bounds, the number of iterations of this kind of algorithm would be exponential in the number of variables. In addition, each iteration

has an operation count in the order of the number of variables. Clearly, the conventional algorithm would have difficulty in solving problems with a large number of variables.

To develop efficient algorithms, we first reformulate the auction-based dispatch as a general minimization problem so that both generators and loads can be handled in the same manner. Then an algorithm to solve the auction-based dispatch problem with only quadratic bidding functions is proposed. To handle cases with both quadratic and linear incremental bidding functions, a second algorithm is developed. These two algorithms can find the optimal solution to the auction-based dispatch problem efficiently with the number of iterations no greater than the number of variables. In addition, every iteration has a computation complexity in the order of the number of variables. As a result, our algorithms have a total computation complexity in the order of the square of the number of variables, which is much more efficient than the conventional algorithm.

1.4.2 Objective 2: Manage Congestion Efficiently and Reasonably by Using a New OPF Method

The OPF model is considered as probably the most effective method to manage congestion of strongly networked transmission systems. Reference [28] provides a typical formulation of this model. In this formulation all generators and loads participate in congestion management. That means the OPF model would have too many variables for big size systems, which is hard to solve.

In this research we propose a new OPF method to efficiently relieve congestion. Our method is based on the sensitivity factors combined with the technique of aggregation. According to the sensitivity factors of all generators with regard to the congested lines, we will identify effective generators that have big influence on these congested lines to relieve the congestion. Since only a limited number of generators participate, our congestion management is sure to be much faster than the method in [20]. To further reduce the number of variables and speed up the calculation, we aggregate

generators that have similar effects in terms of their sensitivity factors. Consequently our OPF method is very efficient in the meantime can provide sufficient accuracy.

1.4.3 Objective 3: Develop a Probabilistic Method to Evaluate Composite Power System Long-term Reliability with Both Adequacy and Security Included

In reliability analysis, security means not only static problems such as line overload but also dynamic problems like transient stability caused by faults. However, most of the work on reliability either ignores the dynamic aspect of security or uses deterministic methods to analyze the dynamic process. Both ways cannot exactly reflect dynamic security's effect on composite power system long-term reliability.

In this dissertation, we develop a probabilistic method to evaluate the long-term reliability in both adequacy and security. The effects of both static and dynamic security are considered. This method is based on the sequential Monte Carlo simulation approach, which can capture the stochastic properties of contingencies. More importantly, the sequential Monte Carlo simulation approach can easily describe the dynamic and static processes following a contingency. We also develop a 3-state transition model for transmission lines in order to consider the impacts of both permanent and transient faults on system reliability. Furthermore, to reflect the effects of the system dynamic process, two new reliability indices, Mean Loss of Load During Restoration *(MLLDR*) and Mean Instability Occurrence Rate (*MIOR*), are introduced for this integrated reliability evaluation. Finally the effects of both security and adequacy are compared to demonstrate that adequacy is the major issue of the long-term reliability.

1.4.4 Objective 4: Study Means That Could Be Employed to Improve Composite Power System Reliability Efficiently

Conventionally to improve composite power system reliability, people would construct a robust system, i.e., building more plants, more transmission lines, etc. This

option, however, is hard to implement considering the high cost associated with it and limits such as environment.

We propose to use Flexible AC Transmission System (FACTS) to enhance reliability. It has been well known that the FACTS can offer a variety of benefits to power systems such as enhancement of transient stability, improvement of voltage stability, and direct control over power flow [29-35]. But little work has been done to investigate their effects on reliability. Reference [36] shows TCSC, a member of FACTS, can significantly improve the reliability of a two-parallel-line system. However, it is not clear if this result is still valid for larger and more practical systems and for different operating conditions. Our research will examine the effects of TCSC as well as SVC and TCPAR on composite power system reliability. These three devices can control reactance, voltage and phase angle respectively. We first investigate the structures of these devices. Next we build their reliability models and steady state operational models. Then we incorporate these devices into OPF to reduce the load curtailment after contingencies. To find out their efficiency, we will test them under various circumstances.

1.5 Organization of the Dissertation

In this chapter we introduce our research with a review of the deregulated power systems, and the short-term and long-term reliability. Then we discuss some of the existing problems associated with the short-term and long-term reliability in the deregulated power systems, and present the proposed new methods to handle them. In Chapter II, we investigate the formulation of the auction-based dispatch and present efficient algorithms to solve the auction-based dispatch. In Chapter III, by using the sensitivity factors and the technique of aggregation we develop a new OPF method to manage congestion efficiently. In Chapter IV, a method is proposed to probabilistically assess composite power system long-term reliability with both adequacy and security included by using the sequential Monte Carlo simulation method. Then we investigate

the impacts of FACTS on composite power system reliability in Chapter V. Finally we summarize our work and offer suggests for future work in Chapter VI.

CHAPTER II

AUCTION-BASED DISPATCH IN DEREGULATED POWER SYSTEMS

2.1 Introduction

In the vertically regulated power systems, loads are fixed and the economic dispatch is used to determine generation amounts amongst various generating units. On the other hand, in the deregulated power systems, electricity is traded in markets between generators and loads. Basically there are two types of electric power markets: bilateral markets and pool markets. In a bilateral market, generators and loads enter into direct negotiations to determine the quantities and prices of electricity being traded. In a pool market, the amounts and prices of generations and loads are decided by a central auction, namely the auction-based dispatch.

Like the economic dispatch, the auction-based dispatch aims to achieve economic efficiency. However, it is more complicated than the economic dispatch in the following respects:

- Loads are not necessarily fixed.
- Both generators and loads can submit bids to the auction.
- Besides convex quadratic bidding functions, concave quadratic and linear incremental bidding functions also appear in the auction.

Obviously the formulation and algorithm of the auction-based dispatch would be different from those of the economic dispatch. This chapter is thus focused on these two issues, namely the formulation and algorithm of the auction-based dispatch.

We first review the formulation of the classic economic dispatch using the law of supply and demand. Then we extend our research to the auction-based dispatch and investigate its formulation by the law of supply and demand. Next we develop efficient algorithms to solve the auction-based dispatch with different types of bidding functions.

Specifically, the first algorithm solves the dispatch problem in which the objective function contains only quadratic bidding functions. The second algorithm deals with the situation where the objective function contains both quadratic and linear incremental bidding functions. The two algorithms presented have reduced the total computation complexity to $O(n^2)$, compared with the conventional one whose total computation complexity is $O(n \cdot 3^n)$ (where *n* is the number of variables). We finally demonstrate the efficiency of our algorithms through examples.

2.2 Investigation of the Formulation of the Auction-based Dispatch by the Law of Supply and Demand

So far there are still arguments about the formulation of the auction-based dispatch. Notice that both the auction-based dispatch and classic economic dispatch attempt to attain maximum economic efficiency. That implies they can be considered as market activities and ought to satisfy market rules. If we think of generators as sellers and loads as buyers, these two types of dispatches should obey the law of supply and demand.

In this section, we will first examine the formulation of the classic economic dispatch and see whether or not it satisfies the law of supply and demand. Then we will extend our work to the auction-based dispatch. That is we will investigate its formulation mainly from the viewpoint of the law of supply and demand.

2.2.1 Formulation of the Classic Economic Dispatch

In the operation of a vertically integrated power system, loads are supposed to be covered fully and generations are distributed among units by an economic dispatch program. The objective of the economic dispatch is to achieve a power balance between supply and demand with the least cost [37-39]. Below is the formulation of the economic dispatch.

Objective:

$$Min \quad f = \sum_{i=1}^{m} C_i(P_{gi}) \tag{2.1}$$

Subject to:

$$\sum_{i=1}^{m} P_{gi} = P_L \tag{2.2}$$

$$P_{gi\min} \le P_{gi} \le P_{gi\max} \qquad i = 1,..., m \tag{2.3}$$

where

P_{gi} : Real power generation of the ith generator.

$P_{gi\max}, P_{gi\min}$: Real power limits of the ith generator.

m : Number of generators.

P_L : Fixed load demand.

$C_i(P_{gi})$: Cost function of the ith generator.

In terms of the Kuhn-Tucker theorem [40-42], the necessary conditions for optimal problem (2.1) ~ (2.3) can be summarized as

$$\begin{cases} \dfrac{dC_i}{dP_{gi}} = \lambda \quad for \quad P_{gi\min} < P_{gi} < P_{gi\max} \\ \dfrac{dC_i}{dP_{gi}} \le \lambda \quad for \quad P_{gi} = P_{gi\max} \\ \dfrac{dC_i}{dP_{gi}} \ge \lambda \quad for \quad P_{gi} = P_{gi\min} \end{cases} \tag{2.4}$$

where λ is the Lagrange multiplier. Next we check if the economic dispatch obeys the law of supply and demand. In other words, we will examine whether or not the solution obtained by the law of supply and demand satisfies the conditions in (2.4).

Generally, the cost function of a generator is represented by a quadratic function with positive coefficients.

$$C_i(P_{gi}) = a_{gi}P_{gi}^2 + b_{gi}P_{gi} + c_{gi} \quad (\$/h) \tag{2.5}$$

where coefficients a_{gi}, b_{gi} and c_{gi} are all greater than zero.

In terms of the theory of economics, a supply curve is the marginal cost curve, namely the derivative of the cost function [43]. Therefore the supply curve of a generator is

$$p_{gi} = \frac{dC_i}{dP_{gi}} = 2a_{gi}P_{gi} + b_{gi} \quad (\$/MWh) \tag{2.6}$$

where p_{gi} represents the price or the marginal cost. Since $a_{gi} > 0$, the supply curve is linear incremental. Fig. 2.1 below shows this point.

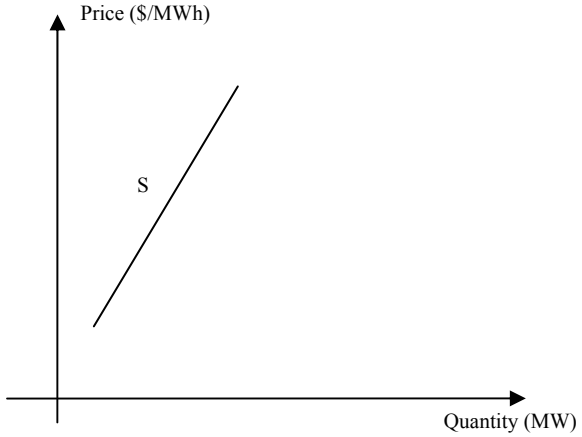

Fig. 2.1. Supply Curve of a Generator in the Classic Economic Dispatch

The economic dispatch involves many generators. Obviously the total supply in the dispatch is the summation of the supplies of all generators. We define the market supply curve as the total supply at every possible price. That means to achieve the market supply curve, we can simply add the power quantity each generator will supply at every possible price. In terms of (2.6), we know that the power a generator can supply at a price is

$$P_{gi} = \frac{p_{gi} - b_{gi}}{2a_{gi}} \tag{2.7}$$

Therefore the total quantity that all generators can supply at every price is

$$P_G = \sum_i \frac{p - b_{gi}}{2a_{gi}} = \left(\sum_i \frac{1}{2a_{gi}} \right) p - \sum_i \frac{b_{gi}}{2a_{gi}} \tag{2.8}$$

Or

$$p = \frac{1}{\sum_i \frac{1}{2a_{gi}}} P_G + \frac{\sum_i \frac{b_{gi}}{2a_{gi}}}{\sum_i \frac{1}{2a_{gi}}} \tag{2.9}$$

Equation (2.9) represents the market supply curve. Variable P_G stands for the quantity this market supplies and variable p means the market price. As all a_{gi}'s and b_{gi}'s are greater than zero, the market supply curve is a linear incremental curve. (Here we do not consider the limits of generators, which will be discussed later.) Fig. 2.2 gives an example of the market supply curve with two generators. In the figure, S_1 and S_2 are the individual supply curves of the two generators. S is the market supply curve.

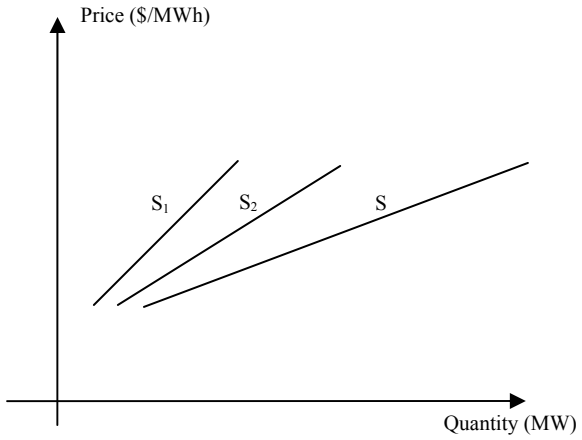

Fig.2.2. Individual Supply Curves and Market Supply Curve
in a Two-generator Economic Dispatch

In the economic dispatch, the total amount of loads is fixed. That implies the corresponding market demand curve is perfectly inelastic. (See Fig. 2.3 below.)

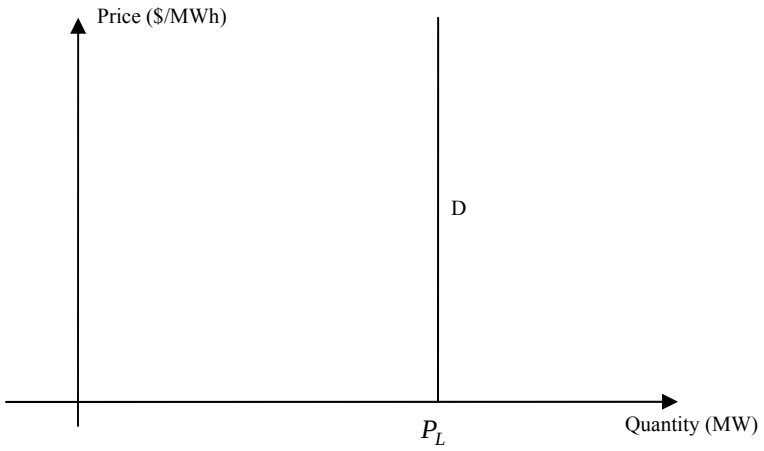

Fig. 2.3. Market Demand Curve of the Loads in the Economic Dispatch

The above figure indicates that regardless of the price, the amount of electricity demanded by the loads is always P_L.

So far we have obtained the market supply curve and market demand curve. From the perspective of economics, a market should operate at the equilibrium that is the intersection of the market supply curve and demand curve. The equilibrium is essentially the stable point of the market, which gives the information of both the price and quantity of the market. In the classic economic dispatch, the quantity is already known, namely P_L. Therefore we only need the equilibrium to determine the price.

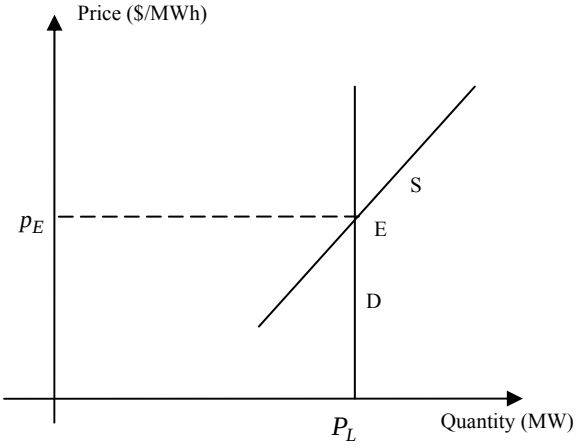

Fig. 2.4. Market Supply and Demand Curves of the Classic Economic Dispatch

In Fig. 2.4, curves S and D are the market supply and demand curves respectively. Point E is the market equilibrium. At this point, the quantity supplied by the market equals the quantity demanded by the market. That means,

$$P_G = P_L \tag{2.10}$$

Assume that all generators are within the limits when the market operates at the equilibrium. Based on the earlier discussion about the relations between individual supply curves and the market supply curve, we have

$$\sum_i P_{gi} = P_G = P_L \tag{2.11}$$

$$p_E = p_{gi} = \frac{dC_i}{dP_{gi}} \tag{2.12}$$

where p_{gi} stands for the price of the *ith* generator. And p_E is the price at the equilibrium. It can be seen that actually (2.12) is necessary condition (2.4) with all generations within the limits. And the Lagrange multiplier λ is the price p_E equivalently.

Let us consider the situation in which some generations are at the lower limits or upper limits when the market operates at equilibrium E. In the figure below, S_1 and S_2 represent the supply curves of generators 1 and 2. Curve S is the market supply curve and vertical line D is the market demand curve. The market equilibrium is point E.

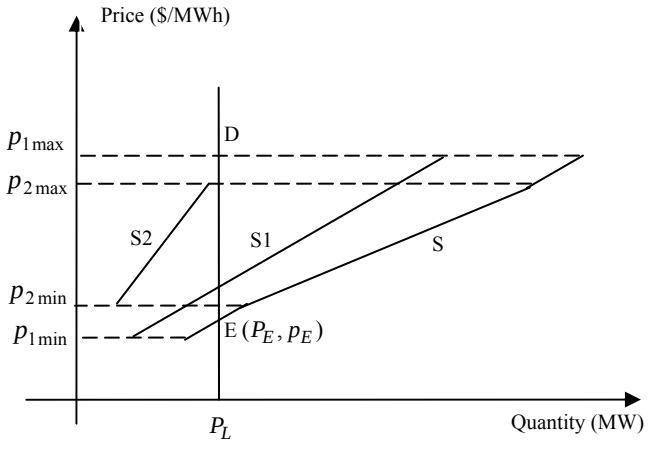

Fig. 2.5. Supply Curves with Different Price Ranges

From Fig. 2.5 it can be seen that the price range of supply curve S_1, [$p_{1\min}$, $p_{1\max}$] is bigger than that of S_2, [$p_{2\min}$, $p_{2\max}$]. That implies for the price range [$p_{1\min}$, $p_{2\min}$], generator 2 has to operate at the lower limit whereas for the price range [$p_{2\max}$, $p_{1\max}$], generator 2 has to operate at the upper limit. Therefore the market supply curve, which is the summation of the quantities supplied by the two generators, is expressed as follows:

$$p = \begin{cases} 2a_{g1}\left(P_G - P_{g2\min}\right) + b_{g1} & p_{1\min} \le p < p_{2\min} \\ \left(\dfrac{1}{2a_{g1}} + \dfrac{1}{2a_{g2}}\right)^{-1}\left(P_G + \left(\dfrac{b_{g1}}{2a_{g1}} + \dfrac{b_{g2}}{2a_{g2}}\right)\right) & p_{2\min} \le p < p_{2\max} \\ 2a_{g1}\left(P_G - P_{g2\max}\right) + b_{g1} & p_{2\max} \le p \le p_{1\max} \end{cases} \tag{2.13}$$

where $P_{g2\min}$ and $P_{g2\max}$ are the lower and upper output limits of generator 2. Equation (2.13) shows that the market supply curve is a collection of line segments instead of a straight line when the two generators' supply curves have different price ranges.

The equilibrium price p_E locates in the price range of supply curve S_1, i.e., $p_{1\min} < p_E < p_{1\max}$. Based on the relationship between individual supply curves and the market supply curve, we can derive

$$p = p_1 = \frac{dC_1}{dP_{g1}} \tag{2.14}$$

On the other hand,

$$p < p_{2\min} \tag{2.15}$$

And we know that generator 2 operates at its lower limit. That means,

$$p_{2\min} = \frac{dC_2}{dP_{g2}} \tag{2.16}$$

Combining (2.15) and (2.16), we conclude

$$p_E < \frac{dC_2}{dP_{g2}} \tag{2.17}$$

By thinking of market price p_E as Lagrange multiplier λ, we can see that (2.14) and (2.17) exactly match necessary condition (2.4) with generations within the limits and at the lower limits. For generators hitting upper limits situation, we can similarly prove that necessary condition (2.4) observes the law of supply and demand.

In summary, the above analysis reveals that the formulation of the classic economic dispatch exactly follows the law of supply and demand. Further, Lagrange multiplier λ can be used as the clearing price of the market.

2.2.2 Formulation of the Auction-based Dispatch

Like the classic economic dispatch, the auction-based dispatch is to dispatch generations to meet the needs of loads. However, instead of fixed values, loads will purchase electricity according to the price. When the price is high, loads will tend to buy less electricity. When the price is low, they will tend to buy more. In other words, loads are variables in the auction-based dispatch. Due to the fact that both the generators and loads are variables, people are arguing about the formulation of the auction-based dispatch. References [26] and [27] propose to maximize the market saving from the angle of generators whereas [28] minimizes consumers' payment. On the other hand, in [17] the objective is to maximize the social welfare, which is the bid difference between the loads and generators.

As discussed earlier, the auction-based dispatch should satisfy the law of supply and demand. Therefore to justify the formulation of this dispatch, we will resort to the supply and demand analysis.

We assume that the competition in power markets is perfect. In an auction-based dispatch, each generator submits its own bidding function. For a perfectly competitive electricity market, the bidding function of a generator is the same as the cost function. Therefore our earlier discussions about the supply curve in the classic economic dispatch can be applied here. For example, the supply curve of a generator in the auction-based dispatch is linear incremental. The market supply curve is simply a straight line if all individual supply curves have the same price ranges.

Unlike the classic economic dispatch that has fixed demand, the auction-based dispatch has variable loads. And each load has its own bidding function. Like the bidding function of a generator, usually a load's bidding function is represented by a quadratic function. Thus the demand curve, the derivative of the load's bidding function, is a linear function. In terms of the law of demand, we know that the power quantity demanded is inversely related to its price. In other words, the slope of the demand curve is negative as shown in Fig. 2.6.

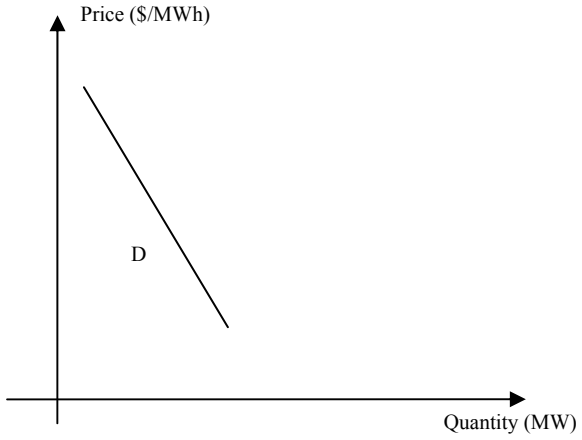

Fig. 2.6. Demand Curve of a Load in the Auction-based Dispatch

According to the above figure, the demand curve of a load, say load *i* can be expressed as

$$p_{li} = 2a_{li}P_{li} + b_{li} \quad (\$/MWh) \tag{2.18}$$

where p_{li} represents the price and P_{li} stands for the power quantity demanded. Coefficient a_{li} is less than zero. According to (2.18), we can obtain the bidding function as follows.

$$D_i(P_{li}) = a_{li}P_{li}^2 + b_{li}P_{li} + c_{li} \quad (\$/h) \tag{2.19}$$

We can see the bidding function of a load is a concave function, which is different than the bidding function of a generator that is convex.

The market demand curve is the summation of individual demand curves. That means to create the market demand curve, we can simply add the quantities demanded by all loads at every possible price. In Fig. 2.7 below, curves D_1 and D_2 are the demand curves of two individual loads. Curve D is the market demand curve, which is created by adding D_1 and D_2 horizontally.

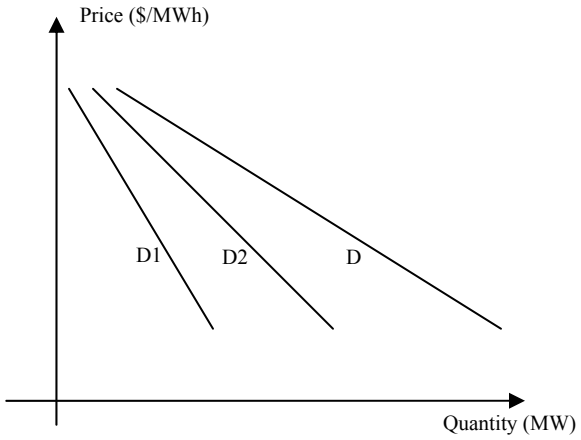

Fig. 2.7. Individual Demand Curves and Market Demand Curve in an Auction-based Dispatch

Similar to the process we derived the equation for the market supply curve in the classic economic dispatch, we can obtain the equation for the market demand curve as follows.

$$p = \frac{1}{\sum_i \frac{1}{2a_{li}}} P_L + \frac{\sum_i \frac{b_{li}}{2a_{li}}}{\sum_i \frac{1}{2a_{li}}} \tag{2.20}$$

This equation assumes that all loads' demand curves have the same price range. If the price ranges of the individual demand curves are different, then the market demand curve will become a collection of line segments instead of a simple straight line. In a word, the market demand curve is handled in the same way as the market supply curve.

As discussed previously, a market operates at the equilibrium where the market supply curve and market demand curve intersect. The equilibrium determines the price and quantity of the market. Since both the generators and loads are variables, normally we cannot know the market price or market quantity before we obtain the equilibrium. This is different from the classic economic dispatch which already has the demand set before the dispatch.

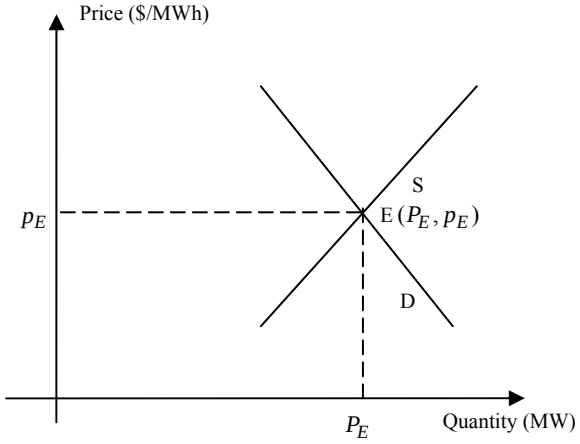

Fig. 2.8. An Auction-based Dispatch with the Market Supply and Demand Curves

Fig. 2.8 shows an auction-based dispatch with market supply curve S and market demand curve D intersecting at point E. The market quantity and price are P_E and p_E respectively. According to the relations between the individual curves and market curve, we can derive the following equations.

$$\sum_i P_{gi} = P_E = \sum_j P_{lj} \tag{2.21}$$

And

$$p_E = p_{gi} = \frac{dC_i}{dP_{gi}} \tag{2.22}$$

$$p_E = p_{lj} = \frac{dD_j}{dP_{lj}} \tag{2.23}$$

where p_{gi}, P_{gi} are the price and quantity of generator i. And p_{lj}, P_{lj} are the price and quantity of load j. We point out that in the above equations it is assumed that all generators and loads are within the limits.

Equations (2.21)-(2.23), which are obtained from the law of supply and demand, involve both the generators and loads. This implies that the formulation of the auction-based dispatch should take into account both the generators and loads. References [26, 27] consider only the generators or the loads. On the other hand, reference [17] considers both the generators and loads in the objective function. Thus its formulation seems more reasonable. Below we will verify this. That means we will check the optimal conditions of this formulation and see if these conditions match the conclusions obtained from the supply and demand analysis.

The formulation of the auction-based dispatch in [17] is as follows.

Objective:

$$Max \quad f = \left(\sum_{j=1}^{k} D_j(P_{lj}) - \sum_{i=1}^{m} C_i(P_{gi}) \right) \tag{2.24}$$

Subject to:

$$\sum_{i=1}^{m} P_{gi} - \sum_{j=1}^{k} P_{lj} = 0 \tag{2.25}$$

$$P_{gi\min} \le P_{gi} \le P_{gi\max} \qquad i = 1,..., m \tag{2.26}$$

$$P_{lj\min} \le P_{lj} \le P_{lj\max} \qquad j = 1,..., k \tag{2.27}$$

where

P_{lj} : Real power amount of jth load.

$P_{lj\max}, P_{lj\min}$: Maximum and minimum requirements of jth load.

P_{gi} : Real power amount of ith generator.

$P_{gi\max}, P_{gi\min}$: Real power limits of ith generator.

k : Number of loads.

m : Number of generators.

$D_j(P_{lj})$: Bidding function of jth load with a form of $a_{lj}P_{lj}^2 + b_{lj}P_{lj} + c_{lj}$.

$C_i(P_{gi})$: Bidding function of ith generator with a form of $a_{gi}P_{gi}^2 + b_{gi}P_{gi} + c_{gi}$.

Equation (2.24) shows that the purpose of this formulation is to maximize the bidding function difference between the loads and generations. This difference is defined as the social welfare [44].

Employing the Kuhn-Tucker theorem, we can achieve the necessary conditions for auction-based dispatch problem (2.24) ~ (2.27) as follows

$$\begin{cases} \dfrac{dC_i}{dP_{gi}} = \lambda & for \quad P_{gi\min} < P_{gi} < P_{gi\max} \\ \dfrac{dC_i}{dP_{gi}} \le \lambda & for \quad P_{gi} = P_{gi\max} \\ \dfrac{dC_i}{dP_{gi}} \ge \lambda & for \quad P_{gi} = P_{gi\min} \end{cases} \tag{2.28}$$

$$\begin{cases} \dfrac{dD_j}{dP_{lj}} = \lambda & for \quad P_{lj\min} < P_{lj} < P_{lj\max} \\ \dfrac{dD_j}{dP_{lj}} \le \lambda & for \quad P_{lj} = P_{lj\min} \\ \dfrac{dD_j}{dP_{lj}} \ge \lambda & for \quad P_{lj} = P_{lj\max} \end{cases} \tag{2.29}$$

where λ is the Lagrange multiplier. If we think of the equilibrium price p_E as the Lagrange multiplier λ, then the conclusions by the analysis of supply and demand, i.e., (2.22) and (2.23), are exactly the necessary conditions in (2.28) and (2.29) for the no limit violation case. Earlier we have proved that when some generators are at the limits, the conclusions by the analysis of supply and demand are still the same as the necessary condition of the classic economic dispatch. Similarly, if the limits of the generators and loads are included in the auction-based dispatch, we can follow the same idea to prove that the conclusions by the law of supply and demand still match the necessary conditions in (2.28) and (2.29).

The exact match between the conclusions by the law of supply and demand, and the necessary conditions of formulation (2.24) - (2.27) verifies the reasonability of using the social welfare as the objective of the auction-based dispatch.

According to the above analysis, we find that Lagrange multiplier λ can be used as the clearing price. As a matter of fact, some power markets around the world such as CalPX forward energy markets and Norwegian energy markets are adopting this pricing mechanism [17], which is called the uniform price rule [45].

Finally we take a look at two extremities of load demand curves. Earlier we used a straight line with a negative slope to represent a demand curve. In deregulated power systems, a load can also have a demand curve with the slope being zero as shown in Fig. 2.9.

Fig. 2.9. A Load with a Zero Slope Demand Curve

Fig. 2.9 implies that the load is willing to purchase power up to a specified price p. For such a demand curve, the corresponding bidding curve is a linear incremental function not a quadratic function.

$$D_i(P_{li}) = b_{li}P_{li} + c_{li} \quad (\$/h) \tag{2.30}$$

where $b_{li} > 0$.

The other extremity of loads is that a load has a fixed demand regardless of the price. Loads in the classic economic dispatch belong to this type. And the slope of the demand curve in this situation can be considered as negative infinity (See Fig. 2. 3). The corresponding bidding function is

$$D_i(P_{li}) = a_{li}P_{li}^2 + b_{li}P_{li} + c_{li} \quad (\$/h) \tag{2.31}$$

where $a_{li} = -\infty$.

By observing the bidding functions in (2.30) and (2.31), we find that in fact (2.19) can be used a general bidding function for all kinds of loads. Coefficient a_{li} in (2.19) is zero or negative infinity for the two extremities respectively. For other cases, a_{li} is between zero and negative infinity. Since loads in the classic economic dispatch can be represented by the bidding functions in the auction-based dispatch, we can claim that the classic economic dispatch is a special case of the auction-based dispatch.

2.3 Reformulation of the Auction-based Dispatch

Based on the discussions in section 2.2, we know that (2.24)–(2.27) are a good formulation for the auction-based dispatch. In terms of this formulation, we can see that the auction-based dispatch is more complicated than the classic economic dispatch in the following respects:

- Loads no longer need to be covered completely.
- Since loads are now variables, the total amount of generations becomes uncertain.
- The objective function is not a simple summation of the cost functions of the generators. It becomes the difference in bidding functions between the loads and generators. In addition to quadratic bidding curves, linear incremental bidding curves are also involved in the objective function.

The conventional algorithm for solving such a dispatch problem given by (2.24)-(2.27) would be to examine all the possible state combinations. Each combination could give a solution having a computation complexity in the order of *n*, where *n* is the total number of the generators and loads. If the solution satisfies the optimality conditions derived from the Kuhn-Tucker conditions, then it is the optimal solution to the dispatch problem. Since each generator or load can have three states, i.e., on the upper limit, on

the lower limit, or within bounds, the number of possible combinations could be 3^n. Thus, the conventional algorithm has a total computation complexity $O(n \cdot 3^n)$. For systems with a large number of generators and loads this complexity can become expensive computationally. In the following, we present efficient algorithms that can solve the auction-based dispatch within *n* iterations and each iteration only has a computation complexity in the order of *n*.

2.3.1 Reformulation of the Problem

In terms of the properties of the bidding functions of generators and loads, we modify the formulation so that the auction-based dispatch can be solved efficiently.

First, we modify objective function (2.24) into:

$$\begin{aligned} Min \quad F &= -f = \sum_{i=1}^{m} C_i(P_{gi}) - \sum_{j=1}^{k} D_j(P_{lj}) \\ &= \sum_{i=1}^{m} C_i(P_{gi}) + \sum_{j=1}^{k} \left(- D_j(P_{lj})\right) \end{aligned} \tag{2.32}$$

Then let $P_{lj}^{New} = -P_{lj}$.

With these two changes, we can reformulate the auction-based dispatch problem as a general minimum optimal problem:

Objective:

$$Min \quad F = \sum_{i=1}^{n} B_i(x_i) = \sum_{i=1}^{n} (a_i x_i^2 + b_i x_i + c_i) \tag{2.33}$$

Subject to:

$$\sum_{i=1}^{n} x_i = 0 \tag{2.34}$$

$$x_{i\min} \le x_i \le x_{i\max} \qquad i = 1,\ldots,n \tag{2.35}$$

where

x_i refers to P_{gi} or P_{lj}^{New}.

B_i represents the bidding function of P_{gi} or P_{lj}^{New}.

n is the number of x_i and is equal to $(m+k)$, the total number of the generators and loads.

After the reformulation, B_i, a term of the objective function, is a convex quadratic function with $a_i > 0$ or a linear incremental function with $a_i = 0$. $x_i \ge 0$ if this variable represents a generator whereas $x_i \le 0$ if it corresponds to a load.

Many methods such as the Interior Point (IP) Method and the Gradient Method [46, 47] can solve the above optimal problem (2.33) – (2.35). Among these methods, the IP method is considered as an efficient tool to solve both linear and nonlinear optimal programming [47]. Thus we use the IP method as an example to discuss the solution and computation complexity of (2.33) – (2.35).

First inequality constraint (2.35) is converted into equality constraints by adding slack variables. Then objective function (2.33) is augmented by a penalty function [48]. Therefore formulation (2.33) – (2.35) is transformed into the formulation below:
Objective:

$$Min \quad F - \mu\left(\sum_{i=1}^{n} \ln s_{hi} + \sum_{i=1}^{n} \ln s_{li}\right) \tag{2.36}$$

Subject to:

$$\sum_{i=1}^{n} x_i = 0 \tag{2.37}$$

$$x_i - x_{i\max} + s_{hi} = 0 \tag{2.38}$$

$$-x_i + x_{i\min} + s_{li} = 0 \tag{2.39}$$

In (2.36), μ is a very small positive number. Slack variables s_{hi}, s_{li} are greater than zero. From the above formulation, we can see that the logarithmic penalty function in the objective function can limit variables x_i within their boundaries. In the meantime the very small positive number μ can ensure the optimal solution of (2.36) – (2.39) is the same as that of (2.33) – (2.35).

Compared with formulation (2.33) – (2.35), formulation (2.36) – (2.39) does not contain any inequality constraints. Thus we can construct a Lagrange function for (2.36) – (2.39).

$$\begin{aligned} L = F - \mu\left(\sum_{i=1}^{n} \ln s_{hi} + \sum_{i=1}^{n} \ln s_{li}\right) - \lambda\left(\sum_{i=1}^{n} x_i\right) - \\ \sum_{i=1}^{n} \rho_{hi}\left(x_i - x_{i\max} + s_{ki}\right) - \sum_{i=1}^{n} \rho_{li}\left(-x_i + x_{i\max} + s_{li}\right) \end{aligned} \tag{2.40}$$

where $\lambda, \rho_{hi}, \rho_{li}$ are Lagrange multipliers. The necessary conditions of (2.36) – (2.39) are that the partial derivatives of Lagrange function L with respect to x_i, s_{hi}, s_{li} and $\lambda, \rho_{hi}, \rho_{li}$ are zero. By solving these necessary conditions, we can then obtain the optimal solution x_i for (2.36) – (2.39). This solution is also the optimal solution for (2.33) – (2.35).

In 1984, Karmarkar proposed a well-known polynomial-time IP algorithm which solves linear programming with at most $O(n)$ iterations and a total of $O(n^{3.5})$ computation complexity, where n is the number of variables [49]. Since then, many developments have been achieved on IP algorithms for both linear and nonlinear

programming. Reference [50] develops a primal-dual path-following IP algorithm that can solve convex quadratic programming with a total complexity of $O(n^3)$ arithmetic operations in at most $O(\sqrt{n})$ iterations. By employing this algorithm, our problem (2.33) – (2.35) can be solved with a total of $O(n^3)$ computation complexity.

We point out that the current optimal programming methods like the IP method are aimed at solving general problems. On the other hand, in optimal problem (2.33) – (2.35), the equality constraint is that the summation of all variables is equal to zero. Thus by utilizing this special feature, we develop our own efficient algorithms to solve (2.33) – (2.35) with a total computation complexity only in $O(n^2)$. The details are provided below.

2.3.2 Optimality Conditions

We write the necessary conditions for optimal problem (2.33)-(2.35) in the following way according to the Kuhn-Tucker conditions [40-42]:

$$\begin{cases} \dfrac{dB_i}{dx_i} = \lambda & for \quad x_{i\min} < x_i < x_{i\max} \\ \dfrac{dB_i}{dx_i} \le \lambda & for \quad x_i = x_{i\max} \\ \dfrac{dB_i}{dx_i} \ge \lambda & for \quad x_i = x_{i\min} \end{cases} \tag{2.41}$$

where λ is the Lagrange multiplier.

The above conditions along with equality constraint (2.34) comprise the sufficient conditions because the objective function is convex and the constraints are linear.

2.4 Solution to the Auction-based Dispatch with Quadratic Bidding Functions

This section is solving auction-based dispatch problem (2.24)-(2.27) by assuming that all bidding data are quadratic functions. Specifically, auction problem (2.24)-(2.27) is first reformulated into optimization problem (2.33)-(2.35). Then an algorithm to solve (2.33)-(2.35) is implemented. Finally the solution is converted back into the amounts of generations and loads. Below are the details of the algorithm.

2.4.1 Algorithm

1. Initialize $M = \varnothing$ and $t = 0$.
2. Compute λ and all variables $x_i (i \notin M)$ according to (2.42) and (2.43).

$$\lambda = \frac{t + \sum_{i=1}^{nk} \frac{b_i}{2a_i}}{\sum_{i=1}^{nk} \frac{1}{2a_i}} \tag{2.42}$$

$$x_i = \frac{\lambda - b_i}{2a_i} \quad i = 1,...,nk \tag{2.43}$$

(where $a_i > 0 (i = 1,...,nk)$ and nk is the number of variables $x_i (i \notin M)$.)

3. If all $x_i (i \notin M)$ are within the limits, go to step 6. Otherwise, let $UP = \sum_i \left(x_i - x_{i\max} \right)$ for all $x_i (i \notin M)$ that are above the upper limits and $DN = \sum_i \left(x_{i\min} - x_i \right)$ for all $x_i (i \notin M)$ that are below the lower limits.
4.

- If *UP=DN*, fix variables that are beyond the limits at their corresponding upper or lower limits. And other variables remain unchanged. Then go to step 6.

- Else if $UP<DN$, fix variables below the lower limits at the violated lower limits. Then let $L = \{i | x_i = x_{i\min}, i \notin M\}$ and $M=M\cup L$.
- Else fix variables above the upper limits at the violated upper limits. Then let $U = \{i | x_i = x_{i\max}, i \notin M\}$ and $M=M\cup U$.

5. $t = -\sum_{i\in M} x_i$. Go back to step 2.
6. Print the results and stop.

Equations (2.42) and (2.43) are obtained by using conditions (2.36) on the assumption that all variables $x_i (i \notin M)$ are within the limits. If not all $x_i (i \notin M)$ are within their limits, we will make an adjustment by comparing the total excessive amount of violated upper limits (i.e., *UP*) and the total excessive amount of violated lower limits (i.e., *DN*); and when $UP>DN$, we fix the upper limit violations at their upper limits; otherwise, fix the lower limit violations at their lower limits. Thus, before a solution is obtained, we fix at least one more variable to the upper or lower limit in the iteration. In addition, the fixed variables will remain unchanged in future iterations. As there are only *n* variables, we can obtain a solution with at most *n* iterations. Moreover, it can be proved that the solution satisfies the optimality conditions and thus the solution is optimal. (The detailed proof is given next.) Simple algebraic calculations are used to obtain λ, x_i, etc. for each iteration. The operation count for such calculations is in the order of *n*. Accordingly, this algorithm has a total computation complexity $O(n^2)$. If we use methods such as the IP method to solve optimal problem (2.33) – (2.35), the computation complexity for the auction-based dispatch is $O(n^3)$. If we directly examine all the possible state combinations of generators and loads by the conventional method, i.e., we do not reformulate the auction-based dispatch into (2.33) – (2.35), the computation complexity is $O(n\cdot 3^n)$. These comparisons clearly show the advantage of our reformulation and the efficiency of our algorithm.

2.4.2 Proof

In this section, we give a detailed proof of the algorithm that solves an optimization problem given by (2.33)-(2.35) with all $a_i \neq 0$.

Before a solution is found, during each iteration the algorithm will fix either the upper limit violations or the lower limit violations by comparing *UP* and *DN*. Obviously, if fixed variables satisfy sufficient conditions (2.41) in all the following iterations, the final solution is optimal.

Here, note that even though the proof below involves only one limit direction such as the lower limit, the conclusions can also apply to the other limit direction due to the symmetric property of lower and upper.

Suppose that an iteration fixes the lower limit violations, i.e., setting those variables below the lower limits at the lower limits. Clearly, the sum of other unfixed variables will have to decrease in the next iteration so that the summation of all variables can remain the same. This indicates that at least one unfixed variable will decrease. For unfixed variables,

$$\frac{dB_i}{dx_i} = 2a_i x_i + b_i = \lambda \tag{2.44}$$

Since $a_i > 0$ for all variables, (2.44) combined with the statement that at least one unfixed variable will decline imply that the Lagrange multiplier λ and all the other unfixed variables will become smaller in the next iteration. In short, $\lambda_{new} < \lambda_{old}$. Note that before fixing the lower limit violations, those variables violating the lower limits have $\frac{dB_i}{dx_i} = \lambda_{old}$. Thus after fixing the lower limit violations, they will have $\frac{dB_i}{dx_i} > \lambda_{new}$. In other words, the fixed variables automatically satisfy sufficient conditions (2.41) in the new iteration. Further, if the following iterations only involve fixing the lower limit violations, then these fixed variables will still satisfy the sufficient conditions because

the Lagrange multiplier keeps decreasing. The problem is that fixing the upper limit violations might be needed in the coming iterations, implying that the Lagrange multiplier could be increasing and possibly violating the sufficient conditions. Below we will show that this possibility will never happen.

Assume in the first iteration $UP_1 < DN_1$. (Note: the subscript indicates the iteration No.) Then we need to fix the lower limit violations. Suppose we keep doing this until iteration *h*, in which $UP_h > DN_h$ and upper limit violations should be fixed. To make it general, we further assume that the process of fixing the upper limit violations does not stop until iteration l. Based on the discussion above, we know that

$$\lambda_1 > \lambda_2 > ... > \lambda_{h-1} > \lambda_h \tag{2.45}$$

And

$$\lambda_h < \lambda_{h+1} < ... < \lambda_{l-1} < \lambda_l \tag{2.46}$$

Concerning variables fixed at the lower limits, we have

$$\frac{dB_i}{dx_i} \geq \lambda_{(h-1)} \tag{2.47}$$

In order to prove that these variables satisfy the sufficient conditions in iterations (*h*+1) to l, we only need to show $\lambda_l < \lambda_{(h-1)}$. To do this, it involves calculations in both iterations (*h*-1) and l.

In step 2 of iteration (h-1), we have

$$\sum_{i \in A_{(h-1)}} x_i + \sum_{i \in B_{(h-1)}} x_i + \sum_{i \in C_{(h-1)}} x_i = t_{(h-1)} \tag{2.48}$$

where $A_{(h-1)}$ consists of unfixed variables that violate or are at the upper limits in iteration (h-1). $B_{(h-1)}$ consists of unfixed variables that are within the limits. And $C_{(h-1)}$ only contains unfixed variables which violate or are at the lower limits. This iteration has $UP_{(h-1)} < DN_{(h-1)}$, which implies

$$\sum_{i \in A_{(h-1)}} (x_i - x_{i\max}) < \sum_{i \in C_{(h-1)}} (x_{i\min} - x_i) \tag{2.49}$$

and

$$\sum_{i \in A_{(h-1)}} x_i + \sum_{i \in C_{(h-1)}} x_i < \sum_{i \in A_{(h-1)}} x_{i\max} + \sum_{i \in C_{(h-1)}} x_{i\min} \tag{2.50}$$

In short, we get an inequality as follows:

$$\sum_{i \in A_{(h-1)}} x_i + \sum_{i \in B_{(h-1)}} x_i + \sum_{i \in C_{(h-1)}} x_i < \sum_{i \in A_{(h-1)}} x_{i\max} + \sum_{i \in B_{(h-1)}} x_i + \sum_{i \in C_{(h-1)}} x_{i\min} \tag{2.51}$$

The variables in set $C_{(h-1)}$ will be fixed at the lower limits and added to set $M_{(h-1)}$ to form M_h. In iterations $h,...,(l-1)$, we fix the upper limit violations. Thus some variables in sets $A_{(h-1)}$ and $B_{(h-1)}$ will be fixed at the upper limits and set M will be updated correspondingly.

Now let us look at iteration l. Step 2 of this iteration gives

$$\sum_{i \in A_l} x_i + \sum_{i \in B_l} x_i + \sum_{i \in C_l} x_i = t_l \tag{2.52}$$

where sets A_l, B_l and C_l have the same definition as $A_{(h-1)}$, $B_{(h-1)}$ and $C_{(h-1)}$ except that the index is referred to iteration l, not $(h-1)$. In terms of the definitions of t and M,

$$t_l = -\sum_{i \in M_l} x_i = t_{(h-1)} + \left(- \sum_{i \in M_l, i \notin M_{(h-1)}} x_i \right) \tag{2.53}$$

We define L_f as the set that consists of variables that are newly fixed at either the upper or lower limits in iterations $(h-1)$ through $(l-1)$. Thus (2.53) can be written into the equation below,

$$t_l = t_{(h-1)} - \sum_{i \in L_f} x_i \tag{2.54}$$

We further define set L_u such that $L_u = \left(A_l \cup B_l \cup C_l \right)$. Therefore (2.52) can be written in the following form:

$$\sum_{i \in L_u} x_i^l + \sum_{i \in L_f} x_i^l = t_{(h-1)} \tag{2.55}$$

Here we use x_i^l to indicate that this variable takes the value associated with iteration l.

Based on the earlier analysis, we know that $\left(A_{(h-1)} \cup B_{(h-1)} \cup C_{(h-1)} \right) = (L_u \cup L_f)$. We therefore can also rewrite (2.51) in terms of sets L_u and L_f:

$$\sum_{i \in L_u} x_i^L + \sum_{i \in L_f} x_i^L < \sum_{i \in L_u} x_i^R + \sum_{i \in L_f} x_i^R \tag{2.56}$$

where x_i^L or x_i^R means that the variable is in iteration $(h-1)$ on the left or right side of (2.51) respectively.

Suppose $\lambda_l \geq \lambda_{(h-1)}$. Then based on (2.43) and tracking the terms in sets L_u and L_f of (2.55) and (2.56), we can easily show

$$\sum_{i \in L_u} x_i^l + \sum_{i \in L_f} x_i^l \geq \sum_{i \in L_u} x_i^R + \sum_{i \in L_f} x_i^R \tag{2.57}$$

Note that essentially (2.56) is (2.50). According to (2.57), (2.56), and (2.48), we have

$$\sum_{i \in L_u} x_i^l + \sum_{i \in L_f} x_i^l > t_{(h-1)} \tag{2.58}$$

This violates (2.55). Thus it concludes that $\lambda_l < \lambda_{(h-1)}$, and proves our theorem.

2.4.3 Classic Economic Dispatch as a Special Case of Our Algorithm

Our algorithm can also be effectively applied to the classic economic dispatch problem since it is a special case of the auction-based dispatch, in which loads are known. Accordingly, variable *t* has an initial value that is equal to the summation of all loads. Reference [46] presents an efficient algorithm to solve the classic economic dispatch. Our algorithm here further improves the one developed in [46] as follows:

- The algorithm in [46] consists of 3 separate sub-algorithms to handle the situations related to upper limit violations only, lower limit violations only, and both upper and lower limit violations. We only use one simple algorithm to deal with all three situations.
- Essentially, both algorithms resolve the situations similarly with only lower or upper limit violations. For the situation with both upper and lower limit violations, the algorithm in [46] compares the total excessive amount of violated lower limits and the total excessive amount of violated upper limits only in the first iteration, then decides which type of limits should be fixed first. This algorithm will keep

fixing that type of limits until all violated limits of that type are fixed. Then it will turn to fixing the limits of the other type if the optimal solution is still not yet found. On the other hand, our algorithm fixes the limits by comparing the total excessive amount of violated lower limits and the total excessive amount of violated upper limits during all iterations.

The advantages of our algorithm over the one in [46] are:

- Our algorithm and thus programming is much more concise.
- The brute force method that may encounter in [46] will never occur in our algorithm.

Later on, we will use a simple case study to show the differences between the two algorithms and the advantages of our algorithm.

2.5 Solution to the Auction-based Dispatch with Both Quadratic and Linear Incremental Bidding Functions

Besides quadratic bidding curves, loads can have linear incremental bidding curves with $D_j(P_{lj}) = a_{lj}P_{lj}^2 + b_{lj}P_{lj} + c_{lj}$ ($a_{lj} = 0$, $b_{lj} > 0$). Here we assume that these b_{lj} are different. (If some b_{lj} are identical, we can combine the corresponding variables together.) To solve such a dispatch problem, we still rearrange it into optimization problem (2.33)-(2.35). Since some a_i in objective function (2.33) could be zero, we cannot simply employ the algorithm presented in the previous section because (2.43) may have zero denominators. We develop another algorithm in the following to bypass the difficulty.

2.5.1 Algorithm

By conditions (2.41), we know that among variables with a_i being zero, there is at most one variable within the limits; and others either at the upper or lower limits.

We define *Z* as the set whose variables have the property of $a_i = 0$ and set *Y* as the remaining variables with $a_i \neq 0$. Hence we can solve λ in (2.42) by the following equation:

$$\lambda = \lim_{a\to 0}\left(\frac{t+\sum_{i\in Y}\frac{b_i}{2a_i}+\sum_{i\in Z}\frac{b_i}{2a}}{\sum_{i\in Y}\frac{1}{2a_i}+\sum_{i\in Z}\frac{1}{2a}}\right) = \lim_{a\to 0}\left(\frac{2a\left(t+\sum_{i\in Y}\frac{b_i}{2a_i}\right)+\sum_{i\in Z}b_i}{a\sum_{i\in Y}\frac{1}{a_i}+z}\right) = \frac{\sum_{i\in Z}b_i}{z} \quad (2.59)$$

In the above equation, *z* refers to the number of variables in set *Z*. Likewise *y* is the number of variables in set *Y*.

Based on the above information, we develop an algorithm for optimization problem (2.33)-(2.35) in which some a_i are zero.

1. Initialize $M = \varnothing$ and $t = 0$.
2. Obtain λ according to (2.59) for all variables in sets *Z* and *Y*.
3. For the variables in *Z*, if $\lambda > b_i$, set the corresponding x_i to $x_{i\max}$; if $\lambda < b_i$, set the corresponding x_i to $x_{i\min}$.
4. For the variables in *Y*, calculate x_i using the following equation

$$x_i = \frac{\lambda - b_i}{2a_i} \quad (i \in Y) \quad (2.60)$$

If $x_i > x_{i\max}$, set the corresponding x_i to $x_{i\max}$; If $x_i < x_{i\min}$, set the corresponding x_i to $x_{i\min}$; Otherwise, x_i retains the same value, i.e., still within the limits.

5.

- If $\lambda \neq b_i$ for all $i \in Z$, let $S = \sum_{i\in Z} x_i + \sum_{i\in Y} x_i$.
  - If *S*=*t*, go to step 8.

- Else if $S>t$, let $L = \{i | \lambda - b_i < 0, i \in Z\}$ and $Z=Z-L$. Set the variables in L to the lower limits and let $M=M \cup L$.
- Else $S<t$, let $U = \{i | \lambda - b_i > 0, i \in Z\}$ and $Z=Z-U$. Set the variables in U to the upper limits and let $M=M \cup U$.

■ Else $\lambda = b_k$ (for a $k \in Z$), let $S = \sum_{i \in Z, i \neq k} x_i + \sum_{i \in Y} x_i$

- If $S + x_{k\min} \leq t \leq S + x_{k\max}$, let $x_k = t - S$. Go to step 8.
- Else if $S + x_{k\min} > t$, let $L = \{i | \lambda - b_i \leq 0, i \in Z\}$ and $Z=Z-L$. Set the variables in L to the lower limits and let $M=M \cup L$.
- Else $S + x_{k\max} < t$, let $U = \{i | \lambda - b_i \geq 0, i \in Z\}$ and $Z=Z-U$. Set the variables in U to the upper limits and let $M=M \cup U$.

6. $t = -\sum_{i \in M} x_i$.
7. If $Z \neq \varnothing$, go back to step 2. Otherwise, employ the algorithm developed in section 2.4 to obtain the solution for variables in set Y.
8. Print the results and stop.

2.5.2 Proof

As shown, in each iteration, we decide the values of variables in sets Z and Y using conditions (2.41) by assuming the current λ is $\lambda_{optimal}$, the one associated with the optimal solution.

Note that set Z is changing during the iterations. Here we use z_0 to represent the initial number of variables in Z. Suppose initially $b_1 < b_2 < \cdots < b_{z_0}$ for set Z. Evidently $\lambda_{optimal}$ can only be one of the 3 possibilities, i.e., $\lambda_{optimal} > b_{z_0}$, $b_{z_0} \geq \lambda_{optimal} \geq b_1$, or $\lambda_{optimal} < b_1$.

We first obtain λ by (2.59). Obviously, $b_{z_0} \geq \lambda \geq b_1$. Assume $\lambda \neq b_i$ for all $i \in Z$. (If $\lambda = b_k$ (for a $k \in Z$), we can handle it in a similar way.) In step 5, if $S=t$, this means equality constraint (2.34) is satisfied. In addition, all variables satisfy sufficient conditions (2.41). Thus the solution is optimal. If $S>t$, λ of this iteration must be bigger than $\lambda_{optimal}$. Suppose $\lambda < \lambda_{optimal}$, then based on (2.41), we can easily deduce that the sum of all variables associated with $\lambda_{optimal}$ would be greater than zero, which violates (2.34). In order to achieve a smaller λ in the next iteration, we let $Z=Z-L$, i.e., we remove variables with $b_i > \lambda$. Obviously λ by (2.59) in the following iterations can only be smaller than the current one. This indicates that

- Variables in L that are fixed at the lower limits can always satisfy sufficient conditions (2.41).
- The search range for $\lambda_{optimal}$ is reduced.

If $S<t$, we can reach similar conclusions.

Initially the number of variables in Z is z_0. Before a solution is obtained, during each iteration from steps 1 to 6, at least one more variable in Z will be fixed at the limit and removed from Z. Moreover, the search range for $\lambda_{optimal}$ is reduced. That means λ by (2.59) can only be one of the 3 possibilities: always increasing, always decreasing, or oscillating with the value closer to $\lambda_{optimal}$. Therefore we can find out whether $\lambda_{optimal}$ is within or beyond b_i ($i = 1, \cdots, z_0$) with at most z_0 iterations. If $\lambda_{optimal}$ is located between b_i ($i = 1, \cdots, z_0$), i.e., $b_{z_0} \geq \lambda_{optimal} \geq b_1$, steps 1-6 can solve the problem by ending up with $S=t$ or $x_k = t - S$. Since fixed variables always satisfy the sufficient conditions, the solution is optimal. If $\lambda_{optimal}$ is beyond $b_i (i = 1, ..., z_0)$, all variables from set Z would be fixed at either the upper or lower limits and satisfy sufficient conditions (2.41). Then we only need to consider variables in set Y that have quadratic bidding functions. Therefore we can apply the algorithm developed in section 2.4. This algorithm would take at most y iterations to find out the optimal solution for the variables in set Y.

Accordingly, it would take no more than (z_0 +y) iterations in total to obtain the optimal solution for all variables in sets *Z* and *Y*.

Note that (z_0 +y) is actually equal to *n*, the total number of variables. That means that this algorithm can obtain the optimal solution within *n* iterations. In addition, each iteration has a computation complexity in the order of *n.* Therefore, this algorithm has a total computation complexity in the order of n^2, the same as the one with quadratic bidding functions.

2.6 Case Studies

The proposed algorithms will be tested on some numerical examples to demonstrate our approach. We will first consider cases with quadratic bidding functions only. Then, we will include linear incremental bidding functions in the auction-based dispatch. Here, only small size problems are presented for easy verification. We have applied to large size problems without any difficulty.

2.6.1 Quadratic Bidding Functions Only

2.6.1.1 Case 1

Table 2.1. Data for Generators and Loads in Case 1

	Type	Bidding data ($/h)	Limits (MW)
1	Generator	$0.01P_{g1}^2 + 12P_{g1} + 300$	[50, 500]
2	Generator	$0.012P_{g2}^2 + 6P_{g2} + 400$	[100, 500]
3	Load	$-0.016P_{l1}^2 + 35P_{l1}$	[0, 400]
4	Load	$-0.017P_{l2}^2 + 34P_{l2}$	[0, 700]

Table 2.1 gives the data for generators and loads. By applying the algorithm to the auction-based dispatch with quadratic bidding functions, we first obtain the solution to optimization problem (2.33)-(2.35) as:

$$x = [344.44 \quad 500 \quad -400 \quad -444.44]$$
$$\lambda = [19.3250 \quad 18.5830 \quad 18.8889]$$

It is noted that:

- The negative signs are for load variables.
- Optimization problem (2.33)-(2.35) is solved in 3 iterations, in which λ oscillates and then converges to the optimal value.
- The solution satisfies the optimality conditions.

After converting the above solution back to generations and loads, the solution to auction problem (2.24)-(2.27) is as follows:

$$P_g = [344.44 \quad 500](MW)$$
$$P_l = [400 \quad 444.44](MW)$$

It can be seen that generator 2 and load 1 hit the upper limits and that others are within the limits.

2.6.1.2 Case 2

Table 2.2. Data for Generators and Loads in Case 2

	Type	Bidding data ($/h)	Limits (MW)
1	Generator	$0.01P_{g1}^2 + 12P_{g1} + 300$	[50, 200]
2	Generator	$0.011P_{g2}^2 + 13P_{g2} + 400$	[100, 310]
3	Generator	$0.009P_{g3}^2 + 11P_{g3} + 300$	[50, 400]
4	Generator	$0.0095P_{g4}^2 + 14P_{g4} + 400$	[100, 300]
5	Generator	$0.05P_{g5}^2 + 15P_{g5} + 300$	[50, 200]
6	Generator	$0.013P_{g6}^2 + 6P_{g6} + 400$	[100, 550]

Table 2.2. (continued)

	Type	Bidding data ($/h)	Limits (MW)
7	Load	$-0.03P_{l1}^2+10P_{l1}$	[0, 300]
8	Load	$-0.017P_{l2}^2+35P_{l2}$	[0, 500]
9	Load	$-0.015P_{l3}^2+35P_{l3}$	[0, 600]
10	Load	$-0.018P_{l4}^2+33P_{l4}$	[0, 700]
11	Load	$-0.0182P_{l5}^2+37P_{l5}$	[0, 400]

The data for generators and loads are shown in Table 2.2. The solution to problem (2.33)-(2.35) is:

$$x=\begin{bmatrix}200 & 294.1314 & 400 & 287.9416 & 50 & 518.1112\\ 0 & -456.7385 & -517.6370 & -375.8086 & -400\end{bmatrix}$$
$$\lambda=\begin{bmatrix}18.6561 & 19.7992 & 19.4709\end{bmatrix}$$

The above results show that though there are more variables than case 1, case 2 takes the same number of iterations to find the optimal solution.

Equivalently, we easily find the solution to auction problem (2.24)-(2.27) as follows:

$$P_g=\begin{bmatrix}200 & 294.1314 & 400 & 287.9416 & 50 & 518.1112\end{bmatrix}(MW)$$
$$P_l=\begin{bmatrix}0 & 456.7385 & 517.6370 & 375.8086 & 400\end{bmatrix}(MW)$$

Generators 1 and 3 hit the upper limits whereas generator 5 hits the lower limit. Load 5 is at the upper limit and load 1 is at the lower limit. Note that even though we have more variables on the limits, the number of iterations is not increased.

2.6.1.3 Case 3

In this case study, we will solve an economic dispatch problem to show that our algorithm improves the one developed in [39].

Table 2.3. Data for Generators in Case 3

Generator	Fuel-cost data $C_i(P_{gi})$ (\$/h)	Limits (MW)
1	$0.01P_{g1}^2 + 12P_{g1} + 300$	[80, 450]
2	$0.012P_{g2}^2 + 6P_{g2} + 400$	[100, 700]
3	$0.016P_{g3}^2 + 25P_{g3} + 250$	[0, 200]
4	$0.017P_{g4}^2 + 20P_{g4} + 350$	[60, 300]

Table 2.3 shows the data for generators. The load is 1200MW.

■ *Iteration 1*

The two algorithms have the same result in the first iteration. Both assume that all the 4 variables are within the limits. Then by (2.37) and (2.38), the following can be obtained:

$$\begin{cases} \lambda_1 = 22.4481 \\ P_g = \left[522.41 \quad 685.34 \quad -79.75 \quad 72.00\right](MW) \end{cases}$$

$UP_1 = 522.41 - 450 = 72.41$; $DN_1 = 0 - (-79.75) = 79.75$. As $UP_1 < DN_1$, both algorithms fix variable P_{g3} at the lower limit.

■ *Iteration 2*

$P_{g3} = 0$. By using (2.37) and (2.38), we obtain

$$\begin{cases} \lambda_2 = 21.7895 \\ P_g = \left[489.47 \quad 657.89 \quad 0 \quad 52.63\right](MW) \end{cases}$$

$UP_2 = 489.47 - 450 = 39.47$; $DN_2 = 60 - 52.63 = 7.37$. As $UP_2 > DN_2$, our algorithm will fix P_{g1} at its upper limit. Whereas the algorithm in [39] will continue setting P_{g4} to its lower limit.

■ *Iteration 3*

For our algorithm, $P_{g1} = 450$; $P_{g3} = 0$. By using (2.37) and (2.38), we obtain

$$\begin{cases} \lambda_3 = 22.3448 \\ P_g = [450 \quad 681.03 \quad 0 \quad 68.97](MW) \end{cases}$$

We stop here because P_{g2}, P_{g4} are within the limits. By checking sufficient conditions (2.36), we can see that this solution is optimal.

On the other hand, it can be easily seen the algorithm in [39] will be ended with brute force enumeration and the computation load is exponentially growing with the system size *n*.

2.6.2 With Quadratic and Linear Incremental Bidding Functions

2.6.2.1 Case 4

Table 2.4. Data for Generators and Loads in Case 4

	Type	Bidding data ($/h)	Limits (MW)
1	Generator	$0.01P_{g1}^2 + 12P_{g1} + 300$	[0, 400]
2	Generator	$0.015P_{g2}^2 + 6P_{g2} + 400$	[0, 300]
3	Load	$34P_{l1}$	[0, 300]
4	Load	$35P_{l2}$	[0, 500]

The data for generators and loads are given in Table 2.4. By implementing the algorithm for the auction-based dispatch with both quadratic and linear incremental bidding functions, we first obtain the solution to problem (2.33)-(2.35):

$$x = [400 \quad 300 \quad -200 \quad -500]$$
$$\lambda = [34.5 \quad 34]$$

In this case, only 2 iterations are needed to find the optimal solution. The solution to auction problem (2.24)-(2.27) is:

$$P_g = [400 \quad 300](MW)$$
$$P_l = [200 \quad 500](MW)$$

It can be seen that load 2 is at the upper limit whereas load 1 is within the limits. This is expected since the bidding cost of load 2 is always higher than that of load 1, and load 1 cannot get any power unless load 2 is fully supplied.

2.6.2.2 Case 5

Table 2.5. Data for Generators and Loads in Case 5

	Type	Bidding data ($/h)	Limits (MW)
1	Generator	$0.01P_{g1}^2 + 12P_{g1} + 300$	[0, 400]
2	Generator	$0.015P_{g2}^2 + 6P_{g2} + 400$	[0, 300]
3	Generator	$0.011P_{g3}^2 + 11P_{g3} + 300$	[0, 400]
4	Generator	$0.013P_{g4}^2 + 13P_{g4} + 400$	[0, 300]
5	Load	$34P_{l1}$	[0, 300]
6	Load	$35P_{l2}$	[0, 200]
7	Load	$33P_{l3}$	[0, 300]
8	Load	$36P_{l4}$	[0, 200]
9	Load	$37P_{l5}$	[0, 100]
10	Load	$-0.03P_{l6}^2 + 25P_{l6}$	[0, 150]

Table 2.5 gives the data for generators and loads. Again, by using the algorithm for the auction-based dispatch with both quadratic and linear incremental bidding functions, we can obtain the solution to problem (2.33)-(2.35):

$$x = \begin{bmatrix} 335.2554 & 300 & 350.2322 & 219.4272 & & \\ -300 & -200 & -300 & -200 & -100 & -104.9149 \end{bmatrix}$$
$$\lambda = [35 \quad 33.5 \quad 33 \quad 18.0336 \quad 18.7051]$$

From the values of the λ, we know that the algorithm in section 2.4 is also involved in the process. It first takes 3 iterations to judge the location of $\lambda_{optimal}$. After finding out that $\lambda_{optimal}$ is smaller than the marginal costs of the variables with linear incremental bidding curves, we employ the algorithm in section 2.4 with 2 more iterations to find the solution. Therefore, in total, it takes 5 iterations to obtain the optimal solution.

The solution to auction problem (2.24)-(2.27) is:

$$P_g = [335.2554 \quad 300 \quad 350.2322 \quad 219.4272](MW)$$
$$P_l = [300 \quad 200 \quad 300 \quad 200 \quad 100 \quad 104.9149](MW)$$

The above answer indicates that loads 1 to 5 hit the upper limits whereas load 6 is within its limits since the bidding costs of loads 1 to 5 are so high that they should be covered first before load 6 can be supplied.

2.7 Conclusions

By using the law of supply and demand, this chapter investigates the formulation of the auction-based dispatch and illustrates that it is reasonable to adopt the social welfare as the objective function. Then efficient algorithms to solve the auction-based dispatch are developed. With appropriate formulations, two algorithms solving the auction-based dispatch are presented for different types of bidding functions. It is proved that both algorithms have a total computation complexity in the order of the square of the number of variables. By comparison, the conventional algorithm has an exponential computation complexity. Accordingly, the algorithms presented here are much more effective and efficient. The numerical experiments further verify the efficiency and accuracy of the proposed algorithms.

CHAPTER III

CONGESTION MANAGEMENT BY USING SENSITIVITY FACTORS AND THE TECHNIQUE OF AGGREGATION

3.1 Introduction

In chapter II, an intensive study has been carried out for the formulation and algorithm of the auction-based dispatch. The purpose of the auction-based dispatch is to encourage competition among the generators and loads so that maximum economic efficiency can be achieved. However, this type of dispatch is a pure market activity and neglects the constraints of the transmission system. Under this dispatch, people tend to buy power from the cheapest sources. As a result, the transmission system is congested more often than before deregulation [20]. Accordingly reliability level has declined in the deregulated environment. Obviously, to maintain the system reliability, it is important to eliminate congestion efficiently.

In deregulated power systems, transmission congestion is defined as the condition that there is not sufficient transmission capacity to simultaneously implement all transactions in electricity markets [19]. The management of congestion is one of the fundamental problems of deregulated power systems. There are many methods to manage congestion. One of them is the OPF model [17, 18]. This model is arguably the most accurate and effective method for strongly networked transmission systems [20]. Below is the formulation of this model, which is based on the DC power flow.

Objective:

$$Max \quad f = \left(\sum_{j=1}^{r} D_j(P_{lj}) - \sum_{i=1}^{m} C_i(P_{gi}) \right) \tag{3.1}$$

Subject to:

$$\sum_{i=1}^{m} P_{gi} - \sum_{j=1}^{r} P_{lj} = 0 \tag{3.2}$$

$$P_{gi\min} \le P_{gi} \le P_{gi\max} \qquad i = 1,...,m \tag{3.3}$$

$$P_{lj\min} \le P_{lj} \le P_{lj\max} \qquad j = 1,...,r \tag{3.4}$$

$$|P_k| \le P_{k\max} \qquad k = 1,...,t \tag{3.5}$$

Some notations for this formulation are as follows:

P_{lj} : Real power amount of jth load.

$P_{lj\max}, P_{lj\min}$: Maximum and minimum requirements of jth load.

P_{gi} : Real power amount of ith generator.

$P_{gi\max}, P_{gi\min}$: Real power limits of ith generator.

r : Number of loads.

m : Number of generators.

t : Number of congested lines.

$C_i(P_{gi})$: Bidding function of ith generator with a form of $a_{gi}P_{gi}^2 + b_{gi}P_{gi} + c_{gi}$.

$D_j(P_{lj})$: Bidding function of jth load with a form of $a_{lj}P_{lj}^2 + b_{lj}P_{lj} + c_{lj}$.

$P_{k\max}$: The thermal limit of congested line k.

Obviously this formulation can successfully eliminate congestion. In the meantime, it can maintain market efficiency because its objective is to maximize the social welfare, i.e., the difference of bids between the loads and generators. That means this formulation realizes the two major objectives of congestion management, i.e., maintaining security and market efficiency [20]. However, since all generators and loads are involved in the above formulation, the optimization program will have too many variables for large size systems, which makes it hard and slow to solve.

In this chapter, we propose a new OPF method to resolve congestion. This method is based on the sensitivity factors combined with the technique of aggregation. According to the sensitivity factors of all generators with regard to the congested lines, we will identify effective generators that have big influence on these congested lines to relieve congestion. Since only a limited number of generators participate, our congestion management is sure to be much faster than conventional method (3.1) – (3.5). To further

reduce the number of variables and speed up the calculation, we aggregate generators that have similar impact in terms of their sensitivity factors. The case studies on the IEEE RTS-96 system demonstrate that the method proposed here is much faster than the conventional method in the elimination of congestion. Meanwhile, the social welfare decreases little with our method. Thus our method is very effective in managing congestion.

3.2 Calculation of Sensitivity Factors

Though the AC power flow is the most accurate tool in power system studies, it is complicated and slow. On the other hand, the DC power flow is very simple and fast. Meanwhile it can provide sufficient accuracy. Therefore our method is based on the DC power flow.

For the DC power flow, the bus angles and the injected powers have the following relationship.

$$P_{Inj} = B\theta \tag{3.6}$$

where:

B is the admittance matrix: $B_{ij} = -\frac{1}{x_{ij}} \quad B_{ii} = \sum_{j \neq i} \frac{1}{x_{ij}}$; and x_{ij} is the reactance between buses i and j.

P_{Inj} is the vector of injected powers.

θ is the vector of bus angles.

It is noted that (3.6) does not include the reference bus whose angle is zero. That means the dimensions of P_{Inj}, B, and θ are $(N-1)\times 1$, $(N-1)\times(N-1)$, and $(N-1)\times 1$ respectively if there are N buses.

As we know, a line flow in the DC model can be simply represented by the equation below.

$$P_{ij} = \frac{\theta_i - \theta_j}{x_{ij}} \tag{3.7}$$

Thus we define a matrix *C* to reflect the relations between the bus angles and the line flows of interest to us.

$$P_v = C\theta \tag{3.8}$$

where P_v is a vector containing the line flows we are interested in. For instance, they could be tie-line flows. With regard to matrix *C*, each row has at most 2 non-zero elements. Suppose row *m* corresponds to a line connected between buses i and j, neither of which is the reference bus. Further, the flow direction is from i and j. Then we have $c_{mi} = \frac{1}{x_{ij}}; \quad c_{mj} = -\frac{1}{x_{ij}}$ while other elements in row *m* are zero. If either of the two buses, say bus i, is the reference bus, then only c_{mj} is non-zero in row *m*. The reason is that matrix *C* does not have a column corresponding to the reference bus.

Based on (3.7) and (3.8), we can express the line flows in terms of the injected powers.

$$P_v = (CB^{-1})P_{Inj} = SP_{Inj} \tag{3.9}$$

We define matrix *S*, namely (CB^{-1}) as the sensitivity matrix of the injected powers with regard to the line flows which are of interest to us.

3.3 Selection of Effective Generators to Participate in Congestion Management

Generators normally have a higher priority than loads in congestion management. Therefore in our work, we assume that only generators participate in congestion management.

We want the congestion to be eliminated with as little change of generation as possible. To realize this, we will adjust generators that have big effects on the congested lines and ignore generators whose effects are small. For instance, suppose line *k* is congested. From (3.9), we have

$$\Delta P_k = \sum_{l \in S_g} s_{kl} \cdot \Delta P_{gl} \tag{3.10}$$

where ΔP_k is the change needed to get rid of the congestion. ΔP_{gl} is the output change of generator l and s_{kl} is the sensitivity factor of this generator with regard to line *k*. Set S_g contains all the generators.

Suppose we only adjust two generators, say generators i and j.

$$\Delta P_k = s_{ki}\Delta P_{gi} + s_{kj}\Delta P_{gj} \tag{3.11}$$

Notice that power needs to be balanced all the time. If we increase the output of one generator, we need to decrease the output of the other generator by the same amount. In other words, $\Delta P_{gi} = -\Delta P_{gj}$. Thus (3.11) can be rewritten as

$$\Delta P_k = \left(s_{ki} - s_{kj}\right)\Delta P_{gi} \tag{3.12}$$

Equation (3.12) tells us that if we want to relieve the congestion with the smallest adjustment, we should choose two generators such that the difference between their

corresponding sensitivity factors is biggest. In other words, these two generators together have the biggest effect on this congested line. Similarly, if we need to choose more than two generators, we can follow the same idea. That means we will select several times with each time involving two biggest effect generators. The detailed procedure can be referred to the algorithm below.

3.4 Determination of Zones

After we select some generators for relieving a congested line, we will divide them into several zones according to their sensitivity factors. Suppose for a congested line, say *k*, we have chosen generators $g_1, g_2, ...g_q$. The sensitivity factors associated with these generators are $s_{k,g1}$, $s_{k,g2}$, ..., $s_{k,gq}$. Further we assume that $s_{k,g1} > s_{k,g2} > \cdots > s_{k,gq}$. Let $D_k = s_{k,g1} - s_{k,gq}$ and choose an integer β, e.g. 5. We will determine zones with boundaries as follows: $[s_{k,g1}, \quad s_{k,g1} - D_k / \beta]$, $[s_{k,g1} - D_k / \beta, \quad s_{k,g1} - 2D_k / \beta]$, …, $[s_{k,gq} + D_k / \beta, \quad s_{k,gq}]$. In terms of the position of the sensitivity factor, we can decide which zone a generator belongs to. This method of determination of zones indicates that any two generators within the same zone will have a difference of their sensitivity factors less than D_k / β. Unlike conventional methods which decide a zone in terms of the geographical location, we use sensitivity factors. This can guarantee that generators within the same zone have similar effects on the congested lines.

Concerning the case of multiple congested lines, it may happen that two generators are selected in the same zone for a congested line while in different zones for another congested line. For such situations, we have to place these two generators into different zones when we want to relieve all the congested lines.

3.5 Aggregation and Disaggregation of Generators

3.5.1 Aggregation

In this part, we will aggregate generators within the same zone into a single generator. Specifically, we will derive the expressions of the output, lower/upper limits, and the bidding function of the new aggregate generator. We will also express the flows of congested lines in terms of aggregate generators.

3.5.1.1 Outputs and Lower/Upper Limits of Aggregate Generators

To obtain the aggregate output and lower/upper limits, we can simply sum up the individual values. For instance, let us consider a zone, say Z_j. The aggregate values of the output and lower/upper limits are

$$P_{Gj}^{'} = \sum_{l \in Z_j} P_{gl} \tag{3.13}$$

$$P_{Gj\min}^{'} = \sum_{l \in Z_j} P_{gl\min} \tag{3.14}$$

$$P_{Gj\max}^{'} = \sum_{l \in Z_j} P_{gl\max} \tag{3.15}$$

where $P_{Gj}^{'}$, $P_{Gj\min}^{'}$ and $P_{Gj\max}^{'}$ are the output, lower and upper limits of the aggregate generator. P_{gl} , $P_{gl\min}$ and $P_{gl\max}$ are the output, lower and upper limits of generator l in zone Z_j.

3.5.1.2 Bidding Functions of Aggregate Generators

The bidding function of a generator has the following form:

$$C_i(P_{gi}) = a_{gi}P_{gi}^2 + b_{gi}P_{gi} + c_{gi} \quad (\$/h) \tag{3.16}$$

where $a_{gi} > 0, b_{gi} > 0, c_{gi} > 0$.

Thus the supply curve, the derivative of the bidding function, is

$$MC_i = 2a_{gi}P_{gi} + b_{gi} \quad (\$/MWh) \tag{3.17}$$

where *MC* is the price or the marginal cost.

That is

$$P_{gi} = \frac{MC_i - b_{gi}}{2a_{gi}} \tag{3.18}$$

According to studies in chapter II, the supply curve of the aggregate generator is the horizontal summation of the supply curves of all individual generators. Specifically, the power quantity of the aggregate supply curve at a price is the sum of the power quantities of all individual supply curves at this price. Therefore the expression of the aggregate supply curve in a zone, say Z_j is

$$P_{Gj}^{'} = \sum_{i \in Z_j} \frac{MC_j^{'} - b_{gi}}{2a_{gi}} = \left(\sum_{i \in Z_j} \frac{1}{2a_{gi}} \right) MC_j^{'} - \sum_{i \in Z_j} \frac{b_{gi}}{2a_{gi}} \tag{3.19}$$

Or

$$MC_j^{'} = \frac{1}{\sum_{i \in Z_j} \frac{1}{2a_{gi}}} P_{Gj}^{'} + \frac{\sum_{i \in Z_j} \frac{b_{gi}}{2a_{gi}}}{\sum_{i \in Z_j} \frac{1}{2a_{gi}}} \tag{3.20}$$

where $P_{Gj}^{'}$ and $MC_j^{'}$ are the power quantity and price of the aggregate supply curve. By integrating supply curve (3.20), we can obtain the bidding function of the aggregate generator. We also point out that (3.20) assumes all individual generators have the same price range. In terms of discussions in chapter II, the aggregate supply curve will become a collection of linear functions when the individual supply curves have different price ranges. For instance, let us consider a price range, say $[MC_{k1},\ \ MC_{k2}]$. Suppose set W_j consists of generators at the limits whereas set L_j is composed of generators within the limits. The expression for the supply curve will be

$$MC_j^{'} = \frac{1}{\sum_{i \in W_j} \frac{1}{2a_{gi}}} \left(P_{Gj}^{'} - \sum_{i \in L_j} P_{gi,\lim it} \right) + \frac{\sum_{i \in W_j} \frac{b_{gi}}{2a_{gi}}}{\sum_{i \in W_j} \frac{1}{2a_{gi}}} \tag{3.21}$$

where $P_{gi,\lim it}$ refers to the lower or upper limit.

3.5.1.3 Expression of the Flows of Congested Lines by Using Aggregate Generators

After we select generators and divide them into zones according to sections 3.3 and 3.4, we can express the flow changes of congested lines as follows:

$$\Delta P_k = \sum_{j=1}^{NZ} \left(\sum_{i \in Z_j} s_{ki} \cdot \Delta P_{gi} \right) \qquad k = 1, \cdots, t \tag{3.22}$$

where NZ is the number of zones and Z_j stands for zone j. To apply the aggregation method, we need to convert ΔP_{gi} the amount change of an individual generator in a zone into $\Delta P_{Gj}^{'}$ the amount change of an aggregate generator.

Notice that sensitivity factors within the same zone are close to one another. That is for any p, q belonging to Z_j, we have

$$s_{kp} \approx s_{kq} \tag{3.23}$$

This implies

$$s_{kp} \approx s_{kq} \approx \frac{\sum_{i \in Z_j} s_{ki}}{nj} \tag{3.24}$$

where nj is the number of the generators in zone Z_j.

Therefore

$$\sum_{i \in Z_j} s_{ki} \cdot \Delta P_{gi} \approx \frac{\sum_{i \in Z_j} s_{ki}}{nj} \left(\sum_{i \in Z_j} \Delta P_{gi} \right) \tag{3.25}$$

Recall that the aggregate generator's output is the summation of that of every generator in the same zone. That means $\left(\sum_{i \in Z_j} \Delta P_{gi} \right)$ is in fact $\Delta P'_{Gj}$ the amount change of the aggregate generator in zone j. Thus (3.25) indicates that we can use the average of the sensitivity factors in a zone to represent the sensitivity factor of the aggregate generator with regard to the congested line. If we define $\frac{\sum_{i \in Z_j} s_{ki}}{nj}$ as s'_{kj}, then we can rewrite (3.22) in terms of the aggregate generators.

$$\Delta P_k = \sum_{j=1}^{NZ} s'_{kj} \cdot \Delta P'_{Gj} \quad k = 1, \cdots, t \tag{3.26}$$

3.5.1.4 Congestion Management by Using Aggregate Generators

After we aggregate selected generators and express the congested lines in terms of the aggregated generators, we can relieve the congestion by running the following optimal program.

Objective:

$$Min \quad f = \sum_{j=1}^{NZ} C'_j(P'_{Gj}) \tag{3.27}$$

Subject to:

$$\sum_{j=1}^{NZ} (P'_{Gj} - P'_{Gj0}) = 0 \tag{3.28}$$

$$P'_{Gj\min} \le P'_{Gj} \le P'_{Gj\max} \qquad j = 1,..., NZ \tag{3.29}$$

$$\Delta P_k = \sum_{j=1}^{NZ} s'_{kj} (P'_{Gj} - P'_{Gj0}) \qquad k = 1,..., t \tag{3.30}$$

where P'_{Gj0} and P'_{Gj} are the outputs of aggregate generator j before and after the congestion management respectively. $C'_j(P'_{Gj})$ stands for the bidding function of aggregate generator j. And t is the number of congested lines.

In comparison with formulation (3.1) – (3.5), our formulation only involves effective generators. Further the number of variables is reduced by the technique of aggregation. Therefore fast and stable computation would be expected for our congestion management. In the meantime, since we only aggregate generators with close sensitivity factors, our aggregation method can still retain accuracy.

As we know, before congestion management, the generations and loads are dispatched under the rule of maximum social welfare. That means congestion management will unavoidably reduce the social welfare and affect the market efficiency. A good congestion management should not only efficiently eliminate congestion but also maintain market efficiency as much as possible. Our method only adjusts generators that have biggest effects on the congested lines. Thus the amount adjusted is small and correspondingly the market efficiency could be retained.

In a word, congestion management by using (3.27)-(3.30) is fast and can maintain market efficiency. Thus it is a good management. Later on we will use the IEEE RTS-96 system to demonstrate the efficiency and effectiveness of our method.

3.5.2 Disaggregation

After we run (3.27) – (3.30) and obtain the aggregate outputs and aggregate marginal costs, we can return to each zone to calculate the individual generations in this zone. Since generators within the limits in the same zone have the same marginal cost, we can easily obtain the outputs of these generators.

$$MC_i = MC_j^{'} \quad (i \in Z_j) \tag{3.31}$$

$$P_{gi} = \frac{MC_i - b_{gi}}{2a_{gi}} \tag{3.32}$$

where MC_i is the marginal cost of generator i which is in zone Z_j. And P_{gi} is the output of generator i.

3.6 Algorithm for Congestion Management

We make the following assumptions for the congestion management.

- Generators have a higher priority over loads in the congestion management. Usually we will adjust generators only.
- There are N buses. The N^{th} bus is the reference bus and the first m buses are generator buses.

Based on the above assumptions, we develop an algorithm to relieve congestion. The details are given below:

1. Calculate matrices B and C in (3.6) and (3.8).
2. Calculate S, the sensitivity matrix of the generations with regard to the congested lines, using (3.9). Therefore the following equation can be achieved.

$$\begin{bmatrix} \Delta P_1 \\ \vdots \\ \Delta P_t \end{bmatrix} = \begin{bmatrix} s_{11} & s_{12} & \cdots & s_{1m} \\ \vdots & \vdots & \cdots & \vdots \\ s_{t1} & s_{t2} & \cdots & s_{tm} \end{bmatrix} \begin{bmatrix} \Delta P_{g1} \\ \Delta P_{g2} \\ \vdots \\ \Delta P_{gm} \end{bmatrix} \tag{3.33}$$

where

$\begin{bmatrix} \Delta P_1 & \cdots & \Delta P_t \end{bmatrix}^T$ is the vector of desired correction on the congested lines.

$\begin{bmatrix} \Delta P_{g1} & \Delta P_{g2} & \cdots & \Delta P_{gm} \end{bmatrix}^T$ represents the change of the generations.

$\begin{bmatrix} s_{11} & s_{12} & \cdots & s_{1m} \\ \vdots & \vdots & \cdots & \vdots \\ s_{t1} & s_{t2} & \cdots & s_{tm} \end{bmatrix}$ is the sensitivity matrix S.

3. Choose α less than 1 for use in the following steps, e.g. α = 0.25. Define $\beta = \left\lceil \frac{1}{\alpha} \right\rceil$, i.e., the smallest integer greater than or equal to $\frac{1}{\alpha}$.
4. For k from 1 to t (t is the number of congested lines), do steps 5 through 8.
5. Calculate the difference between the biggest and the smallest sensitivity factors among $s_{kj}\,(j = 1, \cdots, m)$ for the k^{th} congested line.

$$D_k = s_{k,p} - s_{k,q} \tag{3.34}$$

where $s_{k,p} = \max\{s_{k,j}, \quad j = 1,\cdots,m\}$ and $s_{k,q} = \min\{s_{k,j}, \quad j = 1,\cdots,m\}$

6. Calculate $D_k \cdot \alpha$ to be the threshold.

7. Select effective generators for management of the k^{th} congested line. The detailed procedure is as follows.

   7.1 Initialize iteration index $i = 1$.

   7.2 Initialize sets $M_k = \{p_1, q_1\}$ and $R_k = \{j \mid j = 1,2,\cdots,m, \quad j \neq p_1, j \neq q_1\}$, where p_1 is the generator whose sensitivity factor is the biggest of all $s_{kj}(j = 1,2,\cdots,m)$ and q_1 is the generator whose sensitivity factor is the smallest of all $s_{kj}(j = 1,2,\cdots,m)$.

   7.3 Set $d_{k,1} = D_k$.

   7.4 While $d_{k,i} \geq D_k \cdot \alpha$, repeat steps 7.5 to 7.8.

   7.5

   - If $i = 1$, calculate $\Delta P_{gp_i}^{\max}$ and $\Delta P_{gq_i}^{\max}$ the maximum allowed changes of generators p_i and q_i by performing the capacity routine defined as follows:

     - If we need to decrease the flow on the k^{th} congested line to eliminate the congestion, i.e., $\Delta P_k < 0$, then

$$\Delta P_{gp_i}^{\max} = P_{gp_i} - P_{gp_i}^{\min} \tag{3.35}$$

$$\Delta P_{gq_i}^{\max} = P_{gq_i}^{\max} - P_{gq_i} \tag{3.36}$$

     - Else

$$\Delta P_{gp_i}^{\max} = P_{gp_i}^{\max} - P_{gp_i} \tag{3.37}$$

$$\Delta P_{gq_i}^{\max} = P_{gq_i} - P_{gq_i}^{\min} \tag{3.38}$$

- Else compare $\Delta P_{gp_{(i-1)}}^{\max}$ and $\Delta P_{gq_{(i-1)}}^{\max}$, calculate $\Delta P_{gp_i}^{\max}$, $\Delta P_{gq_i}^{\max}$ and update M_k, R_k as follows:
  - If $\Delta P_{gp_{(i-1)}}^{\max} > \Delta P_{gq_{(i-1)i}}^{\max}$, let $\Delta P_{gp_i}^{\max} = \Delta P_{gp_{(i-1)}}^{\max} - \Delta P_{gq_{(i-1)}}^{\max}$. Calculate $\Delta P_{gq_i}^{\max}$ by performing half of the capacity routine using (3.36) or (3.38), which depends on the sign of ΔP_k. Let $M_k = M_k \cup \{q_i\}$ and $R_k = R_k - \{q_i\}$.
  - Else if $\Delta P_{gp_{(i-1)}}^{\max} < \Delta P_{gq_{(i-1)i}}^{\max}$, let $\Delta P_{gq_i}^{\max} = \Delta P_{gq_{(i-1)}}^{\max} - \Delta P_{gp_{(i-1)}}^{\max}$. Calculate $\Delta P_{gp_i}^{\max}$ by performing half of the capacity routine using (3.35) or (3.37), which depends on the sign of ΔP_k. Let $M_k = M_k \cup \{p_i\}$ and $R_k = R_k - \{p_i\}$.
  - Else calculate $\Delta P_{gp_i}^{\max}$ and $\Delta P_{gq_{(i}}^{\max}$ by performing the capacity routine using (3.35) and (3.36) or (3.37) and (3.38), which depends on the sign of ΔP_k. Let $M_k = M_k \cup \{p_i, q_i\}$ and $R_k = R_k - \{p_i, q_i\}$.

7.6 Set $i = i + 1$.

7.7

- If $\Delta P_{gp_{(i-1)}}^{\max} > \Delta P_{gq_{(i-1)}}^{\max}$, let $p_i = p_{(i-1)}$. Find the generator whose sensitivity factor is the smallest of all $s_{kj}(j \in R_k)$ and designate it as q_i.
- Else if $\Delta P_{gp_{(i-1)}}^{\max} < \Delta P_{gq_{(i-1)}}^{\max}$, let $q_i = q_{(i-1)}$. Find the generator whose sensitivity factor is the biggest of all $s_{kj}(j \in R_k)$ and designate it as p_i.
- Else find the generator whose sensitivity factor is the biggest of all $s_{kj}(j \in R_k)$ and designate it as p_i. Then find the generator whose sensitivity factor is the smallest of all $s_{kj}(j \in R_k)$ and designate is as q_i.

7.8 Let $d_{k,i} = s_{k,p_i} - s_{k,q_i}$.

8. Divide selected generators, i.e., those generators in set M_k, into zones according to their sensitivity factors:

8.1 Calculate D_k / β to be the step size. (See step 3 for the definition of β.)

8.2 Based on the sensitivity factors, determine zones with boundaries as follows: $[s_{k,p}, \quad s_{k,p} - D_k / \beta]$, $[s_{k,p} - D_k / \beta, \quad s_{k,p} - 2D_k / \beta]$,…, $[s_{k,q} + D_k / \beta, \quad s_{k,q}]$. (The definition of $s_{k,p}$ and $s_{k,q}$ is given in step 5.) In terms of the positions of the sensitivity factors, we can decide which generators are within the same zone.

9. Map generators in the same zone into a single generator according to (3.13)-(3.15) and (3.21).
10. Express the congested lines in terms of the aggregate generators according (3.26).
11. Run optimization program (3.27) – (3.30) to relieve the congestion and obtain the outputs and marginal costs of the aggregate generators.
12. Obtain the marginal costs and outputs of the individual generators in the original system by using (3.31) and (3.32).

3.7 Case Studies

Let us consider the IEEE RTS-96 system as shown in Fig. 3.1. This system is developed by modifying and updating the IEEE RTS-79 system. The RTS-96 system has 119 lines including 5 tie-lines, and 73 buses. The data for the tie-lines can be found in Table 3.1. Other data can be referred to the appendix and [51].

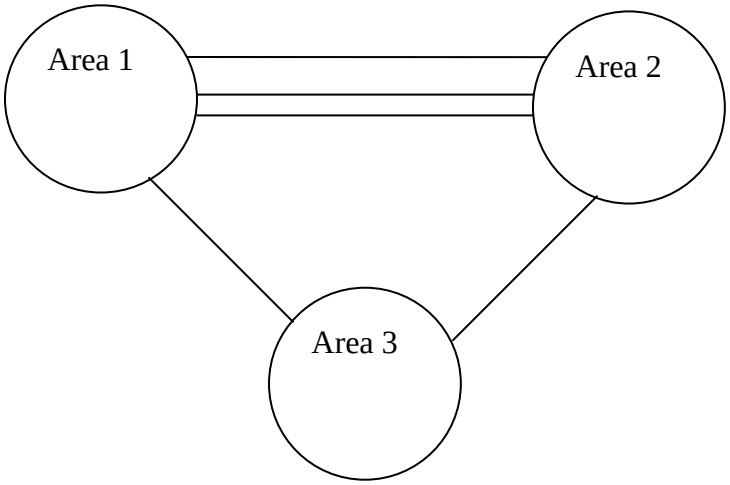

Fig. 3. 1. IEEE RTS-96 System

Table 3.1. Data of Tie-lines

Tie-line No.	From (Area, Bus)	To (Area, Bus)	R (p.u.)	X (p.u.)	B (p.u.)	Current limits (p.u.)
1	(1, 107)	(2, 203)	0.0140	0.0537	0.0147	0.5
2	(1, 113)	(2, 215)	0.0033	0.0250	0.0527	0.5
3	(1, 123)	(2, 217)	0.0033	0.0247	0.0517	1
4	(3, 325)	(1, 121)	0.0040	0.0323	0.0677	1
5	(3, 318)	(2, 223)	0.0043	0.0347	0.0727	1

In the system, the bilateral market has a transaction 50MW from bus 101 in area 1 to bus 201 in area 2. On the other hand, the pool market is decided by the auction-based dispatch. (The bidding functions of generators and loads are provided in the appendix.) The pool generations are shown in the 4^{th} column in Table 3.2 below (The lower limits of the generators are 0.). The loads are covered fully. And the social welfare, namely the bid difference between loads and generations is 156430($/h).

Table 3.2. Pool Generations

Generator No.	Gen. bus ID	$P_{g\,\max}$ (MW)	P_g (MW)
1	101	192	163.91
2	102	192	163.91
3	107	300	288.91
4	113	591	431.13
5	115	215	196.7
6	116	155	155
7	118	400	346.7
8	121	400	346.7
9	122	300	300
10	123	660	461.93
11	201	192	143.08
12	202	192	143.08
13	207	300	300
14	213	591	431.13
15	215	215	171.7
16	216	155	155
17	218	400	346.7
18	221	400	346.7
19	222	300	300
20	223	660	461.93
21	301	192	178.82
22	302	192	178.82
23	307	300	300
24	313	591	431.13
25	315	215	196.7
26	316	155	155

According to the results of measurements, we discover that tie-lines 1 and 2 are congested, namely above the thermal limits.

Table 3.3. Tie-line Flows

Tie-line No.	From (Area, Bus)	To (Area, Bus)	Currents (p.u.)	Limits (p.u.)
1	(1, 107)	(2, 203)	0.5246	0.5
2	(1, 113)	(2, 215)	0.8071	0.5
3	(1, 123)	(2, 217)	0.5074	1
4	(3, 325)	(1, 121)	0.8931	1
5	(3, 318)	(2, 223)	0.5835	1

It is noted that in Table 3.3 the limits refer to maximum allowable currents. We will relieve the congestion by adjusting the real powers of generators only. Before the adjustment,

$$\sqrt{\left(P_{ij}^0\right)^2+\left(Q_{ij}^0\right)^2}=V_i^0 I^0 \tag{3.39}$$

where P_{ij}^0, Q_{ij}^0 stand for the real and reactive powers along line *ij*. V_i^0 is the voltage magnitude at bus *i* and I^0 is the current of line *ij*. If we only adjust the real powers, we can assume that the reactive powers and voltage magnitudes are not changed [52]. That is,

$$\sqrt{\left(P_{ij}^0+\Delta P_{ij}\right)^2+\left(Q_{ij}^0\right)^2}=V_i^0 I^{\max} \tag{3.40}$$

where ΔP_{ij} is the desired real power flow change on line *ij* to reduce the current to the limit. For tie-line 1 which is between bus 107 and bus 203, we have $S_{107,203}^0 = 0.5265 + j0.1084$ (p.u.) and $V_{107}^0 = 1.025$ (p.u.). By using (3.40), we obtain

$\Delta P_{107,203} = -0.0256$ (p.u.). Concerning tie-line 2 that is connected between buses 113 and 215, we have $S^0_{113,215} = -0.8178 + j0.0945$ (p.u.) and $V^0_{113} = 1.020$ (p.u.). Again by using (3.40), we obtain $\Delta P_{113,215} = 0.3167$ (p.u.). With the desired real power flow changes of the two tie-lines available, we now can apply the algorithm proposed earlier to eliminate the congestion.

Based on steps 1 and 2 in the algorithm, we obtain the sensitivity factors of generators with regard to the two congested tie-lines as shown in Table 3.4 below. (Bus 325 is the reference bus.)

Table 3.4. Sensitivity Matrix: Only Generator Buses

Generator No.	Generator bus ID	Tie-Line 1	Tie-Line 2
1	101	0.11344	0.25017
2	102	0.11450	0.25233
3	107	0.58949	0.068949
4	113	0.02669	0.50694
5	115	0.013702	0.045691
6	116	0.013771	0.056319
7	118	0.0044245	0.017475
8	121	0.003192	0.011515
9	122	0.0048737	0.018817
10	123	0.0072166	0.064346
11	201	-0.13032	-0.01928
12	202	-0.12693	-0.01968
13	207	-0.097211	-0.0232
14	213	-0.052724	-0.0227
15	215	-0.008571	-0.1733
16	216	-0.009421	-0.08522
17	218	-0.000893	-0.01464

Table 3.4. (continued)

Generator No.	Generator bus ID	Tie-Line 1	Tie-Line 2
18	221	-0.001737	-0.03376
19	222	-0.001416	-0.0253
20	223	-0.011018	-0.00677
21	301	-0.000547	-0.00034
22	302	-0.000543	-0.00033
23	307	-0.000512	-0.00031
24	313	-0.000387	-0.00024
25	315	-0.000884	-0.00054
26	316	-0.001118	-0.00069
27	318	-0.002958	-0.00182
28	321	-0.001173	-0.00072
29	322	-0.001599	-0.00098
30	323	-6.13E-05	-3.77E-05

We will only select generators that have big effects on the congested lines for the congestion management. In terms of the algorithm, we first choose a coefficient α as 0.25. Then from the above table we learn that the difference between the biggest and the smallest sensitivity factors for tie-line 1 is

$$D_1 = (0.58949 - (-0.13032)) = 0.7198$$

That means the threshold for tie-line 1 is $D_1 \cdot \alpha = 0.7198 \times 0.25 = 0.18$. We thus can pick effective generators to relieve tie-line 1 according to step 7 in the algorithm. Specifically,

[Step 7.1]: $i = 1$.

[Step 7.2]: Generator 3's sensitivity factor is the biggest among all sensitivity factors while generator 11's sensitivity factor is the smallest. Therefore $p_1 = 3; q_1 = 11$ and $M_1 = \{3,11\}$, $R_1 = \{j \mid j = 1,2,...,30 \quad j \neq 3, j \neq 11\}$.

[Step 7.3]: $d_{1,1} = D_1 = 0.7198$.

[Step 7.4]: $d_{1,1} = 0.7198 > D_1 \cdot \alpha = 0.18$. Therefore do steps 7.5 through 7.8

[Step 7.5]: Since $i = 1$, perform the capacity routine of p_1, q_1. As $\Delta P_1 = -0.0256 < 0$, we use (3.35) and (3.36).

$$\Delta P_{gp_1}^{\max} = P_{gp_1} - P_{gp_1}^{\min} = 288.91 - 0 = 288.91$$

$$\Delta P_{gq_1}^{\max} = P_{gq_1}^{\max} - P_{gq_1} = 192 - 143.08 = 48.92$$

[Step 7.6]: $i = i + 1 = 1 + 1 = 2$.

[Step 7.7]: $\Delta P_{gp_1}^{\max} > \Delta P_{gq_1}^{\max}$, therefore $p_2 = p_1 = 3$ and $q_2 = 12$ because generator 12's sensitivity factor is the smallest in set R_1.

[Step 7.8]: $d_{2,1} = 0.58949 - (-0.12693) = 0.71642$.

Since $d_{2,1} > D_1 \cdot \alpha$, we repeat steps 7.5 through 7.8:

[Step 7.5]: As $i > 1$ and $\Delta P_{gp_1}^{\max} > \Delta P_{gq_1}^{\max}$, we have $\Delta P_{gp_2}^{\max} = \Delta P_{gp_1}^{\max} - \Delta P_{gq_1}^{\max}$ =288.91-48.92 = 239.99. Then perform the capacity routine of q_2 using (3.36),

$$\Delta P_{gq_2}^{\max} = P_{gq_2}^{\max} - P_{gq_2} = 192 - 143.08 = 48.92$$

Update M_1= M_1 U $\{q_2\}$={3, 11, 12} and R_1 = R_1 - $\{q_2\}$ = $\{ j \mid j = 1,2,...,30, j \neq 3, j \neq 11, j \neq 12 \}$

[Step 7.6]: $i = i + 1 = 2 + 1 = 3$.

[Step 7.7]: $\Delta P_{gp_2}^{\max} > \Delta P_{gq_2}^{\max}$. Thus $p_3 = p_2 = 3$ and $q_3 = 13$.

[Step 7.8]: $d_{3,1} = 0.58949 - (-0.097211) = 0.686701$.

Since $d_{3,1} > D_1 \cdot \alpha$, we continue doing steps 7.5 through 7.8. We repeat the above procedure until $i = 6$ for which $p_6 = 2; q_6 = 20$ and $d_{6,1} = 0.1255 < D_1 \cdot \alpha = 0.18$. Therefore we terminate the iteration. The final result is $M_1 = \{3,11,12,13,14,20\}$. Notice that for generator 13, the maximum allowed change is 0. Therefore we only select generators 3, 11, 12, 14 and 20 to manage the congestion of tie-line 1.

Similarly for congested tie-line 2, we select the following generators: 1, 2, 4, 15 and 18. That means we totally select generators 1, 2, 3, 4, 11, 12, 14, 15, 18 and 20 to relieve the congestion of the whole system.

Suppose we first do not consider the method of aggregation, i.e., we do not group generators with close sensitivity factors. We can therefore skip steps 8 through10 and obtain the following results by running (3.27)-(3.30) without any aggregation.

Table 3.5. Generations after the Congestion Management (Without Aggregation)

Generator No.	ΔP_g (MW)	P_g (MW)
1	17.0663	180.9763
2	17.2588	181.1688
3	-15.2562	273.6538
4	36.7974	467.9274
11	-3.6922	139.3878
12	-3.8297	139.2503
14	-5.016	426.114
15	-27.661	144.039
18	-10.6532	336.0468
20	-4.9994	456.9306

With this new set of generations in Table 3.5, we check the currents by running the AC power flow and find that all currents are within the limits. Tie-lines 1 and 2 which were overloaded earlier now have $I_1 = 0.4955(p.u.)$ $I_2 = 0.4921(p.u.)$, which are less than the limits 0.5 (p.u.). That means our sensitivity factor-based method solves the congestion problem. The two currents are not exactly 0.5 because our algorithm is based on the DC model.

When we determine ΔP_{ij} the desired real power flow change to eliminate the congestion, we use (3.40), which considers the effects of both real and reactive power

flows. As we know, for loads, the power factors are normally close to 1 or are corrected so that they are close to 1. That implies real powers are much bigger than reactive powers in a power system. Correspondingly, on transmission lines, real power flows are much bigger than reactive power flows. For such cases, we can neglect the effect of reactive power flows and directly use the DC model to solve ΔP_{ij}. In other words, rather (3.40), we will use the following equation:

$$| \Delta P_{ij} | = | P_{ij} - P_{ij}^{\max} | \tag{3.41}$$

where $P_{ij}^{\max} = I^{\max}$ in p.u. For our test system, in the initial state, tie-lines 1 and 2 are overloaded and the power flows (in p.u.) are:

$$S_1^0 = 0.5265 + j0.1084; \qquad S_2^0 = -0.8178 + j0.0945$$

Here we can clearly see that the reactive power flows are much smaller than the real power flows. That means we can apply (3.41). The current limits for the two tie-lines are both 0.5. Therefore we can easily obtain the desired real power flow changes to eliminate the congestion as follows:

$$\Delta P_1 = -0.0265; \qquad \Delta P_2 = 0.3178$$

By comparison, the results by using (3.40) are -0.0256 and 0.3167 respectively. The two sets of results are very close. That verifies the effectiveness of (3.41).

With $\Delta P_1, \Delta P_2$ available, we re-run our algorithm. The results are given in Table 3.6.

Table 3.6. A Comparison between the Generations Obtained by Using Equations (3.40) and (3.41)

Generator No.	P_g (MW)		Difference (%)
	Using (3.40)	Using (3.41)	
1	180.9763	181.0319	0.0307
2	181.1688	181.2252	0.0311
3	273.6538	273.4804	-0.0634
4	467.9274	468.0793	0.0325
11	139.3878	139.4109	0.0166
12	139.2503	139.2715	0.0152
14	426.114	426.1112	-0.0007
15	144.039	143.9431	-0.0666
18	336.0468	336.0189	-0.0083
20	456.9306	456.9223	-0.0018

In Table 3.6, the columns labeled as “using (3.40)” and “using (3.41)” mean the desired real power flow changes are solved by using (3.40) and (3.41) separately. This table clearly shows that the two sets of generations are very close. Concerning the currents, all lines are within the limits by using (3.41). For tie-lines 1 and 2, $I_1 = 0.4949(p.u.)$ $I_2 = 0.4920(p.u.)$. They are very close to those obtained by (3.40). Based on the results of generations and currents, we can see that when real power flows are much bigger than reactive power flows, and reactive power flows are near zero, equation (3.41) can also lead to successful elimination of congestion.

In practice, it may happen that reactive sources are not enough to correct power factors to near 1. As a result, for such loads, reactive powers are big. Correspondingly, transmission lines around such loads could have big reactive power flows. If that is the case, equation (3.41), which neglects reactive power flows, might not be effective in

eliminating congestion. To demonstrate this, we increase the reactive powers of the loads around the two tie-lines to 3 times the original values. Specifically, we change the following loads:

Table 3.7. Change of Some Loads

Load bus No.	Before the change		After the change	
	Load (p.u.)	Power factor	Load (p.u.)	Power factor
107	1.25 + j0.25	0.9806	1.25 + j0.75	0.8575
108	1.71 + j0.35	0.9797	1.71 + j1.05	0.8522
113	2.65 + j0.54	0.9799	2.65 + j1.62	0.8532
201	1.08 + j0.22	0.9799	1.08 + j0.66	0.8533
203	1.80 + j0.37	0.9795	1.80 + j1.11	0.8512
209	1.75 + j0.36	0.9795	1.75 + j1.08	0.8510
215	3.17 + j0.64	0.9802	3.17 + j1.92	0.8553
216	1.00 + j0.20	0.9806	1.00 + j0.60	0.8575

These loads are connected to the buses of the tie-lines or the lines closest to the tie-lines. Table 3.7 reveals that before the change, the loads have power factors close to 1. After we increase the reactive powers, the power factors decrease to around 0.85. With these new values of loads, we check the power flows and find that for tie-lines 1 and 2 the reactive power flows have increased greatly while the real power flows only change slightly:

Table 3.8. Power Flows (p.u.) along Tie-lines 1 and 2

	Before the load change	After the load change
Tie-line 1	0.5265 + j0.1084	0.5421+j0.4021
Tie-line 2	-0.8178 + j0.0945	-0.8368+j0.3010

According to Table 3.8, obviously these two tie-lines violate the current limits 0.5 p.u. To relieve the congestion, we first need to know the desired real power flow changes on the two congested tie-lines. By using (3.40), we have

$$\Delta P_{107,203} = -0.2243; \quad \Delta P_{113,215} = 0.4251$$

By using (3.41), we have

$$\Delta P_{107,203} = -0.0421; \quad \Delta P_{113,215} = 0.3368$$

Note: 107 and 203 are the bus IDs of tie-line 1. Similarly 113 and 215 are the bus IDs of tie-line 2.

We can then employ our algorithm of congestion management to get rid of the overload. The results of generations, power flows and currents on the two tie-lines are listed in Tables 3.9 and 3.10.

Table 3.9. Generations after the Congestion Management by Using Equations (3.40) and (3.41) Respectively

Gen. No.	P_g (MW)		Difference (%)
	By using (3.40)	By using (3.41)	
1	185.9891	181.994	-2.148
2	186.2204	182.1971	-2.1605
3	240.2881	270.481	12.5653
4	486.1635	470.7048	-3.1797
11	146.5861	139.8156	-4.6188
12	146.2159	139.6547	-4.4873
14	427.8752	426.0677	-0.4224
15	134.6666	142.2911	5.6618
18	334.2382	335.516	0.3823
20	457.2517	456.7728	-0.1047

Table 3.10. Line Flows and Currents by Using Equations (3.40) and (3.41) Respectively

		Before congestion management	After congestion management	
			By using (3.40)	By using (3.41)
Line Flow (p.u.)	Tie-Line 1	0.5421+j0.4021	0.3039+j0.3880	0.4979+j0.3929
	Tie-Line 2	-0.8368+j0.3010	-0.4265+j0.2863	-0.4838+j0.2878
Current (p.u.)	Tie-Line 1	0.6585	0.4808	0.6188
	Tie-Line 2	0.8719	0.5036	0.5519

The above table clearly shows that when we use (3.41), we cannot eliminate the congestion. On the other hand, we can still eliminate the congestion with (3.40). The currents are not exactly adjusted to the desired value 0.5 because our algorithm of congestion management is based on the DC power flow.

Based on the above examples, we can see that in a power system

- If loads have power factors close to 1, then we would expect that real power flows dominate transmission lines. Therefore we can use either (3.40) or (3.41) to calculate the desired real power flow change to get rid of the congestion. Then we can effectively eliminate the congestion by applying our algorithm of congestion management.
- If some loads have small power factors and this leads to big reactive power flows along congested lines, then basically we cannot use (3.41) to calculate the desired real power flow change to get rid of the congestion. Yet, we can still use (3.40) and then apply our algorithm of congestion management to eliminate the congestion.

We next discuss the implementation of the aggregation method and then compare the results with those obtained without the aggregation method. The loads are the original values. Therefore tie-lines 1 and 2 have very small reactive power flows. That means we can use either (3.40) or (3.41). Here we choose the simpler one (3.41).

As we have chosen α to be 0.25, according to step 3 in the algorithm, $\beta = \left[\frac{1}{\alpha}\right] = 4$. Then based on step 8 of the algorithm, we can calculate the zone boundaries for generators selected for relieving tie-line 1. That is,

[0.58949, 0.4095]; [0.4095, 0.2296]; [0.2296, 0496]; [0.0496, -0.1303]

According to the positions of the sensitivity factors in the above zones, we can easily deduce that generator 3 itself is one zone while generators 11, 12, 14, and 20 are within the same zone. With regard to tie-line 2, similarly the selected generators can be divided into three zones, namely [1, 2], [4], and [15, 18]. In other words, generators 1 and 2 are within the same zone; generator 4 itself is a zone while generators 15 and 18 are in the same zone. Combining all the zones together, we finally have the zones as shown below for the two congested lines.

[1, 2], [3], [4], [11, 12, 14, 20], [15, 18]

We therefore can map all the selected generators into 5 zones. The output limits and the bidding functions are converted according to (3.14), (3.15) and (3.21). With regard to the expression for the flows of the congested lines, in terms of step 10 of the algorithm, we have

$$\Delta P_1 = 0.1140\Delta P'_{G1} + 0.5895\Delta P'_{G2} + 0.0267\Delta P'_{G3} - 0.0802\Delta P'_{G4} - 0.0052\Delta P'_{G5}$$

$$\Delta P_2 = 0.2512\Delta P'_{G1} + 0.0689\Delta P'_{G2} + 0.5069\Delta P'_{G3} - 0.0171\Delta P'_{G4} - 0.1035\Delta P'_{G5}$$

where $\Delta P_1 = -0.0265(p.u.)$; $\Delta P_2 = 0.3178(p.u.)$ are the amounts needed to eliminate the congestion.

By applying optimization program (3.27) – (3.30) to the aggregated system, we achieve the following results (in p.u.)

$$\Delta P'_{G1} = 0.3581 \quad \Delta P'_{G2} = -0.1601 \quad \Delta P'_{G3} = 0.3838 \quad \Delta P'_{G4} = -0.1840 \quad \Delta P'_{G5} = -0.3977$$

Thus we can easily obtain the outputs and marginal costs of the aggregate generators. Next we use (3.31) and (3.32) to obtain the outputs of all individual generators at each zone. The detailed solution is provided in Table 3.11.

Table 3.11. Generations with and without Aggregation

Gen. No.	P_g		
	With aggregation(MW)	Without aggregation (MW)	Difference (%)
1	181.8174	181.0319	0.4339
2	181.8174	181.2252	0.3268
3	272.9061	273.4804	-0.21
4	469.5099	468.0793	0.3056
11	138.0496	139.4109	-0.9765
12	138.0496	139.2715	-0.8774
14	427.1064	426.1112	0.2336
15	151.8122	143.9431	5.4668
18	326.8122	336.0189	-2.7399
20	457.614	456.9223	0.1514

Some discussions about the results are as follows.

- By checking the currents under the AC environment, we find that no overloads exist. Tie-lines 1 and 2 which were overloaded previously have $I_1 = 0.4948(p.u.)$ $I_2 = 0.4923(p.u.)$, slightly less than the limits 0.5 (p.u.). That means the aggregation method effectively solves the congestion problem.
- In the above table, we also list the results obtained without grouping any selected generators into zones. It can be seen that the generations obtained with the aggregation are very close to those obtained without the aggregation method. Only generators 15 and 18 have relatively big differences. The reason is that though they are in the same zone, their sensitivity factors are in fact not so near each other. For instance, their factors are -0.1733 and -0.03376 respectively for tie-line 2. To achieve a better solution, we can further divide them into different zones. Actually

the present solution is not too bad: the biggest difference for the two methods is only 5.4668%, which is for generator 15.

- The objective functions with and without the aggregation method are the same: 156390 ($/h). This value is near that of the auction-based dispatch without considering any line limits, i.e., 156430 ($/h). The difference is only $\frac{(156390-156430)}{156430}\times 100\% = -0.0256\%$. That implies our congestion management reduces the social welfare very little and hence is a good management.
- The algorithm is implemented in Matlab language and tested on a PC with 1.24GHz AMD processor. If we let all generators participate in the congestion management, i.e., we use conventional method (3.1)-(3.5), the objective function is 156394 ($/h), slightly better than that of our method. The time consumption of the conventional method is 4.6260 (s). On the other hand, for our sensitivity factor-based method, if we do not employ the technique of aggregation, i.e., we skip steps 8-10 in our algorithm, the computation time is only 0.8120(s). If we use the aggregation technique, i.e., we run the whole algorithm, the computation time can be further reduced to 0.2910(s). This clearly shows that our sensitivity factor-based method, especially the one with aggregation, has a huge advantage in speed.

Table 3.12. A Comparison among Different Methods

	Conventional method	Sensitivity factor-based method	
		without aggregation	with aggregation
Number of variables	30	10	5
Computation time (s)	4.6260	0.8120	0.2910

The comparison in Table 3.12 reveals that our sensitivity factor-based method significantly reduces the number of variables. Correspondingly, the computation time is reduced greatly. For simplicity, we call the conventional method as method 1, the sensitivity factor-based method without aggregation as method 2, and the sensitivity

factor-based method with aggregation as method 3. Further, we define m as the ratio of the numbers of variables of two methods. For instance, when we consider methods 1 and 2, $m = \frac{30}{10} = 3$. According to the above table, we discover that the time ratio of two methods is somewhere between $O(m)$ and $O(m^2)$. Specifically, for methods 1 and 2, we have

$$m = 3 < \frac{4.6260}{0.8120} = 5.6970 < 9 = m^2$$

For methods 2 and 3, we have

$$m = \frac{10}{5} = 2 < \frac{0.8120}{0.2910} = 2.7904 < 4 = m^2$$

As we know, the main time consumption load for the above three methods is the solution of optimal program (3.1)-(3.5) or (3.27)-(3.30). Concerning the running time of an optimal program, there are two factors: the number of iterations and the computation time during each iteration. Recall that both (3.1)-(3.5) and (3.27)-(3.30) have linear constraints with the objective function being a quadratic function. That means each iteration solves a linear system such as $Ax=b$. Suppose A is a $n \times n$ matrix. The computation complexity for solving x is $O(n^3)$ for a full matrix A. For a sparse A, the computation complexity could be reduced to $O(n^2)$ or even $O(n)$. Since we utilize the sparse technique in the calculations, the computation complexity for each iteration is $O(n^2)$ or even $O(n)$, where n is the number of variables. With regard to the number of iterations, the three methods have the following results: 20, 11 and 7. That means when the number of variables decreases, the number of iterations decreases too. Combining the effects of these two factors, namely the number of iterations and the computation time for each iteration, we can see that the time ratio of two methods could be greater than $O(m)$, where m is the ratio of the numbers of variables of two methods. On the other hand, we notice that the number of iterations will reduce at a smaller rate than the number of variables. For instance, method 1 has 3 times variables of method 2 whereas

method 1's number of iterations is only $\frac{20}{11}$ times that of method 2. Further, besides the computation time for running optimal program (3.27)-(3.30), method 2 has an extra time for the selection of sensitivity factors compared to method 1. With regard to method 3, there is another extra time for aggregation in addition to the time for the selection of sensitivity factors. All these account for the fact that our case studies have a time ratio less than $O(m^2)$.

In a word, the sensitivity factor-based method, especially the one with aggregation, can reduce the number of variables greatly and thus reduce the time of computation significantly. Specifically, the time saved due to the reduction of the number of variables is better than $O(m)$.

As a conclusion, our congestion management method which is based on the sensitivity factors and the technique of aggregation is fast and accurate in calculation meanwhile can maintain market efficiency. Therefore it is a good method to manage congestion.

3.8 Conclusions

This chapter develops a new OPF method based on the sensitivity factors and the technique of aggregation to manage congestion efficiently. Unlike the conventional method which involves all generators and loads, our method selects only effective generators to eliminate congestion. Moreover, generators that have similar effects are aggregated. The selection and aggregation of effective generators lead to much fewer variables in congestion management than the conventional method. As a result, our method is much faster than the conventional method. The case studies on the IEEE RTS-96 system verify that the method proposed here can not only gain speed of solution but also maintain market efficiency. Thus it is a very effective method for congestion management.

CHAPTER IV

COMPOSITE POWER SYSTEM LONG-TERM RELIABILITY EVALUATION FOR ADEQUACY AND SECURITY

4.1 Introduction

Composite power system reliability evaluation can be subdivided into the domains of adequacy and security [9]. In the long-term reliability, though security is not the major issue, it could lead to a large loss of load. This is true especially for dynamic security problems. Thus like adequacy, security should be paid attention to in the long-term reliability study. So far people have incorporated static effects of security into the long-term reliability analysis both deterministically and probabilistically [23]. However, for dynamic effects of security, people tend to use deterministic methods. As a consequence, results could be conservative [11]. Thus it is important and necessary to develop a method to probabilistically evaluate the dynamic effects as well as the static effects of security on the long-term reliability.

In this chapter, a method based on the system state transition sampling approach, one of the sequential Monte Carlo simulation methods, is developed to probabilistically evaluate composite power system long-term reliability in both adequacy and security. The static and dynamic effects of security are incorporated. In order to consider the effects of dynamic security, we assume that a contingency on a transmission line is a fault. Further we make a distinction between permanent faults and transient faults. In the past work on reliability, only the effects of permanent faults are considered. However, according to experiences, transient faults account for more than 80% of the total faults [53]. Under transient faults the system may lose stability and has to cut load to ensure security. That implies reliability analysis should also take transient faults into account. In our work, the reclosing time together with the fault duration are used to distinguish between transient and permanent faults. And a three-state transition model for

transmission lines is proposed to include the effects of transient faults and permanent faults.

There are several uncertainties affecting transient stability calculation, for instance, locations of faults, fault-clearing phenomena, etc [54]. Here we use random numbers to represent the locations of faults. Random variables combined with probability distribution functions such as normal and Rayleigh functions are used to sample the values for the clearing time, reclosing time and fault duration. These techniques can well catch the stochastic properties of the dynamic process of the system.

Conventional reliability indices mainly focus on the static behavior of the system and cannot reflect the effects of the system dynamic process. The feature of the dynamic process is that though the time is short, it can have significant impacts on system reliability. For instance, when the system loses stability, loads might have to be shed and the amount could be large. If only the traditional indices such as *EENS* are used, the severe system situation under instability will not be reflected. Hence we introduce the index: Mean Loss of Load during Restoration (*MLLDR*) to evaluate this situation. We also use a new index: Mean Instability Occurrence Rate (*MIOR*) to show the capability of the system to sustain faults and maintain stability.

Finally to demonstrate our methodology of probabilistic evaluation of adequacy and security, and the proposed techniques for describing the stochastic properties of the dynamic process, a reliability evaluation is made on the WSCC 9-bus system. The results clearly show that dynamic security could lead to a large loss of load but the major issue in the long-term reliability is still adequacy.

4.2 Composite Power System Reliability Evaluation Using the System State Transition Sampling Approach

There are two types of probabilistic methods for evaluating composite power system reliability. One is the contingency enumeration method, and the other being the Monte Carlo simulation methods [24]. For the latter, there are two main approaches, i.e.,

the state sampling and sequential simulation approaches [13]. Both the contingency enumeration method and the state sampling Monte Carlo simulation method do not consider the effect of time. On the other hand, the sequential Monte Carlo simulation method is very suitable for considering time-related events.

Our reliability study intends to incorporate the effects of faults. That means we need to deal with time-related variables such as

- The residence time of each system state
- The time instant of fault occurrence

According the above discussion, only the sequential Monte Carlo simulation method can handle time-related variables. Therefore we adopt this method as the tool to evaluate reliability probabilistically in both adequacy and security.

The sequential Monte Carlo simulation method we use is the system state transition sampling approach. This approach is focused on state transition of the whole system instead of individual components. Since there is no need to calculate and store the chronological component state transition processes, this approach is faster and requires less memory storage than the state duration sampling approach, another sequential Monte Carlo simulation method. The only disadvantage of the system state transition sampling approach is that it assumes that the state residence times of all components follow exponential distributions. However, we point out that in composite power system reliability evaluation, exponential distributions are most commonly used [24].

Suppose there are *n* components in the system and the state duration of component *i* follows an exponential distribution with the means as $\frac{1}{\rho_i}$, where ρ_i is the transition rate of component *i*. It can then be proved that the state duration of the whole system also follows an exponential distribution with the means as $\frac{1}{\sum_i \rho_i}$ [24]. Therefore according to the property of an exponential distribution, the system state duration *T* can be expressed by the equation below.

$$T = -\frac{\ln U}{\sum_{i=1}^{n} \rho_i} \tag{4.1}$$

In the above equation, U is a uniformly distributed random number between [0, 1]. Transition rate ρ_i depends on the present state of component i. For instance, suppose component i has two states, namely the up and down states. If the present state is the up state, ρ_i is the failure rate. If the present state is the down state, ρ_i is the repair rate.

As we know, the state transition of the system is caused by the state transition of a component. Suppose there are n components in a system. Correspondingly, the system has n possible reached states. The probability that the transition of the system results from the transition of component j can be expressed by the following equation.

$$P_j = \frac{\rho_j}{\sum_{i=1}^{n} \rho_i} \tag{4.2}$$

Obviously,

$$\sum_{j=1}^{n} P_j = 1 \tag{4.3}$$

Therefore, we can use a uniformly distributed random number between 0 and 1 to determine the next system state. Specifically, we first calculate the probabilities of the n possible reached states according to (4.2). Then we place these n probabilities in the period [0, 1]. Next we generate a uniformly distributed random number U' between [0, 1]. If U' falls into the segment corresponding to probability P_j, that indicates the transition of the system state is caused by the transition of component j. Fig. 4.1 below illustrates that the transition of component 2 leads to the transition of the system state.

Fig. 4.1. Determination of Next System State
by a Uniformly Distributed Random Number

Basically composite power system reliability evaluation by using the system state transition sampling approach involves the following three steps:

- State selection
- State evaluation
- Reliability index calculation

In brief, each time a system state is selected and then evaluated. If there is a loss of load, reliability indices are updated correspondingly. These processes repeat until certain convergence criterion is reached. In terms of the discussions about the system state transition sampling approach, we can use (4.1) to determine the duration of the present system state. To select the next system state, we can use (4.2) together with a random number. Both (4.1) and (4.2) involve component transition rates which are associated with the transition models of components. Thus below we will first talk about the models of components. Then we will explain state evaluation and reliability index calculation. Finally a methodology to evaluate reliability in both adequacy and security will be presented.

4.3 Transition Model for Transmission Lines Considering Permanent and Transient Faults

In composite power system reliability evaluation, we assume that there are two major types of components, namely generators and transmission lines. For generators, it

is assumed that there are only two states, i.e., the up and down states. The state transition diagram of a generator is shown in Fig. 4.2 below:

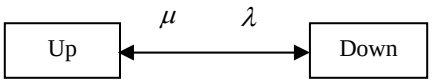

Fig. 4.2. Two–state Transition Model of a Generator

In the above figure, λ stands for the failure rate and μ stands for the repair rate.

Concerning transmission lines, conventionally a two-state model like that in Fig.4.1. is used. However, such a two-state model can only represent one type of faults. In other words, it cannot include the effects of both permanent and transient faults. As we know, in most cases, faults are transient [53]. And it is probable that the system loses stability under a transient fault. Therefore the effects of transient faults should be considered for a comprehensive reliability study. To incorporate the impacts of both permanent and transient faults, we propose a three-state transition model for transmission lines. The details are shown in Fig. 4.3.

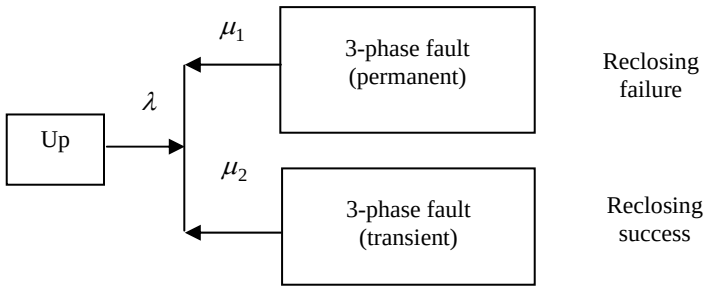

Fig. 4.3. Three-state Transition Model of a Transmission Line
Considering Both Permanent and Transient Faults

In the figure above, λ is the failure rate of the transmission line. μ_1 and μ_2 are the repair rates corresponding to a permanent fault and a transient fault respectively. μ_1 is much smaller than μ_2 because in the former case the fault is permanent. From this figure, it can be seen that we distinguish a permanent or transient fault on a transmission line in terms of the status of the reclosure. Specifically, if the reclosure is successful, the fault is transient. Otherwise it is a permanent fault. To determine the status of the reclosure, the reclosing time together with the fault duration are used. If the fault duration is less than the reclosing time, i.e., the fault has disappeared when the line reconnects, the reclosure is successful. If the fault duration is greater than the reclosing time, the reclosure fails.

According to the above analysis, we can see that the clearing time, reclosing time and fault duration are key parameters for determining the state of a transmission line. All of these three parameters are actually random variables. For instance, though the clearing time is preset, in practice the time at which a breaker opens may deviate from the preset value due to harmonics in the input waveforms, etc. Experiences show that these three parameters satisfy certain distributions. Specifically, the clearing time can be considered as a random variable following a normal distribution. The reclosing time can also be considered to follow a normal distribution. Concerning the fault duration, usually a Rayleigh distribution is used [54, 55]. The parameters for these distributions such as mean time and variance can be obtained from experiments and historic data.

We point out that the location of a fault is uncertain. In this work, a uniformly distributed random number U between [0, 1] is used to represent the fault location [56]:

$$L = U \tag{4.4}$$

where L is the distance percent between the location of the fault and the sending end of the line.

Although in Fig. 4.2, only 3-phase faults are considered (their effects are most severe among all faults), other types of faults such as line-to-line faults can be included

easily. We can simply add the corresponding failure and repair rates of these faults to the model in Fig. 4.2.

After obtaining the transition models for generators and transmission lines, we can calculate the duration of system state by substituting transition rates into (4.1). By plugging transition rates into (4.2) and generating a uniformly distributed random number between [0, 1], we can determine the next system state. For each system state, we should evaluate if the system has a load curtailment or if the system is insecure. If the answer is yes, we need to update reliability indices. The details are given in the following sections.

4.4 State Evaluation

4.4.1 Transient Stability Analysis

In conventional reliability studies, it is assumed the faulted component will be isolated from the system immediately after a contingency occurs. And the system will settle at a steady state instantaneously. However, in practice, the system will experience a dynamic process before reaching a static state.

Suppose the current system state is a contingency state in which there is a 3-phase fault on a transmission line. The system will be in the faulted state until the fault is cleared by the breaker and the line disconnects from the system. After the line is disconnected for a moment, the breaker will attempt to re-closes. At this time instant, if the fault still exists, the reclosure will fail and we consider this fault as a permanent one. On the other hand, if the fault has disappeared when the breaker re-closes, the reclosure will be successful and the fault is considered to be transient. This procedure can be illustrated using a flow chart as shown in Fig. 4.4 below.

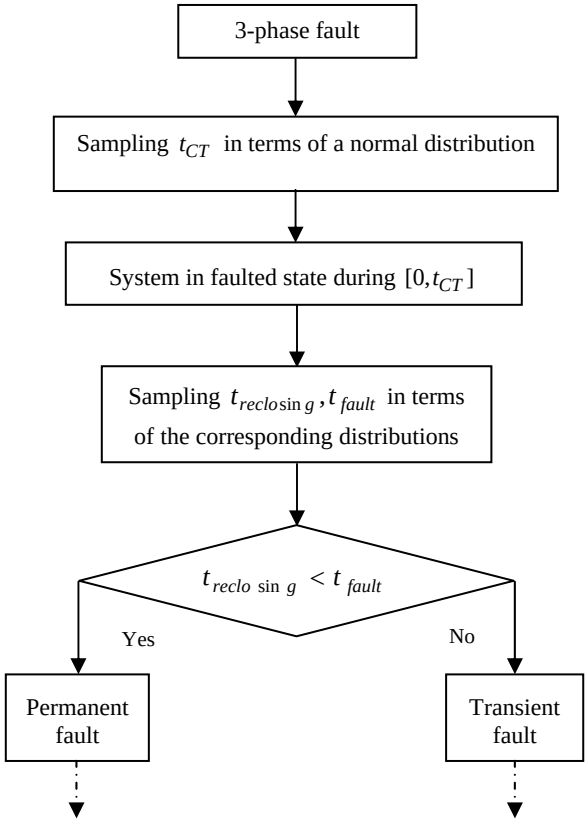

Fig. 4.4. Distinction between a Permanent Fault and a Transient Fault

In the above flow chart, t_{CT} stands for the clearing time and is decided by a normal distribution. $t_{reclosing}$ means the reclosing time, which is also from a normal distribution. t_{fault} refers to the fault duration, which is determined by a Rayleigh distribution.

No matter whether the fault on a transmission line is permanent or transient, we need to judge if the system is stable or not. Here we use the numerical integration method to analyze the transient stability.

Basically, the overall system equations consist of differential and algebraic equations:

$$\dot{X} = f(X, I, V, C) \tag{4.5}$$

$$g(X, I, V) = 0 \tag{4.6}$$

Where:

X is the vector of state variables such as rotor angle δ and rotor angular velocity ω.

I is the vector of injected currents.

V is the vector of bus voltages.

C is the vector of constants such as mechanical powers.

To simplify the matter, we adopt the classic model for generators. And the loads are assumed as constant impedances.

To solve (4.5) and (4.6), we use the partitioned approach along with the fourth order Runge-Kutta method. In this approach, we solve the algebraic and differential equations separately. Notice that state variables cannot change instantly. Thus we solve the algebraic equation (4.6) first to obtain V and I. Then with the known values of V and I together with the value of X at the previous time step, we solve (4.5) for X at the current time step by using the 4^{th} order Runge Kutta method. (The description of the Runge-Kutta method can be found in [57]). We repeat the above procedure until a stopping criterion is reached. Usually the loss of synchronism due to transient stability will become evident within 2 to 3 seconds [53]. Thus in our work, we simulate the behavior of generator rotor angles for 3 seconds. If during this simulation period, the largest rotor angular deviation between any two generators does not exceed the maximum secure angle difference, which is set as 180 degree, we assume the system is stable. Otherwise the system is considered to lose stability. If the system is stable, it will settle down to a steady state soon. If the system loses stability, protection actions will trip the asynchronous generators and then the rest of the system will gradually settle at a stable state, i.e., restorative state. It is called the restorative state because restorative actions will be taken to resynchronize those tripped generators and then reconnect them to the system.

4.4.2 Calculation of Loss of Load Using OPF

When the system reaches a stable state, we will run an Optimal Power Flow (OPF) to calculate the loss of load. The formulation of the OPF is shown as follows.

Objective:

$$f = \min\left(\sum_{i=1}^{n_d}(P_{di} - P_{li})\right) \tag{4.7}$$

Subject to:

$$\begin{cases} P_{gi} - P_{li} - \sum_{j=1}^{n} U_i U_j (G_{ij}\cos\theta_{ij} + B_{ij}\sin\theta_{ij}) = 0 \\ Q_{gi} - Q_{li} - \sum_{j=1}^{n} U_i U_j (G_{ij}\sin\theta_{ij} - B_{ij}\cos\theta_{ij}) = 0 \end{cases} \quad (i = 1, \cdots, n) \tag{4.8}$$

$$\begin{cases} P_{gi\min} \le P_{gi} \le P_{gi\max} \\ Q_{gi\min} \le Q_{gi} \le Q_{gi\max} \end{cases} \tag{4.9}$$

$$\begin{cases} 0 \le P_{li} \le P_{di} \\ 0 \le Q_{li} \le Q_{di} \end{cases} \tag{4.10}$$

$$\frac{P_{li}}{Q_{li}} = \frac{P_{di}}{Q_{di}} \tag{4.11}$$

$$U_{i\min} \le U_i \le U_{i\max} \tag{4.12}$$

$$P_{ij}^2 + Q_{ij}^2 \le S_{ij\max}^2 \qquad ij \in [1, \cdots, n_b] \tag{4.13}$$

where

n, n_b are the numbers of buses and branches respectively;

P_{gi}, Q_{gi} are the real and reactive generations at bus *i*;

$P_{gi\max}, P_{gi\min}$ are the limits of P_{gi};

$Q_{gi\min}, Q_{gi\max}$ are the limits of Q_{gi};

P_{li}, Q_{li} are the real and reactive loads at bus *i* after the redispatch of generations;

P_{di}, Q_{di} are the load demands at bus *i*;

P_{ij}, Q_{ij} are the real and reactive power flows along line *ij*;

$S_{ij\max}$ is the flow limit of line *ij*;

U_i is the voltage magnitude at bus *i*;

$U_{i\min}, U_{i\max}$ are the voltage magnitude limits of bus *i*.

The objective of this OPF is to determine the minimum amount of load curtailment of the whole system. If the objective function is zero, that means there is no load loss for this system state.

4.5 Reliability Indices Associated with Transient Stability

When the OPF determines that there is a loss of load, we need to update reliability indices. Conventional reliability indices are mainly focused on the adequacy aspect of reliability. For instance, the following two indices are widely used in reliability evaluation:

- Expected Energy Not Supplied (MWh/year) --- *EENS*

$$EENS = \frac{\sum_{i=1}^{n} C_i D_i}{TS} \tag{4.14}$$

where C_i (MW) and D_i are the loss of load and the duration of load curtailment system state *i*. *n* is the number of load curtailment system states. *TS* (year) is the total simulation time.

- Loss Of Load Probability ---- *LOLP*

$$LOLP = \frac{\sum_{i=1}^{n} D_i}{TS \times 8760} \tag{4.15}$$

The above two indices are time-related. As we know, when the system loses stability, the restoration period is very short: usually around one hour [57]. On the other hand, when a component is in the down state, normally it will take more than 10 hours to repair the component. That means the severe effect of instability on system reliability cannot be reflected if only *EENS* and *LOLP* are used. Hence we introduce two new indices to reflect the effect of transient stability.

- Mean Instability Occurrence Rate (occ./year) --- *MIOR*

$$MIOR = \frac{\sum_{i=1}^{m} I_i}{TS} \tag{4.16}$$

where m is the total number of transient stability calculation. I_i is 1 if the system is unstable. I_i is 0 if the system is stable.

As discussed previously, instability has great influence on the reliability of power systems especially those operating near their stability limits. Therefore, this index is introduced to reflect the ability of system to sustain faults. To emphasize the effects of transient faults, the index values caused by permanent and transient faults can be calculated respectively.

- Mean Loss of Load during Restoration (MW/occ.) --- *MLLDR*

$$MLLDR = \frac{\sum_{i=1}^{NR} R_i}{NR} \tag{4.17}$$

where *NR* is the total number of restorative states the system experiences during the Monte Carlo simulation. R_i is the load curtailment in restorative state *i*.

Conventionally, when there is a contingency on a transmission line, it assumes that the line is disconnected from the system without any stability problem. Then an OPF program is run to obtain the loss of load of the system. Obviously this can not reflect the practice. When a fault occurs to a transmission line, the system may lose stability and then experience a restoration process. Though the restorative time is short, the loss of load is usually large. Obviously the system is under a severe circumstance. However conventional reliability indices are mainly aimed at adequacy and cannot reflect the loss of load in the restoration. To give a more comprehensive description of the system under instability, we introduce the index *MLLDR*, which measures the mean loss of load during the restorative state. Like the first introduced index *MIOR*, we can calculate *MLLDR* under permanent and transient faults respectively to show the effects of these two types of faults. We can also compare *MLLDR* with the mean loss of load by the conventional steady state method to illustrate the significant impact of instability.

4.6 Methodology of Composite Power System Reliability Evaluation for Adequacy and Security

Composite power system reliability evaluation in both adequacy and security by using the system state transition sampling approach can be summarized in the following steps:

1. The evaluation starts from the system state in which all components are in the up state.
2. Generate a uniformly distributed random number *U* between [0, 1] to determine the duration of the present system state by using (4.1).
3. Evaluate the present system state. Specifically,

- If the present system state is a contingency state in which a fault occurs to a transmission line, then
  i. Sample fault clearing time $t_{clearing}$ by using a normal distribution.
  ii. Sample breaker reclosing time $t_{reclosing}$ and fault duration t_{fault}.
  iii. Compare $t_{reclosing}$ and t_{fault} to determine if the fault is transient or permanent.
  iv. Assess transient stability by using the time domain simulation method, namely the partitioned approach along with the fourth order Runge-Kutta method.
  v. If the system is unstable, protection actions will trip the asynchronous generators. Run OPF (4.7) – (4.13) to determine the loss of load in the restorative state and then after the restorative state. If the system is stable, Run OPF (4.7) – (4.13) directly to determine the loss of load.
- If the present system state is a contingency state in which a generator is down, run OPF (4.7) – (4.13) to determine the loss of load.
- If the present system state transits from a system state in which a component is repaired, run OPF (4.7) – (4.13) to determine the load curtailment.

4. Update reliability indices by using (4.14) – (4.17) if the system has a loss of load or the system is unstable.
5. If the convergence criterion is satisfied, terminate the simulation. Otherwise proceed to step 6.
6. Generate a uniformly distributed random number U' between [0, 1] to decide the next system state according to the technique described in section 4.2. Return to step 2.

In the above reliability evaluation, when the system loses stability, it will go through a restorative state in which asynchronous generators are disconnected from the system. During this restorative state, people will take actions to resynchronize those tripped generators and then reconnect them back to the system. In other words, during and after the restoration, the system will have different structures, i.e., those

asynchronous generators. Therefore we run OPF twice to calculate the loss of load in these two situations.

In step 5, the convergence criterion is that either of the following two conditions is satisfied:

- The simulation reaches a specified number of years.
- The coefficients of variation of certain reliability indices are all less than a given tolerant error. In the conventional reliability evaluation, usually *EENS* is slowest in convergence among reliability indices. Thus its coefficient of variation is often used as the convergence criterion. As we introduce two new reliability indices *MIOR* and *MLLDR*, we also need to consider their coefficients of variation during simulation.

4.7 Case Studies

4.7.1 Test System

The proposed methodology is applied to the WSCC 9-bus system as shown in Fig. 4.5. The data about power flow and synchronous machines can be found in [58]. The reliability data, such as the failure and repair rates of components, fault duration time etc, are given in Tables 4.1 to 4.5.

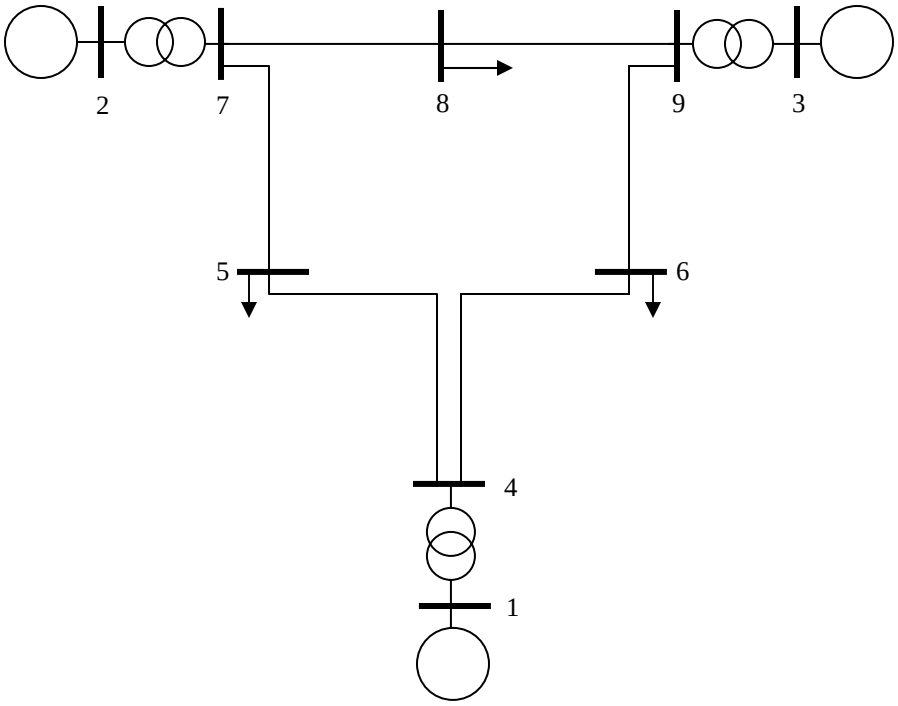

Fig. 4.5. WSCC 9-bus System

Tables 4.1 and 4.2 list the failure rate λ and the repair rate μ of each component.

Table 4.1. Failure / Repair Rates of Generators and Transformers

	No.	λ (occ./ year)	μ (occ./ year)
Generators	1	5	195
	2	5	195
	3	5	195
Transformers	1	4	196
	2	4	196
	3	4	196

Table 4.2. Failure / Repair Rates of Transmission Lines

No.	λ (occ./year)	μ (occ./year)
1	5	193
2	5	193
3	5	193
4	5	193
5	5	193
6	5	193

Note: The repair rates in Table 4.2 are for permanent 3-phase faults. If faults are transient, a very big number can be used to represent the repair rates.

Table 4.3 below shows the probability distribution of the fault clearing time of every transmission line.

Table 4.3. Probability Distribution of the Fault Clearing Time

Line	Type of distribution	Mean time (s)	Variance (s)
1	Normal	0.07	0.01
2	Normal	0.07	0.01
3	Normal	0.06	0.01
4	Normal	0.05	0.01
5	Normal	0.04	0.01
6	Normal	0.03	0.01

Tables 4.4 and 4.5 show the probability distributions of the reclosing time and fault duration.

Table 4.4. Probability Distribution of the Reclosing Time

Line	Type of distribution	Mean time (s)	Variance (s)
1	Normal	0.55	0.02
2	Normal	0.75	0.02
3	Normal	0.65	0.02
4	Normal	0.55	0.02
5	Normal	0.85	0.02
6	Normal	0.65	0.02

Table 4.5. Probability Distribution of the Fault Duration

Line	Type of distribution	*k*
1	Rayleigh	0.29
2	Rayleigh	0.39
3	Rayleigh	0.34
4	Rayleigh	0.28
5	Rayleigh	0.44
6	Rayleigh	0.34

4.7.2 Results and Analysis

As discussed earlier, of the conventional reliability indices, the index *EENS* has the slowest rate of convergence. For the two new introduced indices *MIO*R and *MLLDR*, our simulations show that the latter is slower in convergence. Therefore in the case studies, we consider that the sequential Monte Carlo simulation converges if either of the following two conditions is satisfied: The simulation reaches 800 years or the maximum of coefficients of variation of *EENS* and *MLLDR* is less than 0.04. For our reliability

evaluation of the WSCC 9-bus system, the first convergence condition leads to the termination of the simulation. Below are some of the results.

EENS = 12036.7311(MWh/year)

LOLP = 0.0550

$MLLDR_1$ = 120.0404 (MW/occ.)

$MLLDR_2$ = 41.5675 (MW/occ.)

Cov_1 = 0.0303; Cov_2 = 0.0367; Cov_3 = 0.0466

where:

$MLLDR_1$ is related to permanent faults.

$MLLDR_2$ is related to transient faults.

Cov_1 is the coefficient of variation for *EENS*.

Cov_2 is the coefficient of variation for $MLLDR_1$.

Cov_3 is the coefficient of variation for $MLLDR_2$.

In the reliability evaluation, we calculate *MLLDR* for permanent faults and transient faults separately. Specifically, $MLLDR_1$ is related to permanent faults while $MLLDR_2$ is associated with transient faults. According to the results, we can see that $MLLDR_2$ is smaller than $MLLDR_1$. In other words, transient faults cause less loss of load than permanent faults. The reason is that transient faults mean the reclosure is successful. As a result, the system under transient faults is more robust than the system under permanent faults. Correspondingly, the system with transient faults usually has less loss of load.

The above results about the coefficients of variation reveal that $MLLDR_2$ converges slower than *EENS* and $MLLDR_1$. When the simulation ends, both the coefficients of variation of *EENS* and $MLLDR_1$ are less than the given tolerant error 0.04 while the coefficient of variation of $MLLDR_2$ is greater than the given tolerant error. Though the coefficient of variation of $MLLDR_2$ does not converge to the desired value 0.04, it is very close. Figs. 4.6 – 4.9 below show the convergence processes of some of the indices as the simulation time increases.

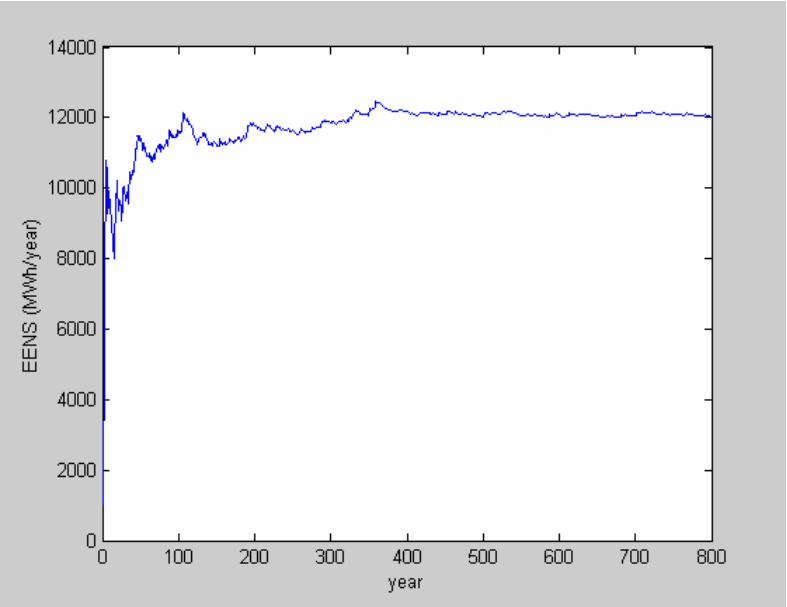

Fig. 4.6. Response of *EENS* with the Simulation

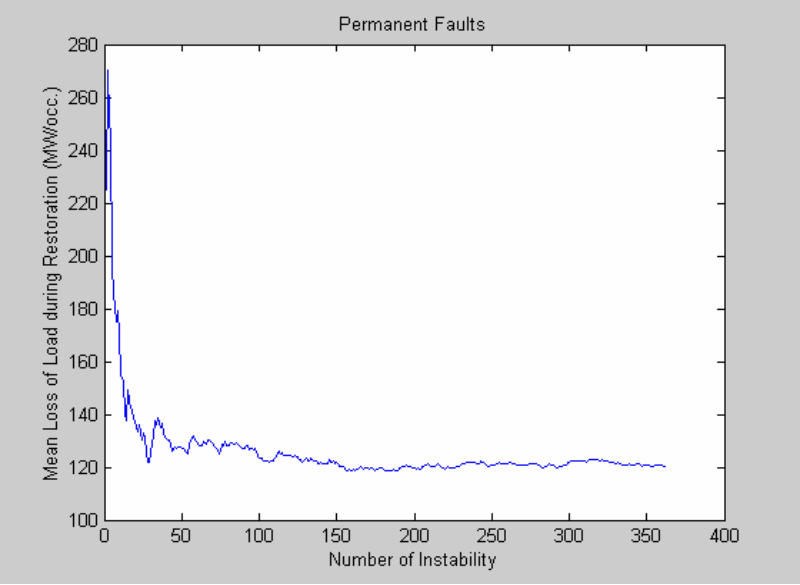

Fig. 4.7. Response of $MLLDR_1$ with the Simulation

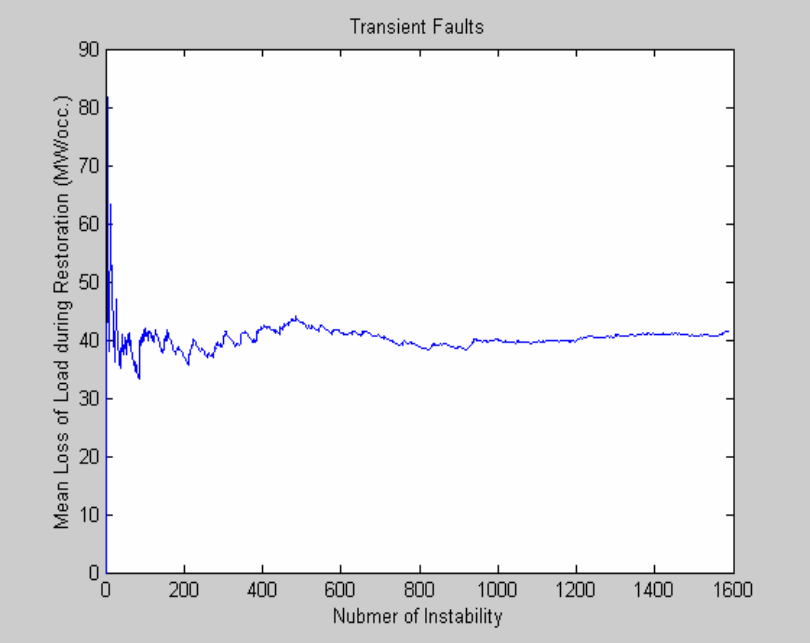

Fig. 4.8. Response of $MLLDR_2$ with the Simulation

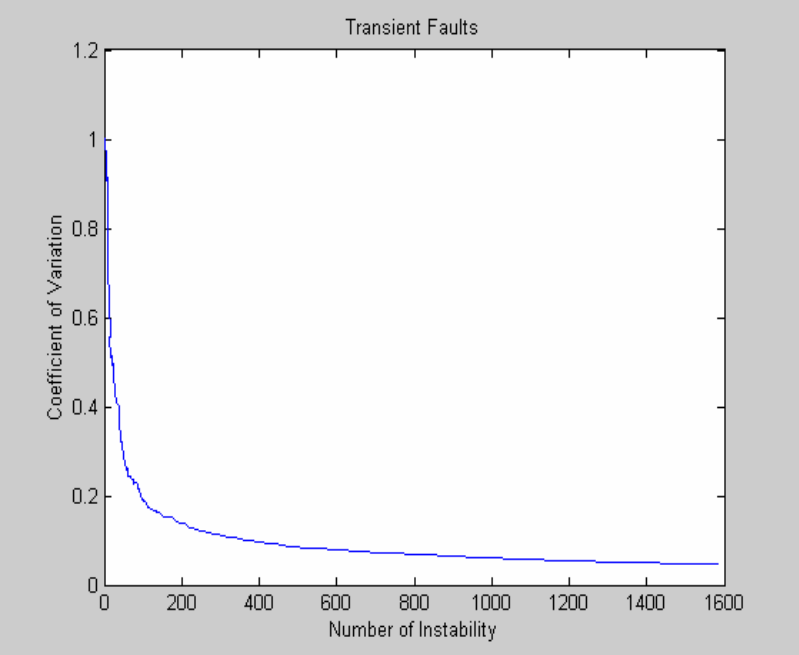

Fig. 4.9. Response of Cov_3 with the Simulation

From the above curves, we can see:

- The reliability indices change greatly at the beginning of the simulation. As the simulation goes by, these indices gradually stabilize at certain values. For instance, the index *EENS* finally stabilize at 12000 (MWh/year).
- Though Cov_3, the coefficient of variation of $MLLDR_2$ has not yet reached the given tolerant error 0.04 at the end of the simulation, it decreases as the number of instability increases. In other words, the whole trend is that Cov_3 will decrease as the simulation time increases. That implies if the simulation is longer, Cov_3 will eventually reach 0.04.

The convergence processes shown in the above figures illustrate that our composite power system reliability evaluation based on the sequential Monte Carlo simulation method is valid.

Like the index *MLLDR*, we also calculate the index *MIOR* for permanent and transient faults respectively. The results are given in the table below.

Table 4.6. *MIOR* under Permanent and Transient Faults

Disturbance type	*MIOR* (occ./year)
Permanent faults	0.4538
Transient faults	1.9825

Table 4.6 shows that *MIOR* related to transient faults is much greater than that related to permanent faults. The reason behind this is that transient faults happen much more frequently than permanent faults. The table below demonstrates this point.

Table 4.7. Information about Reclosing

Reclosing status	Number of occurrence
Success	21542
Failure	4110

Table 4.7 is about the status of reclosing in the whole simulation process. It can be seen that in most cases, the reclosing is successful. Specifically, the percent of successful reclosing is about 84% among all reclosing cases. We distinguish transient and permanent faults in terms of the status of reclosing. Therefore the above table means that among all faults of the simulation, 84% are transient. This accounts for the fact that *MIOR* associated with transient faults is greater than that associated with permanent faults. In practice more than 80% of all faults are transient [53]. This is consistent with our result. That means our input data about the fault duration and reclosing time are reasonable and the simulation reflects the practical operation of power systems.

The above analysis illustrates that transient faults have a big effect on the system reliability. We can also investigate the effect of transient faults from the number of loss of load.

Table 4.8. Number of Loss of Load Caused by Permanent and Transient Faults

Disturbance type	Number of Loss of Load
Permanent faults	755
Transient faults	1101

From Table 4.8, we can see that loss of load caused by transient faults is more often than that caused by permanent faults. Of course for the amount of loss of load, permanent faults have a more significant effect than transient faults. This can be reflected from the fact that $MLLDR_1$ is greater than $MLLDR_2$ (Please see our earlier results for details), where $MLLDR_1$ is related to permanent faults while $MLLDR_2$ is related to transient faults.

We also calculate the mean loss of load by the conventional steady state method. The value is 25.6407 (MW/occ), which is much smaller than $MLLDR_1$ and $MLLDR_2$ whose values are 120.0404 (MW/occ.) and 41.5675 (MW/occ.) respectively. This comparison means that the dynamic security has a significant impact on the loss of load.

The above analysis clearly shows the effect of dynamic security, i.e., it can cause a huge loss of load. However, as we pointed out that the occurrence of dynamic security is very rare. If we consider the loss of energy in the long-term, the influence of dynamic security could be very small. To demonstrate this, we compare the values of *EENS* with dynamic security included and without dynamic security included.

$$\frac{12036.7311 - 11866.2357}{12036.7311} \times 100\% = 1.42\%$$

In the above calculation, the value of *EENS* that considers dynamic security is 12036.7311; and the value of *EENS* without considering dynamic security is 11866.2357. The small difference between the two *EENS*'s implies that dynamic security contributes little to the long-term loss of energy. Therefore we can conclude though dynamic security can cause a serious loss of load, adequacy is still the main issue of the long-term reliability.

4.8 Conclusions

This chapter develops a method to probabilistically evaluate composite power system long-term reliability in both adequacy and security. The method is based on the system state transition sampling approach, one of the sequential Monte Carlo simulation methods. To consider the effects of both permanent and transient faults, a 3-state transition model for transmission lines is developed. To capture the stochastic properties of the dynamic process after a fault, random variables in conjunction with probability distribution functions are used. Two new reliability indices related to transient stability are introduced to give a comprehensive description of the dynamic process following a fault. The study on the WSCC 9-bus system demonstrates that dynamic security has a significant effect on the loss of load but adequacy is still the major issue in the long-term reliability.

CHAPTER V

IMPACTS OF FACTS ON COMPOSITE POWER SYSTEM RELIABILITY

5.1 Introduction

Highly reliable power systems are crucial to the continuing advancement for a society. Since the introduction of markets into power systems, however, reliability level has declined [10, 14]. On the one hand, this indicates that the design and operation of today's power markets are far from mature and perfect. On the other hand, this requires special attention to the improvement of power system reliability. The conventional way to enhance reliability is to construct a robust system, i.e., building more power plants and more transmission lines. However, this way is not easy to implement because of such factors as costs, environment and politics. Alternate efficient methods must be searched for implementation.

In many situations, the inadequacy of power supply after a contingency is caused by the decrease of transfer capability due to the loss of some components such as transmission lines and generators. Therefore techniques which can control power flow and thus improve power transfer situation will be helpful for improving system reliability. FACTS like TCSC, SVC and TCPAR have the ability to alter power flow pattern. More importantly, they can change their parameters smoothly and rapidly, which will allow a more desirable control of power flow. Therefore FACTS are good candidates for power system reliability improvement. In addition, there are fewer restrictions on the installation of FACTS than on the construction of new lines or plants. Thus we propose to use FACTS as the tools for the enhancement of reliability.

There are three important operational parameters FACTS can control, i.e., impedance, voltage, and phase angle. Correspondingly, this chapter will investigate the effects of TCSC, SVC and TCPAR which can control impedance, voltage and phase angle respectively. We first examine the structures and principals of operation of TCSC,

SVC and TCPAR. Then we built their reliability models via the state space approach. Next we dispatch them during contingencies through an OPF program. We finally investigate the impacts of these three devices on composite power system reliability through some case studies.

5.2 Reliability Models of TCSC, SVC, and TCPAR

5.2.1 Reliability Model of TCSC

5.2.1.1 Structure of TCSC

Generally a typical TCSC is made up of a number of modules [29]. For instance, the TCSC in Fig. 5.1 consists of 4 modules.

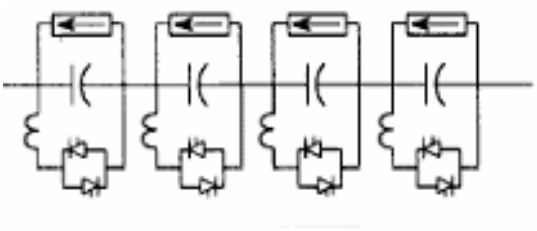

Fig. 5.1. Structure of a 4-module TCSC (Adapted from [29])

From the above figure, we can see that each TCSC module consists of a series capacitor with a parallel path including a thyristor switch and a series inductor. Also in parallel is a metal-oxide varistor (MOV) for overvoltage protection.

5.2.1.2 TCSC Capability Characteristic

Basically, a TCSC module operates in one of the following three modes:

- Thyristor blocked. In this mode, the thyristor is not fired and the module works like a capacitor.
- Thyristor bypassed. The module appears as a small inductor with the full conduction of thyristor.
- Thyristor phase control, i.e., vernier mode. This mode is between the above two extremities. Hence the module can present as a capacitor or inductor.

The reactance-current capability curves of a TCSC module are shown in Fig. 5.2.

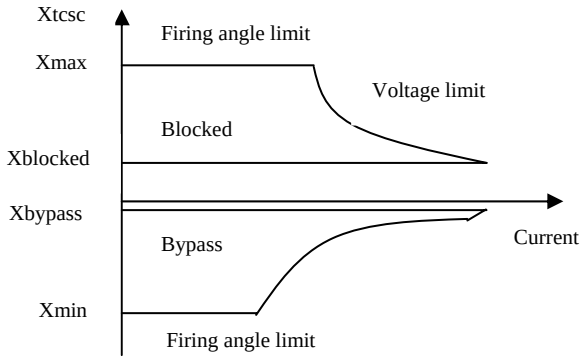

Fig. 5.2. Capability Curves of a Single Module

For a multi-module TCSC, its capability curves are associated with not only the curves of a single module but also the number of modules available. Fig. 5.3 below shows the reactance-current capability curves of a 4-module TCSC with different numbers of modules at work [30].

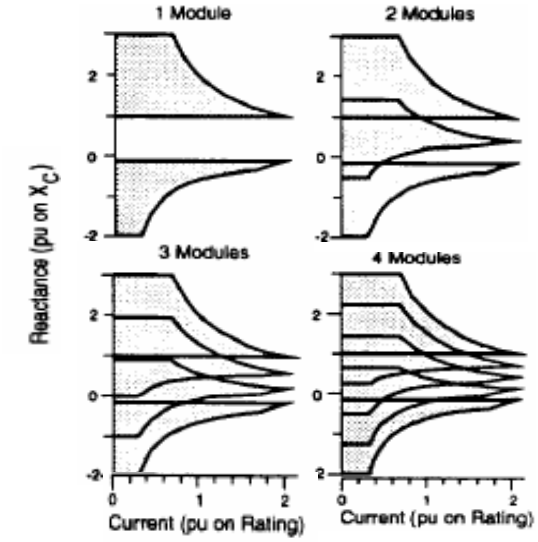

Fig. 5.3. Capability Curves of a 4-modue TCSC
with Different Numbers of Modules at Work (Adapted from [30])

From Figs. 5.2 and 5.3, we can also see that the behavior of a TCSC or the apparent reactance of a TCSC is determined by many factors such as thyristor firing angle, voltage limit etc [31-33]. For steady state reliability analysis, to simplify the matter, it assumes that only the firing angle decides the capacity of the TCSC. That means other factors like the voltage limit are always satisfied so that they can be neglected. Based on the above assumption, the TCSC reactance can be simply expressed as a reactance range like [X_1, X_2]. The figure below shows the steady model of a TCSC on transmission line *ij*.

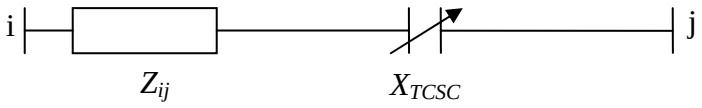

Fig. 5.4. Steady State Model of a TCSC

In Fig. 5.4, Z_{ij} is the impedance of line *ij*. X_{TCSC}, the reactance of the TCSC is variable between range [X_1, X_2]. This range is associated with the number of operational modules. For instance, in Fig. 5.3 there is a gap in the range for one single module. In other words, this reactance range is discontinuous: $X_{TCSC} = \left([X_{\max}, X_{blocked}] \cup [X_{bypass}, X_{\min}]\right)$. When there are 2 or more modules at work, the gap is filled so the entire range is continuous: $X_{TCSC} \in [X_{\max}, X_{\min}]$. (The meanings of $X_{\max}$, X_{blocked}, X_{bypass}, and $X_{\min}$ can be referred to Fig. 5.3.)

5.2.1.3 Reliability Model of TCSC

There are two levels of control and protection of a TCSC corresponding to a single module and the whole TCSC: module control and protection (MCP) and common control and protection (CCP). In addition, for each module, there is a bypass breaker. And there is a bypass breaker for the whole TCSC too. Therefore, the MCP and the module bypass breaker will act when there is a problem in the module. Similarly, the CCP and the TCSC bypass breaker will work for problems in the whole TCSC.

To build the reliability model of a TCSC, we make the following assumptions:

- For each module there are only two states, namely the up and down states.
- Each time there is only one module down.
- When a module fails, there will be 3 possibilities:
  - The bypass breaker across it closes automatically, and the failed module is isolated. Other modules continue to work.
  - Its bypass breaker fails to close; in reaction, the bypass breaker of the TCSC closes automatically and the whole TCSC is bypassed.
  - Both bypass breakers fail to function, and the TCSC goes to emergency state. The TCSC will transit to the bypassed state if the manual control of the bypass breaker of the TCSC switches successfully.

In terms of the above information, we can determine the reliability model for a TCSC. Fig. 5.5 below shows the model of a 4-module TCSC.

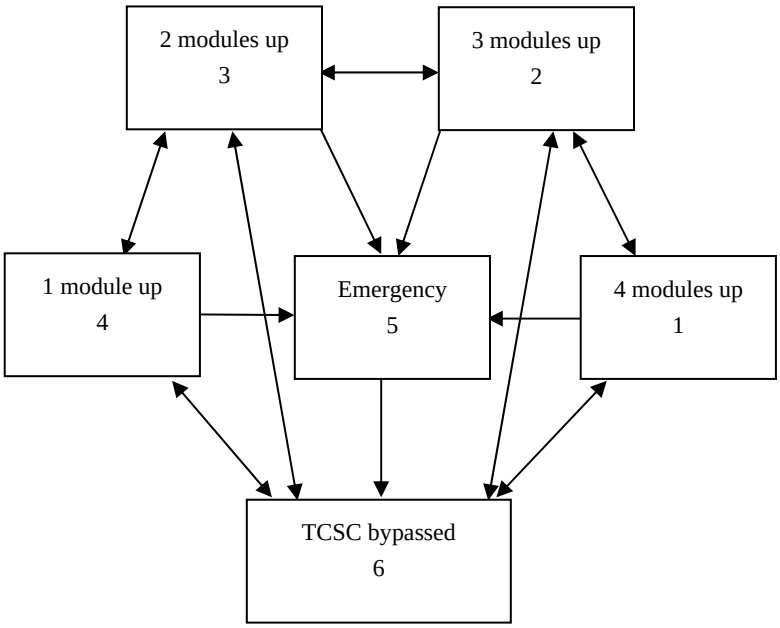

Fig. 5.5. State-space Model of a 4-module TCSC

In the above figure, the number on the bottom of each block stands for the state No. For example, state 5 is the emergency state. The state represents that the TCSC fails and the transmission line where TCSC is placed can no longer transfer any power. In state 6, the TCSC is bypassed because of the closure of the bypass breaker across the TCSC or the bypass breakers across all the modules. Hence the TCSC is essentially short-circuited and contributes nothing to the corresponding line.

The probability of each state in Fig. 5.5 can be calculated by solving the following equation:

$$\begin{cases} pR = 0 \\ \sum_{i=1}^{6} p_i = 1 \end{cases} \tag{5.1}$$

where p is a row vector whose *ith* element p_i is the probability of state i. R is a 6×6 transition rate matrix which is obtained based on the Markov Chains in Fig. 5.5.

5.2.1.4 Reliability Model of a Line with a TCSC

To develop the reliability model of a line with a TCSC, we assume that transmission lines only have up and down states and the TCSC consists of 4 modules. Hence the number of states for the line with the TCSC is $6 \times 2 = 12$, where 6 is the number of states of the TCSC as described in Fig. 5.5 and 2 is the number of states of the transmission line. Table 5.1 lists all the states.

Table 5.1. States of a Line with a 4-module TCSC

State No.	TCSC & Line states	State No.	TCSC & Line states
(1)	4 modules up & line up	(7)	4 modules up & line down
(2)	3 modules up & line up	(8)	3 modules up & line down
(3)	2 modules up & line up	(9)	2 modules up & line down
(4)	1 module up & line up	(10)	1 module up & line down
(5)	Emergency & line up	(11)	Emergency & line down
(6)	TCSC bypassed & line up	(12)	TCSC bypassed & line down

The impact of the states on the transfer capability, which is our major concern in reliability analysis, can be observed in this way:

- If the line is up, then as long as some modules work, in terms of the TCSC capability characteristic discussed earlier, the TCSC can adjust its reactance. Accordingly, the system can operate in a state in which the loss of load is less than it would be without the TCSC. Of course, the effects may differ depending on how

many modules are up. Generally, state (1) has the greatest effects, followed by states (2), (3) and then (4).

- In state (6) or (12), the TCSC is bypassed. So the TCSC is virtually short-circuited. Therefore, the status of the composite component is only decided by the line state.
- The TCSC is in series with the line. Hence the composite component cannot transfer any power when either the TCSC or the line itself is down. Based on this, we can combine states (5), (7)-(12) into one, called “down state”.

According to the above discussions, we can simplify the reliability model of a line with a 4-module TCSC from 12 states to 6 states:

(a) 4 modules up & line up.
(b) 3 modules up & line up.
(c) 2 modules up & line up.
(d) 1 module up & line up.
(e) Down.
(f) TCSC bypassed & line up.

If the TCSC has the characteristic as shown in Fig. 5.3, i.e., when 2 or more modules are at work, the reactance control ranges are the same, we can further combine states a)-c) into one, called “multi-module up & line up”. The states of the line with the TCSC after this combination are shown below.

i. Multi-module up & line up.
ii. 1 module up & line up.
iii. Down.
iv. TCSC bypassed & line up.

Obviously, all the above 3 reliability models, 12-state model, 6-state model and 4-state model, will yield the same results for the system reliability evaluations. The simplest model, namely, 4-state model, will be used throughout the rest of our work.

5.2.2 Reliability Model of SVC

5.2.2.1 Structure of SVC

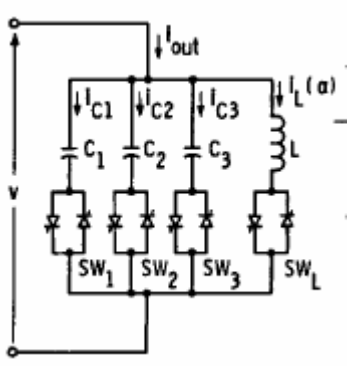

Fig. 5.6. A Basic TSC-TCR Type SVC (Adapted from [59])

A typical SVC is comprised of a number of Thyristor-Switched Capacitors (TSCs) and Thyristor-Controlled Reactors (TCRs). For instance, the SVC in Fig. 5.6 consists of three TSCs and one TCR. In practice, the numbers of TSCs and TCRs are decided by many factors such as maximum reactive power output and current rating of the thyristor valves [59]. That implies we can add more TCRs to increase the inductive reactive power range. Under the control of the thyristor valves, the output of the SVC can vary from the maximum inductive to maximum capacitive power rapidly and continuously.

5.2.2.2 Steady State Model of SVC

In the steady state environment, an SVC can be treated as a PV bus with zero active power. The reactive power of the SVC is within upper and lower limits [60].

$$\begin{cases} Q_{SVC\min} \le Q_{SVC} \le Q_{SVC\max} \\ P_{SVC} = 0 \end{cases} \tag{5.2}$$

We can make better use of an SVC when it is installed in the middle of a transmission line [60]. Fig. 5.7 shows an SVC is placed in the middle of transmission line *ij*. From the figure we can see that a bus, namely bus *q*, is created after the installation of the SVC. This figure also tells us that unlike a TCSC which is a series component, an SVC is a parallel component.

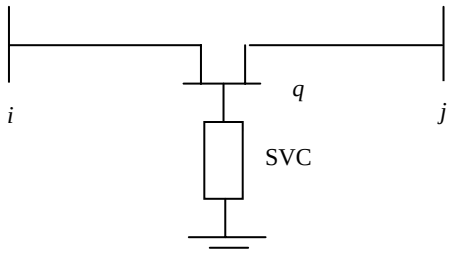

Fig. 5.7. Steady State Model of an SVC

5.2.2.3 Reliability Model of SVC

A TSC-TCR type SVC comprises a certain number of TSCs and TCRs. We are mainly concerned with the failures of these components, which are in parallel. To build the reliability model of an SVC, the following assumptions are made:

- After a TSC or TCR fails, it will be isolated by a bypass breaker. Therefore other normal components can still work.
- If all the TSCs and TCRs of the SVC fail, the SVC will be simply disconnected by a bypass breaker from the transmission line with which the SVC is in parallel.

Here to simplify the matter, we give an example of an SVC consisting of a TSC and a TCR. The state-space model of the SVC is shown in Fig. 5.8:

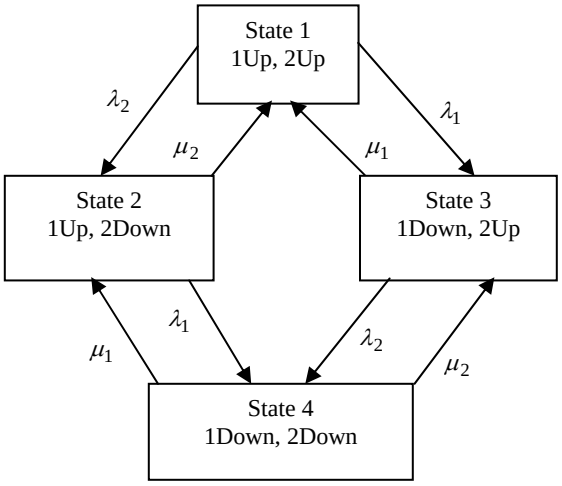

Fig. 5.8. Reliability Model of an SVC with a TSC and a TCR

In the above figure, λ_1, μ_1 are the failure and repair rates of component 1 and λ_2, μ_2 are the failure and repair rates of component 2. Components 1 and 2 refer to the TSC and TCR respectively. Suppose the TSC has a limit of 100MVAR capacitive power and the TCR can consume as much as 100MVAR power. Hence in state 1 where both the TSC and TCR are at work, the SVC can either absorb or generate reactive power and the range is [-100, 100] MVAR. In state 2, the TCR is down and isolated by a bypass breaker from the rest of the SVC. Therefore the SVC can provide [0, 100] MVAR, which comes from the available TSC. State 3 is similar to state 2. The difference is that the SVC now can only absorb reactive power because only the TCR is available. The SVC has no effect in state 4 where both the TSC and TCR are down.

Based on the Markov chains in Fig. 5.8, we can obtain the transition rate matrix as follows:

$$R = \begin{bmatrix} -(\lambda_1 + \lambda_2) & \lambda_2 & \lambda_1 & 0 \\ \mu_2 & -(\lambda_1 + \mu_2) & 0 & \lambda_1 \\ \mu_1 & 0 & -(\mu_1 + \lambda_2) & \lambda_2 \\ 0 & \mu_1 & \mu_2 & -(\mu_1 + \mu_2) \end{bmatrix} \tag{5.3}$$

Then we solve the follow equation:

$$\begin{cases} pR = 0 \\ \sum_{i=1}^{4} p_i = 1 \end{cases} \tag{5.4}$$

where p is a row vector whose ith element p_i is the probability of state i. The probability of each state is:

$$p_1 = \frac{\mu_1 \mu_2}{(\lambda_1 + \mu_1)(\lambda_2 + \mu_2)} \tag{5.5}$$

$$p_2 = \frac{\mu_1 \lambda_2}{(\lambda_1 + \mu_1)(\lambda_2 + \mu_2)} \tag{5.6}$$

$$p_3 = \frac{\lambda_1 \mu_2}{(\lambda_1 + \mu_1)(\lambda_2 + \mu_2)} \tag{5.7}$$

$$p_4 = \frac{\lambda_1 \lambda_2}{(\lambda_1 + \mu_1)(\lambda_2 + \mu_2)} \tag{5.8}$$

With regard to other types of SVC [59], we can follow the same idea to build their reliability models and calculate the probability of each state.

5.2.3 Reliability Model of TCPAR

5.2.3.1 Structure of TCPAR

Fig. 5.9 below shows the structure of a typical TCPAR [61-63]. According to this figure, we can see that a typical TCPAR consists of a series transformer, an excitation transformer and a converter, which is a network of thyristors. A voltage that is perpendicular to the phase voltage of the transmission line V is obtained from the excitation transformer. Through the series transformer, the obtained voltage is injected to the phase voltage of the line to generate a new voltage V'. Through the adjustment of the magnitude of the injected voltage Vq, we can control the phase angle shift between V' and V, namely α.

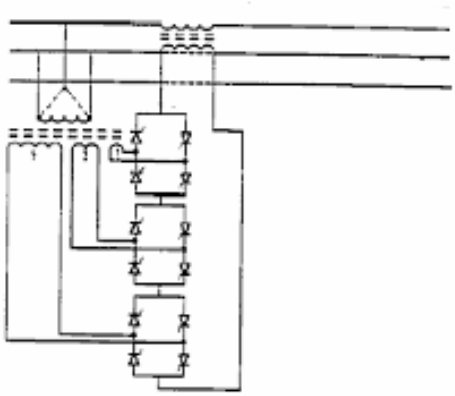

Fig. 5.9. Schematic Diagram of a TCPAR (Adapted from [61])

Usually, there are N windings of the secondary side of each phase of the excitation transformer. The turn ratios of successive windings differ by a factor of three [64]. For example, in the above figure, N is three; and the turn rations are 1:3:9. Each winding is connected to a sub-converter that is in parallel with each other and series with the series transformer. The sub-converter can affect the magnitude and direction of the injected

voltage. Therefore in Fig. 5.9, the total control range of the magnitude of the injected voltage V_q is [-13, 13]. If we know the magnitudes of voltage V and V_q, we can easily obtain the angle α .

5.2.3.2 Steady State Model of TCPAR

Generally, if the series transformer is ideal, i.e., without leakage reactance X and loss R, we can represent a TCPAR by a phase shifting controller with the complex phase angle α [65]. Below is the equivalent circuit of an ideal TCPAR, which is installed on transmission line ij.

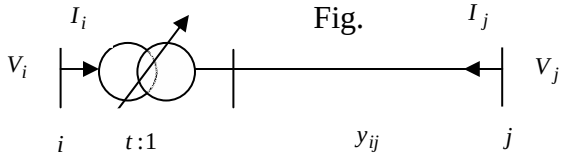

5.10. Steady State Model of a TCPAR

In Fig. 5.10, $t = 1\angle\alpha$ is the turn ratio of the TCPAR; and the phase angle α is within the range $[\alpha_{\min}, \ \alpha_{\max}]$. The current and voltage relations between bus i and bus j are:

$$\begin{bmatrix} I_i \\ I_j \end{bmatrix} = y_{ij} \begin{bmatrix} 1 & -\angle\alpha \\ -\angle -\alpha & 1 \end{bmatrix} \begin{bmatrix} V_i \\ V_j \end{bmatrix} \tag{5.9}$$

where y_{ij} is the admittance of the line. The above equation can also be applied to a conventional phase shift transformer. The advantage of the TCPAR is that it is able to vary the phase angle smoothly and quickly. This makes the control of power flow very desirable.

5.2.3.3 Reliability Model of TCPAR

The failures of either the transformers or the converter, i.e., the network of thyristor, can affect the operation of the whole TCPAR. However, the transformers have very low failure rates [24], especially those of the electronics-based devices. Therefore, to simplify the matter, the failures of the excitation and series transformers are neglected [66]. In other words, here we can only analyze the effect of the failure of the converter. Notice that the converter is in parallel with the transmission line. That means the TCPAR can be viewed as a parallel component if only the failure of the converter is considered.

Without loss of generality, we assume that there are only two sub-converters with the voltage magnitudes proportional to 1:3. And the full angle control range is supposed to be $[-30^{\circ}, \ +30^{\circ}]$. To build the reliability model of the TCPAR, we assume that

- When a sub-converter fails, it will be isolated by a bypass breaker.
- If all sub-converters are down, the TCPAR will be isolated by a bypass breaker so that this TCPAR will have no influence on the corresponding transmission line.

Based on the above information, we can achieve the state-space model of the TCPAR as shown in Fig. 5.11 where $\lambda, \ \mu$ are the failure and repair rates of the sub-converter.

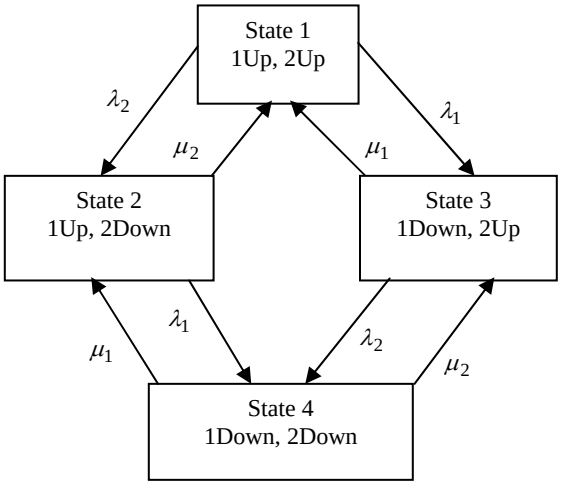

Fig. 5.11. Reliability Model of a TCPAR with Two Sub-converters

Suppose in the above figure, components 1 and 2 stand for the sub-converters with ratios of 1:3. Some comments about the states can be made as follows:

- State 1, namely the one with two sub-converters up, has the angle control range of $[-30^\circ,\ +30^\circ]$ whereas state 4 in which no components are up has no control effect.
- States 2 and 3 each has only a sub-converter up. Obviously, their control ranges are smaller than that of state 1. It can be demonstrated by the relations between voltage magnitude and angle that the control ranges of states 2 and 3 are $[-8.21^\circ,\ +8.21^\circ]$ and $[-23.41^\circ,\ +23.41^\circ]$ separately. The difference in the range is caused by the ratio of the available sub-converter.
- The Markov chains are exactly the same as those in Fig. 5.8. Thus the probabilities of the states in the above figure can be solved in the same way as those in Fig. 5.8. In other words, we can use (5.5) ~ (5.8) to calculate the state probabilities in Fig. 5.11.

Clearly, the technique we adopt to build the reliability model can be extended to a TCPAR with any number of sub-converters.

5.3 Application of TCSC / SVC / TCPAR to Composite Power System Reliability

5.3.1 Reliability Evaluation Method

Building the reliability model of each component in a system and choosing an appropriate evaluation method are the basic and important steps in reliability studies. For a composite power system, there are two major types of components, i.e., generators and transmission lines. We assume that they are represented by an up-and-down two-state transition model. Regarding TCSC, SVC and TCPAR, multi-state models are used and have been discussed in the previous section.

Basically there are two types of probabilistic methods for the evaluation of composite power system reliability. One is the contingency enumeration method and the other is the Monte Carlo simulation method. The former will create a considerable increase in the number of contingency states when dealing with multi-state components. On the other hand, the state sampling approach, one of the Monte-Carlo simulation methods, can easily incorporate the multi-state of the components in the analysis without much increase in the calculation time [24]. Considering the fact that TCSC, SVC and TCPAR are represented by multi-state models, we adopt the state sampling approach to evaluate the reliability of a composite power system with the inclusion of a FACTS device.

For the state sampling approach, the behavior of a component can be depicted by a uniformly distributed random number between [0, 1]. For instance, suppose a component has two states of up and down. Then we can determine the state of this component by generating a random number U between [0, 1]. The details can be found in Table 5.2:

Table 5.2. Determination of Component State by a Random Number

Random number's value	Component state sampled
$[0, p_{up}]$	Up
$[p_{up}, 1]$	Down

In the above table, p_{up} is the probability of the component being in the up state. The table shows that if the random number drawn is located between $[0, p_{up}]$, the component is in the up state. Otherwise it is in the down state. For a multi-state component, we can determine the state similarly by looking at the probability range a random number falls in.

After determining the state of every component, we can easily obtain the state of the whole system, which is the combination of the states of all components. Then we can evaluate this system state. If the system has a loss of load, we need to update reliability indices. We keep on doing the above procedure, i.e., determining component states and system state, evaluating system state and calculating reliability indices, until a certain convergence criteria is reached. Usually the evaluation is considered to be over when the coefficient of variation of the index *EENS* is less than a given tolerant error or a specified number of state samples is reached. The reason that the coefficient of variation of *EENS* is adopted is that in steady state reliability studies this index is slowest in convergence among conventional reliability indices [24].

5.3.2 Formulation of Re-dispatch with the Inclusion of TCSC / SVC / TCPAR

Each time, after we select a system state by the state sampling approach, we need to evaluate the corresponding system situation. If the system does not operate in a secure environment, for example, some thermal or voltage limits are violated, we should re-dispatch the generation. The purpose of the re-dispatch process is to supply as much load as possible meanwhile make the system operate securely. The re-dispatch is achieved

through an expanded OPF, namely the conventional OPF with the inclusion of a TCSC, SVC or TCPAR. Below is the formulation.

Objective:

$$f = \min\left(\sum_{i=1}^{n_d}(P_{di} - P_{li})\right) \tag{5.10}$$

Subject to:

$$\begin{cases} P_{gi} - P_{li} - \sum_{j=1}^{n} U_i U_j (G_{ij}\cos\theta_{ij} + B_{ij}\sin\theta_{ij}) = 0 \\ Q_{gi} - Q_{li} - \sum_{j=1}^{n} U_i U_j (G_{ij}\sin\theta_{ij} - B_{ij}\cos\theta_{ij}) = 0 \end{cases} \quad (i = 1,...,n) \tag{5.11}$$

$$\begin{cases} P_{gi\min} \le P_{gi} \le P_{gi\max} \\ Q_{gi\min} \le Q_{gi} \le Q_{gi\max} \end{cases} \tag{5.12}$$

$$\begin{cases} 0 \le P_{li} \le P_{di} \\ 0 \le Q_{li} \le Q_{di} \end{cases} \tag{5.13}$$

$$\frac{P_{li}}{Q_{li}} = \frac{P_{di}}{Q_{di}} \tag{5.14}$$

$$U_{i\min} \le U_i \le U_{i\max} \tag{5.15}$$

$$P_{ij}^2 + Q_{ij}^2 \le S_{ij\max}^2 \qquad ij \in [1,...,n_b] \tag{5.16}$$

$$X_{TCSC} \in [X_{\max}, X_{\min}] \tag{5.17}$$

$$X_{TCSC} \in \left([X_{\max}, X_{blocked}] \cup [X_{bypass}, X_{\min}]\right) \tag{5.18}$$

$$\begin{cases} Q_{SVC\min} \le Q_{SVC} \le Q_{SVC\max} \\ P_{SVC} = 0 \end{cases} \tag{5.19}$$

$$\alpha_{\min} \le \alpha \le \alpha_{\max} \tag{5.20}$$

where

n, n_b are the numbers of buses and branches respectively;

P_{gi}, Q_{gi} are the real and reactive generations at bus *i*;

$P_{gi\max}, P_{gi\min}$ are the limits of P_{gi};

$Q_{gi\min}, Q_{gi\max}$ are the limits of Q_{gi};

P_{li}, Q_{li} are the real and reactive loads at bus *i* after the redispatch of generations;

P_{di}, Q_{di} are the load demands at bus *i*;

P_{ij}, Q_{ij} are the real and reactive power flows along line *ij*;

$S_{ij\max}$ is the flow limit of line *ij*;

U_i is the voltage magnitude at bus *i*;

$U_{i\min}, U_{i\max}$ are the voltage magnitude limits of bus *i*;

In order to maintain a high level of the system reliability, the objective function we use is to minimize the load curtailment of the whole system. Equations (5.11) ~ (5.16) are the equal and unequal constraints like the power flow balance equations and thermal limits, which are the same as those of the conventional OPF.

Equations (5.17) and (5.18) describe the effect of a TCSC and are obtained based on Figs. 5.2 and 5.3. Equation (5.17) refers to the situation in which 2 or more modules are operational. And (5.18) is for the case when only a single module is operational. (Note: $X_{\max}, X_{blocked}$ stand for the limits of capacitance range while $X_{\min}, X_{bypassed}$ are for inductance limits.) Suppose the 4-state model described in section 5.2.1.4 is used to represent the line with a 4-module TCSC. Equation (5.17) will be used when the line with the TCSC is in state i, namely, multi-module up & line up. If it is in state ii, (5.18) will be applied. For states iii and iv, the OPF problem can be handled in the same way as that without a TCSC.

Equation (5.19) and (5.20) describes the contributions of an SVC and a TCPAR separately. It should be noted that the upper and lower limits of (5.19) and (5.20) are

related to the states of the SVC and TCPAR, which are discussed in sections 5.2.2 and 5.2.3.

Compared with the conventional OPF, our formulation has more control variables related to a TCSC, an SVC or a TCPAR. That means the system has a more flexible control over the operation. Therefore, the load curtailment is expected to be reduced with a TCSC, SVC or TCPAR. In other words, the reliability level can rise.

5.4 Case Studies

The WSCC 9-bus system is used in order to examine the impacts of the employment of a TCSC, SVC or TCPAR on composite power system reliability.

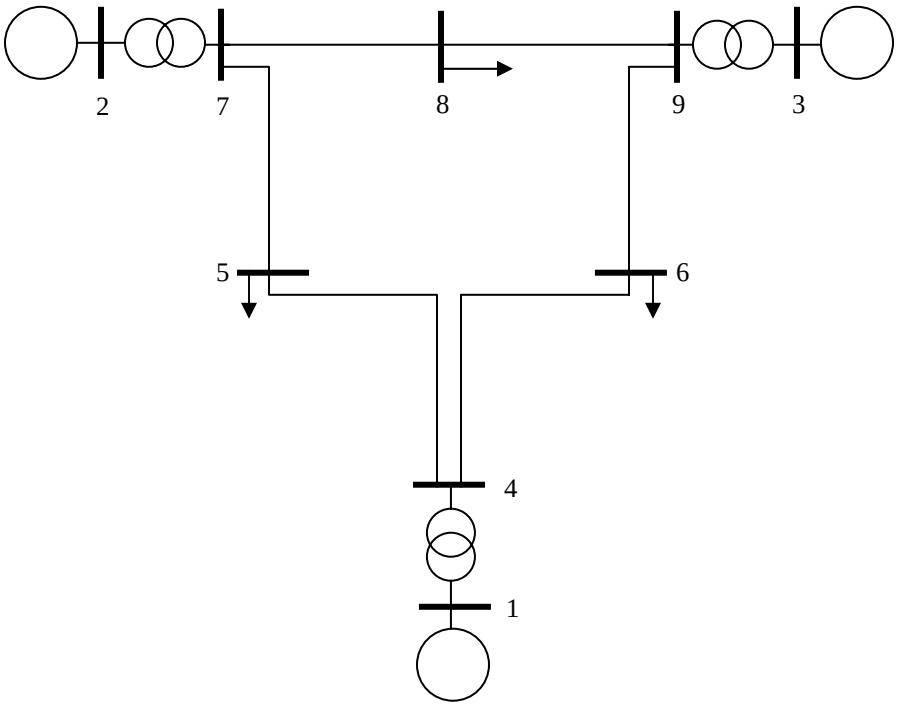

Fig. 5.12. Test System: WSCC 9-bus System

In Table 5.3 we list some data that are closely associated with our study. Other network data can be found in [58].

Table 5.3. Branch Data of the WSCC 9-bus System

Branch	Resistance (p.u.)	Reactance (p.u)	Susceptance (p.u)	Limits (MVA)
1-4	0.0000	0.0576	0.0000	300
4-6	0.0170	0.0920	0.1580	300
6-9	0.0390	0.1700	0.3580	300
3-9	0.0000	0.0586	0.0000	300
8-9	0.0119	0.1008	0.2090	300
7-8	0.0085	0.0720	0.1490	300
2-7	0.0000	0.0625	0.0000	300
5-7	0.0320	0.1610	0.3060	300
4-5	0.0100	0.0850	0.1760	300

Buses 5, 6 and 8 are load points. The base loads are 200+j80, 120+j40 and 130+j45 (MVA) separately.

5.4.1 TCSC

5.4.1.1 TCSC Reliability Data

The TCSC used here consists of 4 modules. The transition rates of the state-space model of this TCSC are listed in Table 5.4.

Table 5.4. Transition Rates (occ./year) of the State-space Model of a 4-module TCSC

$\rho_{12} = 0.0028$	$\rho_{21} = 0.0154$	$\rho_{15} = 0.0005$	$\rho_{61} = 0.0333$	$\rho_{16} = 0.0004$
$\rho_{23} = 0.0021$	$\rho_{32} = 0.0308$	$\rho_{25} = 0.0005$	$\rho_{62} = 0.0333$	$\rho_{26} = 0.0004$
$\rho_{34} = 0.0014$	$\rho_{43} = 0.0462$	$\rho_{35} = 0.0005$	$\rho_{63} = 0.0333$	$\rho_{36} = 0.0004$
$\rho_{46} = 0.0007$	$\rho_{56} = 8584.8$	$\rho_{45} = 0.0005$	$\rho_{64} = 0.0949$	$\rho_{46} = 0.0004$

The parameters of (5.17) and (5.18), i.e., the reactance ranges of the TCSC with different numbers of modules at work, are set as follows in terms of [63]:

- $[-0.5X, 0.5X]$ (2 or more modules up)
- $[-0.5X, -0.15X] \cup [0.1X, 0.5X]$ (one module up)

where X is the reactance of the line where TCSC is placed.

Below we will try several schemes to investigate the influence of a TCSC on the system reliability.

5.4.1.2 TCSC Site Effect

Intuitively, when installed at different locations, the TCSC would have different effects on the system reliability. Below we place the TCSC on different lines and try to find out its optimal location. The reliability index used here is *EENS* of the whole system.

Table 5.5. Effect of TCSC Site on Reliability Improvement

TCSC installation condition	*EENS* (MWh/year)	Reliability Improvement (%)
No TCSC	17524.8390	----------
On line 6-9	9002.0219	48.63
On line 7-8	17278.9508	1.40
On line 5-7	12209.4087	30.33
On line 4-5	15692.5075	10.46

Table 5.5 clearly shows that the TCSC improves the system reliability and the improvement varies greatly with the location of the TCSC. For example, when the TCSC is installed on line 7-8, the improvement of *EENS* is only 1.40%. Due to the fact that the TCSC is an expensive device, it is not a good idea to place the TCSC on this line. However, if we move the TCSC to line 6-9, the improvement is as high as 48.63%. Obviously, the introduction of the TCSC to this place is desirable. The reason for this

big difference is related to many factors. First we take a look at the load pattern. The load at bus 5 is the biggest, 200MW. When the TCSC is installed close to the heavy load bus, the corresponding line can transfer more power than without the TCSC or the TCSC at other locations to fill the load gap caused by contingency. Accordingly the reliability improvement will be apparent. That is the reason why the result is good when the TCSC is installed on line 5-7 or line 4-5. But the enhancement is most significant when the TCSC is installed on line 6-9. That is associated with the line impedance. It can be seen that line 6-9 has the biggest reactance, followed by line 5-7. Compared with them line 4-5 has a much smaller one. That means the power transfer capability can be greatly enhanced if we put the TCSC on lines 6-9 or 5-7. In turn the reliability can be improved a lot for these two cases. Of course, the TCSC can improve the transfer capability of line 4-5 when placed there. But the bottleneck now is the line with big impedance that cannot transfer much power. Therefore the effect is less significant when the TCSC is installed on line 4-5.

From the above analysis, we can see that it is a rather complicated task to find out the optimal location of a TCSC because its effect is in fact determined by many factors such as the topology of the system and the load pattern. According to our case study, to achieve a good improvement of the reliability, we can place a TCSC on a line with big impedance and close to heavy loads.

5.4.1.3 Impact of Thermal Limits

In this case, we change the thermal limits of all lines from 300MVA to 200MVA. We expect the improvements of EENS will decrease.

Table 5.6. Solution for Another Set of Thermal Limits

TCSC installation condition	*EENS* (MWh/year)	Reliability Improvement (%)
No TCSC	25832.2272	----------
On line 6-9	16586.5314	35.79
On line 7-8	25603.6706	0.88
On line 5-7	24097.1527	6.72
On line 4-5	25277.2764	2.15

The first phenomenon we observe from Table 5.6 is that *EENS* rises. That is reasonable as the thermal limits are down.

Compared with the results in Table 5.5, we can find that the improvements of *EENS* in Table 5.6 are smaller. That is expected. Though the TCSC can increase the power transfer capability, the actual power transferred is constrained by the thermal limits. Therefore, the effects will be less if the thermal limits are reduced to some extent. That means the installation of the TCSC on some lines may be unnecessary if the thermal limits are small. The above table also tells us that the impact of thermal limits is more significant when the TCSC is placed near a heavy load point such as on line 5-7 or line 4-5. For instance, when the thermal limit on line 5-7 is 300MVA, the improvement of the reliability is 30.33%. When the thermal limit decreases to 200MVA, the improvement is only 6.72%.

5.4.2 SVC

The SVC employed here consists of a TSC and a TCR. Table 5.7 below shows the reliability data of the SVC.

Table 5.7. Reliability Data of the SVC

	Failure rate (occ./year)	Repair rate (occ./year)
TSC	0.0005	0.0210
TCR	0.0005	0.0210

We still use the WSCC 9-bus system and the conditions are the same as those in the TCSC case, namely section 5.4.1.2. We first assume that the full capacity of the SVC is [-100, 100] MVAR. Then in the second case, we increase the maximum available capacity of the SVC to [-200, 200] MVAR. In both cases, comparative simulations are conducted for the system with and without the SVC. The detailed results are given in Tables 5.8 and 5.9.

Table 5.8. Solutions for a Small Capacity SVC

SVC installation condition	*EENS* (MWh/year)	Improvement (%)
No SVC	17524.8390	----------
On line 6-9	8271.6347	52.80
On line 7-8	8072.6094	53.94
On line 5-7	7736.2841	55.86
On line 4-5	8267.6683	52.82

Table 5.9. Solutions for a Big Capacity SVC

SVC installation condition	*EENS* (MWh/year)	Improvement (%)
No SVC	17524.8390	----------
On line 6-9	8222.3364	53.08
On line 7-8	8008.9859	54.30
On line 5-7	7640.3292	56.40
On line 4-5	8249.5967	52.93

In order to compare the effect of the SVC with that of the TCSC, the SVC is installed on the same transmission lines as those for the TCSC. In terms of the results in the above two tables, we can see that

- The SVC improves the system reliability significantly and the effect is greater than that of the TCSC. As we know, the SVC mainly provides the system with reactive power. The huge impact of the SVC on the reliability indicates that an investment in reactive power is an effective way to enhance the reliability level of the WSCC 9-bus system.
- For the WSCC 9-bus system, which is somewhat symmetric, the location of the SVC seems not to affect the reliability improvement quite much. The biggest improvement happens when the SVC is placed on line 5-7. Notice that bus 5 has the biggest real power as well as reactive power of the system. Based on this and the fact that an SVC can supply reactive power, we could probably place an SVC near a heavy reactive power load in order to improve reliability.
- The double increase of the capacity of the SVC does not further improve the reliability level much. As we know, the bigger the capacity of an SVC is, the higher the cost is. That requires us to conduct a full investigation of the cost-effectiveness so that a tradeoff between the reliability improvement and the SVC capacity can be made.

5.4.3 TCPAR

The TCPAR used here has two sub-converters. Table 5.10 shows the reliability data.

Table 5.10. Reliability Data of a Sub-converter

	Failure rate (occ./year)	Repair rate (occ./year)
Sub-converter	0.0004	0.0300

We assume that the maximum phase angle limits of the TCPAR are $[-30^{\circ}, \ 30^{\circ}]$. Table 5.11 below shows the results when the TCPAR is placed on different lines of the WSCC 9-bus system.

Table 5.11. Solutions with and without a TCPAR

TCPAR installation condition	EENS (MWh/year)	Improvement (%)
No TCPAR	17524.8390	----------
On line 6-9	17480.5355	0.25
On line 7-8	17480.5438	0.25
On line 5-7	17481.0248	0.25
On line 4-5	17482.4044	0.24

For this system, the introduction of the TCPAR to the system almost does not improve reliability. By comparison, in the previous examples, the TCSC and the SVC have shown significant effects in the enhancement of the system reliability. As we know, these three types of FACTS devices are aimed at different controls. TCPAR affects phase angle. SVC provides reactive power while TCSC regulates reactance. The case studies on the WSCC 9-bus system indicate that though FACTS can affect the reliability, their effects can vary greatly. Knowledge of the weakness of the system can help us optimize the employment of a FACTS component. For instance, if the system is in lack of reactive power, an SVC could be a good candidate to improve the reliability. On the other hand, studies of the impacts of FACTS on the reliability can guide us in strengthening and planning of a power system.

Finally we would like to point out that the above reliability evaluation methodology for TCSC, SVC and TCPAR can be extended to analyze the effects of other FACTS members or other devices on composite power system reliability. In brief, we first build the reliability model in terms of the structure and operational principle of a

device. Then we make its equivalent circuit in the steady state. Hence we can apply this device to the reliability study in the procedures like state selection and state evaluation.

5.5 Conclusions

This chapter investigates the impacts of FACTS members TCSC, SVC and TCPAR on composite power system reliability. Through studies on the structures of these three devices, we build their reliability models and the steady state operational models. Then we incorporate them into an OPF program to re-dispatch generations during contingencies. The case studies on the WSCC 9-bus system clearly show that these three FACTS devices can improve the system reliability. And the effects are closely related to such factors as the control properties of these devices, the system structure and the load pattern. Finally, we point out that the methods proposed here to build the reliability models of TCSC, SVC and TCPAR, and to analyze their impacts on composite power system reliability can be applicable to other devices as well.

CHAPTER VI

CONCLUSIONS AND SUGGESTIONS FOR FUTURE WORK

6.1 A Summary of the Research Contributions

This dissertation has developed several new methods to deal with some of the issues related to short-term and long-term reliability in deregulated power systems. These methods solve such problems as “auction-based dispatch in the deregulated power systems”, “congestion management by the OPF model”, “composite power system long-term reliability evaluation with both adequacy and security included”, and “impacts of FACTS on composite power system reliability”.

The major contributions of this dissertation are summarized as follows:

- By the law of supply and demand, we investigate the formulation of the auction-based dispatch in the deregulated power systems and demonstrate that it is reasonable to use the social welfare as the objective function. We then develop two efficient algorithms to solve the auction-based dispatch with different types of bidding functions. The first algorithm deals with the dispatch problem in which the objective function consists of only quadratic bidding functions. The second algorithm handles the situation where the objective function includes both quadratic and linear incremental bidding functions. Both algorithms have a computation complexity in the order of the square of the number of variables. Therefore they are much more efficient than the conventional algorithm that has an exponential computation complexity.
- A new OPF method based on sensitivity factors combined with the technique of aggregation is developed to manage congestion. First, by looking into the sensitivity factors of all generators with regard to the congested lines, we identify effective generators that have big influences on these congested lines to relieve congestion. Then, to further reduce the number of variables and speed up the calculation, we

aggregate generators that have close sensitivity factors. Finally a new OPF method based on the above techniques is proposed to relieve congestion. The case studies demonstrate that this method is much faster than the conventional OPF method meanwhile can maintain market efficiency. Thus it is very effective in managing congestion.

- By using the system state transition sampling approach, one of the sequential Monte Carlo simulation methods, we develop a method to probabilistically evaluate composite power system long-term reliability in both adequacy and security. A 3-state reliability transition model is also developed for transmission lines to include the effects of permanent faults as well as transient faults. To reflect the stochastic features of the system following a fault, random variables together with probability distributions are employed. Finally, in order to give a complete depiction of the dynamic process after a fault, two new reliability indices related to angle stability are introduced. Our study clearly shows that though security can cause a big loss of load, the major issue in the long-term reliability is still adequacy.
- We propose to use FACTS rather than build more transmission lines or power plants to improve composite power system reliability. Compared with building more lines or plants, the employment of FACTS is easy to implement. In the meantime, FACTS can have significant effects on the enhancement of reliability by controlling parameters such as reactance, voltage and phase angle rapidly and smoothly. The method and techniques presented in our work to investigate the impacts of FACTS like TCSC, SVC and TCPAR on composite power system reliability can be applied to other devices easily.

6.2 Suggestions for Future Work

This dissertation addresses some important and basic issues associated with short-term and long-term reliability in deregulated power systems. Yet it should be noted

that there is still plenty of room for further developments in our research. Specifically, our work can be improved in the following respects:

- Congestion management aims at maintaining the operational security of the system, the major aspect of the short-term reliability analysis. Our study does not consider contingencies though the method presented is also applicable to contingency situations. For a complete short-term reliability evaluation, we should take account of contingencies.
- Our research on dynamic effects of security on composite power system long-term reliability evaluation is mainly concerned with angle stability. To exactly describe the physical nature of the stability problem, voltage stability should also be included.
- The investigation of the impacts of FACTS on composite power system reliability is focused on the steady state. In fact, FACTS can improve the behavior of a power system in the static state as well as the dynamic state. Therefore the dynamic properties of FACTS should also be explored for more comprehensive work on reliability improvement.

REFERENCES

[1] H. Rudnick, R. Varela, and W. Hogan, "Evaluation of Alternatives for Power System Coordination and Pooling in a Competitive Environment," *IEEE Trans. Power Systems*, Vol. 12, No. 2, pp. 605 – 613, May 1997.

[2] F. A. Rahimi and A. Vojdani, "Meet the Emerging Transmission Market Segments," *IEEE Computer Applications in Power*, Vol. 12, No. 1, pp. 26-32, Jan. 1999.

[3] Z. Alaywan and J. Allen, "California Electric Restructuring; A Broad Description of the Development of the California ISO," *IEEE Trans. Power Systems*, Vol. 13, No. 4, pp. 1445-1552, Nov. 1998.

[4] G. B. Sheble, "Priced Based Operation in an Auction Market Structure," *IEEE Trans. Power Systems*, Vol. 11, No. 4, pp. 1770-1777, Nov. 1996.

[5] M. Aganagic, K. H. Abdul-Rahman, and J. G. Waight, "Spot Pricing of Capacities for Generation and Transmission of Reserve in an Extended Poolco Model," *IEEE Trans. Power Systems*, Vol. 13, No. 3, pp. 1128-1135, Aug. 1998

[6] F. D. Galiana and M. D. Ilic, "A Mathematical Framework for the Analysis and Management of Power Transactions under Open Access," *IEEE Trans. Power Systems*, Vol. 13, No. 2, pp. 681-687, May 1998.

[7] W. Mielczarski and W. Widjaja, "Analysis of Bids and Re-bids of Generators in the Australian National Electricity Market," *Proc. of the 1999 IEEE/PES Winter Meeting*, New York, NY, Vol. 2, pp. 833-838, Jan. 1999.

[8] J. W. Cheng, F. D. Galiana, and D. T. McGillis, “Studies of Bilateral Contracts with Respect to Steady-State Security in a Deregulated Environment [of Electricity Supply],” *IEEE Trans. Power Systems*, Vol. 13, No.3, pp. 1020-1025, Aug. 1998.

[9] North America Electric Reliability Council, “Reliability Assessment 2001-2010: the Reliability of Bulk Electric Systems in North America,” Report, NERC, Princeton, NJ, Oct. 2001.

[10] A. D. Patton and C. Singh, “The Impact of Restructuring Policy Changes on Power Grid Reliability,” Report, Department of Electrical Engineering, Texas A&M University, 1998.

[11] J. D. McCalley, V. Vittal, and N. Abi-Samra, “An Overview of Risk Based Security Assessment,” *Proc. of the 1999 IEEE/PES Summer Meeting*, Edmonton, Alberta, Canada, Vol. 1, pp. 173 –178, July 1999.

[12] R. Billinton, L. Salvaderi, J. D. McCalley, H. Chao, T. Seitz, et.al, “Reliability Issues in Today’s Electric Power Utility Environment,” *IEEE Trans. Power Systems*, Vol. 12, No. 4, pp. 1708-1714, Nov. 1997

[13] C. Singh, “Electric Power System Reliability,” Course Notes, Department of Electrical Engineering, Texas A&M University, 2001.

[14] J. R. Arce, M. D. Iiic, and F. F. Garces, “Two New Methods to Assess Short-term Transmission Reliability,” *Proc. of the 2001 IEEE/PES Summer Meeting*, Vancouver, British Columbia, Canada, Vol.1, pp. 503-509, July 2001.

[15] J. R. Arce, F. F. Garces, and M. D. Iiic, "Comparison of the Ex-ante and Ex-post Methods for Short-term Reliability Management," *Proc. of the 2002 IEEE/PES Winter Meeting*, New York, NY, Vol. 2, pp. 779-786, Jan. 2002.

[16] J. R. Arce, M. D. Iiic, and F. F. Garces, "Managing Short-term Reliability Related Risks," *Proc. of the 2001 IEEE/PES Summer Meeting*, Vancouver, British Columbia, Canada, Vol.1, pp. 516-522, July 2001.

[17] L. L. Lai, *Power System Restructuring and Deregulation*, Wiley, New York, NY, 2001.

[18] A. K. David, "Dispatch Methodologies for Open Access Transmission Systems," *IEEE Trans. Power Systems*, Vol. 13, No.1, pp. 46 – 53, Feb. 1998.

[19] X. Wang and Y. H. Song, "Advanced Real-time Congestion Management through Both Pool Balancing Market and Bilateral market," *IEEE Power Engineering Review*, Vol. 20, No. 2, pp. 47-49, Feb. 2000.

[20] R. D. Christie, B. F. Wollenberg, and I.Wangensteen, "Transmission Management in the Deregulated Environment," *Proc. of the IEEE*, Vol. 88, No. 2, pp. 170-195, Feb. 2000.

[21] R. Billinton and S.Aboreshaid, "Security Evaluation of Composite Power Systems," *Proc. of IEE-Generation, Transmission and Distribution* Vol. 142, No. 5, pp. 511-516, Sept. 1995.

[22] R. Billinton and Guangbin Lian, "Composite Power System Health Analysis using a Security Constrained Adequacy Evaluation Procedure," *IEEE Trans. Power Systems*, Vol. 9, No.2, pp. 936-941, May 1994.

[23] R. Billinton and E. Khan, “A Security Based Approach to Composite Power System Evaluation,” *IEEE Trans. Power Systems*, Vol. 7, No. 1, pp. 65-72, Feb. 1992.

[24] R. Billinton and W. Li, *Reliability Assessment of Electric Power Systems Using Monte Carlo Methods*, Plenum Press, New York, NY, 1994.

[25] S. Hao, G. A. Angelidis, H. Singh, and A. D. Papalexopoulos, “Consumer Payment Minimization in Power Pool Auctions”, *IEEE Trans. Power Systems*, Vol. 13, No.3, pp. 986-991, Aug. 1998.

[26] K. W. Doty and P. L. McEntire, “An Analysis of Electric Power Brokerage Systems,” *IEEE Trans. Power Apparatus and Systems*, Vol. 101, No. 2, pp. 389-396, Feb. 1982.

[27] G. Fahd, D. A. Richards, and G. B. Sheble, “The Implementation of an Energy Brokerage System Using Linear Programming,” *IEEE Trans. Power Systems*, Vol. 7, No.1, pp. 90-96, Feb. 1992.

[28] L. Philipson and H. L. Willis, *Understanding Electric Utilities and Deregulation*, Marcel Dekker, New York, NY, 1998.

[29] J. J. Paserba, N. W. Miller, E. V. Larsen, and Richard J. Piwko, “A Thyristor Controlled Series Compensation Model for Power System Stability Analysis,” *IEEE Trans. Power Delivery*, Vol. 10, No.3, pp. 1471-1478, July 1995.

[30] E. V. Larsen, K. Clark, S. A. Miske, and J. Urbanek, “Characteristics and Rating Considerations of Thyristor Controlled Series Compensation,” *IEEE Trans. Power Delivery*, Vol. 9, No.2, pp. 992-1000, April 1994.

[31] J. Urbanek, R. J. Piwko, E. V. Larsen, B. L. Damsky, B. C. Furumasu, et al., “Thyristor Controlled Series Compensation Prototype Installation at the Slatt 500KV Substation,” *IEEE Trans. Power Delivery*, Vol. 8, No.3, pp. 1460-1469, July 1993.

[32] X. Zhou and J. Liang, “Overview of Control Schemes for TCSC to Enhance the Stability of Power Systems,” *Proc. of IEE-Generation, Transmission and Distribution*, Vol. 146, No.2, pp. 125-130, Mar. 1999.

[33] G. M. Huang and T. Zhu, “TCSC as a Transient Voltage Stabilizing Controller”, *Proc. of the 2001 IEEE/PES Winter Meeting*, Columbus, OH, Vol. 2, pp. 628-633, Jan. 2001.

[34] P. Preedavichit and S. C. Srivastava, “Optimal Reactive Power Dispatch Considering FACTS Devices,” *Proc. of APSCOM*-97, Hong Kong, China, Vol. 2, pp. 620 –625, Nov. 1997.

[35] C. A. Canizares and Z. T. Faur, “Analysis of SVC and TCSC Controller in Voltage Collapse,” *IEEE Trans. Power Systems*, Vol. 14, No. 1, pp158 –165, Feb. 1999.

[36] R. Billinton, M. Fotuhi-Firuzabad, and S. O. Faried, “Power System Reliability Enhancement Using a Thyristor Controlled Series Capacitor,” *IEEE Trans. Power Systems*, Vol. 14, No.1, pp. 369-374, Feb. 1999.

[37] S. Stoft, “PJM’s Capacity Market in a Price-Spike World,” Report, University of California Energy Institute, Berkeley, CA, May 2000.

[38] J. Yu, “Evaluation of Power System Reliability and Development of Transmission Pricing Method under Deregulation,” Ph. D. Dissertation, Texas A&M University, 2000.

[39] Y. H. Song and X. Wang, *Operation of Market-oriented Power Systems*, Springer, London, UK, 2003.

[40] M. S. Bazaraa and C. M. Shetty, *Nonlinear Programming: Theory and Algorithms*, Wiley, New York, NY, 1994

[41] M. Avriel, *Nonlinear Programming: Analysis and Methods*, Prentice-Hall, Englewood Cliffs, NJ, 1976.

[42] G. P. McCormick, *Nonlinear Programming: Theory, Algorithms, and Applications*, Wiley, New York, NY, 1983.

[43] R. L. Miller, *Economics Today*, Addison-Wesley Publishing Company, New York, NY, 1998.

[44] H. R. Varian, *Intermediate Microeconomics: A Modern Approach*, 5th Edition, Norton, New York, NY, 1999.

[45] F. C. Schweppe, M. C. Caraminis, R. D. Tabors, and R. E. Bohn, *Spot Pricing of Electricity*, Kluwer Academic Publishers, Boston, MA, 1998.

[46] G. M. Huang and K. Song, "A Simple Two Stage Optimization Algorithm for Constrained Power Economic Dispatch," *IEEE Trans. Power Systems*, Vol. 9, No.4, pp. 1818 – 1824, Nov. 1994.

[47] H. Wei, H. Sasaki, J. Kubokawa, and R. Yokoyama, "An Interior Point Nonlinear Programming for Optimal Power Flow Problems with a Novel Data Structure," *IEEE Trans. Power Systems*, Vol. 13, No. 3, pp. 870-877, Aug. 1998.

[48] B. Xu and A. Abur, "State Estimation of Systems with UPFCs Using the Interior Point Method," *IEEE Trans. Power Systems*, Vol. 19, No. 3, pp. 1635-1641, Aug. 2004.

[49] N. Karmarkar, "A New Polynomial-time Algorithm for Linear Programming," *Combinatorica*, Vol. 4, pp. 373-395, 1984.

[50] R. Monteiro and I. Adler, "Interior Path Following Primal-dual Algorithms. Part II: Convex Quadratic Programming," *Mathematical Programming*, Vol. 44, pp. 43-66, 1989.

[51] Reliability Test System Task Force of the application of probability methods subcommittee, "The IEEE Reliability Test System-1996," *IEEE Trans. Power Systems*, Vol. 14, No. 3, pp. 1010-1020, Aug. 1999.

[52] B. Stott and E. Hobson, "Power System Security Control Calculations Using Linear Programming," *IEEE Trans. Power Apparatus and Systems*, Vol. 97, pp. 1713-1719, Sept.1978.

[53] Y. G. Paithankar, *Transmission Network Protection*, Marcel Dekker, New York, NY, 1997.

[54] R. Billinton and S. Aboreshaid, "Stochastic Modelling of High-speed Reclosing in Probabilistic Transient Stability Studies," *Proc. of IEE-Generation, Transmission and Distribution*, Vol. 142, No.4, pp. 350-354, July 1995.

[55] P. Kuruganty and R. Billinton, "Protection System Modeling in a Probabilistic Assessment of Transient Stability," *IEEE Trans. Power Apparatus and Systems*, Vol. 100, pp. 2163-2170, May 1981.

[56] G. M. Huang and Y. Li, "Power System Reliability Indices to Measure Impacts Caused by Transient Stability Crises," *Proc. of the 2002 IEEE/PES Winter Meeting*, New York, NY, Vol. 2, pp. 766-771, Jan. 2002.

[57] P. Kundur, *Power System Stability and Control*, McGraw Hill, New York, NY, 1994.

[58] P. M. Anderson and A. A. Fouad, *Power System Control and Stability*, IEEE Press, New York, NY, 1994.

[59] L. Gyugyi, "Power Electronics in Electric Utilities: Static VAR Compensators," *Proc. of the IEEE*, Vol. 76, pp. 483-494, Apr. 1988.

[60] G. M. Huang and P. Yan, "The Impacts of TCSC and SVC on Power System Load Curtailments," *Proc. of the 2001 IEEE/PES Summer Meeting*, Vancouver, British Columbia, Canada, Vol. 1, pp. 33 –37, July 2001.

[61] N. G. Hingorani, "Flexible AC Transmission," *IEEE Spectrum*, Vol. 30, pp. 40-45, Apr. 1993.

[62] M. R. Iravani, P. L. Dandeno, and D. Maratukulam, “Applications of Static Phase Shifters in Power Systems,” *IEEE Trans. Power Delivery*, Vol. 9, No. 3, pp. 1600-1608, July 1994.

[63] N. G. Hingorani, “FACTS Technology and Opportunities,” *IEE Colloquium on FACTS*, Vol. 5, pp. 4/1-4/10, Jan. 1994.

[64] M. R. Iravani and D. Maratukulam, “Review of Semiconductor-controlled (Static) Phase Shifters for Power Systems Applications,” *IEEE Trans. Power Systems*, Vol. 9, No.4, pp. 1833-1839, Nov. 1994.

[65] E. Acha, V. G. Agelidis, O. Anaya, and T. Miller, *Power Electronic Control in Electrical Systems*, Newnes, Woburn, MA, 2002.

[66] R. Billinton, M. Fotuhi-Firuzabad, S. O. Faried, and S. Aboreshaid, “Impact of Unified Power Flow Controllers on Power System Reliability,” *IEEE Trans. Power Systems*, Vol. 15, pp. 410-415, Feb. 2000.

APPENDIX

IEEE RTS-96 SYSTEM

Table A.1. Generator Data for the IEEE RTS-96 System

Zone No.	Bus ID	$P_{g\,\min}$ (MW)	$P_{g\,\max}$ (MW)	a_{gi}	b_{gi}
1	101	0	192	0.012	15
1	102	0	192	0.012	15
1	107	0	300	0.012	12
1	113	0	591	0.015	6
1	115	0	215	0.01	15
1	116	0	155	0.015	13
1	118	0	400	0.01	12
1	121	0	400	0.01	12
1	122	0	300	0.012	11
1	123	0	660	0.014	6
2	201	0	192	0.012	15.5
2	202	0	192	0.012	15.5
2	207	0	300	0.012	11
2	213	0	591	0.015	6
2	215	0	215	0.01	15.5
2	216	0	155	0.015	13
2	218	0	400	0.01	12
2	221	0	400	0.01	12
2	222	0	300	0.012	11
2	223	0	660	0.014	6
3	301	0	192	0.011	15
3	302	0	192	0.011	15

Table A.1. (continued)

Zone No.	Bus ID	$P_{g\min}$ (MW)	$P_{g\max}$ (MW)	a_{gi}	b_{gi}
3	307	0	300	0.012	11
3	313	0	591	0.015	6
3	316	0	155	0.015	13
3	318	0	400	0.01	12
3	321	0	400	0.01	12
3	322	0	300	0.012	11
3	323	0	660	0.014	6

Note: In Table A.1, generator bidding functions are expressed as $a_{gi}P_{gi}^2 + b_{gi}P_{gi} + c_{gi}$. Since c_{gi} does not affect the results, the table above only gives coefficients a_{gi} and b_{gi}.

Table A.2. Load Data for the IEEE RTS-96 System

Zone No.	Bus ID	$P_{l\max}$ (MW)	a_{li}	b_{li}
1	101	108	-0.013	39
1	102	97	-0.013	39
1	103	180	-0.016	37
1	104	74	0	40
1	105	71	0	40
1	106	136	-0.013	38
1	107	125	-0.013	38
1	108	171	-0.013	37
1	109	175	-0.013	37
1	110	195	-0.015	37
1	113	265	-0.015	36
1	114	194	-0.014	37

Table A.2. (continued)

Zone No.	Bus ID	$P_{l\max}$ (MW)	a_{li}	b_{li}
1	115	317	-0.016	35
1	116	100	-0.014	39
1	118	333	-0.016	35
1	119	181	-0.016	37
1	120	128	-0.013	38
2	201	108	-0.013	39
2	202	97	-0.013	39
2	203	180	-0.016	37
2	204	74	0	40
2	205	71	0	40
2	206	136	-0.013	38
2	207	125	-0.013	38
2	208	171	-0.013	37
2	209	175	-0.013	37
2	210	195	-0.015	37
2	213	265	-0.015	36
2	214	194	-0.014	37
2	215	317	-0.016	35
2	216	100	-0.014	39
2	218	333	-0.016	35
2	219	181	-0.016	37
2	220	128	-0.013	38
3	301	108	-0.013	39
3	302	97	-0.013	39
3	303	180	-0.016	37
3	304	74	0	40

Table A.2. (continued)

Zone No.	Bus ID	$P_{l\max}$ (MW)	a_{li}	b_{li}
3	305	71	0	40
3	306	136	-0.013	38
3	307	125	-0.013	38
3	310	195	-0.015	37
3	313	265	-0.015	36
3	314	194	-0.014	37
3	315	317	-0.016	35
3	316	100	-0.014	39
3	318	333	-0.016	35
3	319	181	-0.016	37
3	320	128	-0.013	38

It is noted that in Table A.2,

- Load bidding functions are expressed as $a_{li}P_{li}^2 + b_{li}P_{li} + c_{li}$. Since c_{li} does not affect the results, the table above only gives coefficients a_{li} and b_{li}.
- $P_{l\min} = 0$.

VITA

Yishan Li was born in Quanzhou, Fujian province of China on October 20th, 1974. He received his B.S. and M.S. degrees from the Department of Electrical Engineering at Shanghai Jiao Tong University in 1997 and 2000 respectively. Since August 2000, he has been with Texas A&M University, working towards his Ph.D. degree in the Electrical Engineering Department. During his Ph.D. program, he has been a research assistant for his advisor, Dr. Garng M. Huang. He also worked as a graduate teaching assistant for the ELEN 214, 220 and 248. His research interests include power system reliability, power system operation & control, and power markets.

Yishan Li can be reached at

New South District, Apt. 17-301
Huaqiao University,
Quanzhou, Fujian, 362011,
China